



**Universidade do Minho**  
Escola de Engenharia

Kadriye Tuzlakoğlu

***Fiber-Based Structures from Natural Origin  
Polymers for Tissue Engineering Approches***



**Universidade do Minho**

Escola de Engenharia

Kadriye Tuzlakoğlu

***Fiber-Based Structures from Natural Origin  
Polymers for Tissue Engineering Approches***

Tese de Doutoramento em Ciência e Tecnologia de  
Materiais - Área de Biomateriais

Trabalho efectuado sob a orientação do  
**Professor Doutor Rui Luís Gonçalves dos Reis**

Dezembro de 2007

É AUTORIZADA A REPRODUÇÃO PARCIAL DESTA TESE,  
APENAS PARA EFEITOS DE INVESTIGAÇÃO, MEDIANTE DECLARAÇÃO  
ESCRITA DO INTERESSADO, QUE A TAL SE COMPROMETE.

*To My Father*





## **ACKNOWLEDGEMENTS**

It has been a long journey and I was lucky to have come in touch with many people. I would like to express my appreciation for those who directly or indirectly affected the course of this journey.

Firstly, I would like to thank my supervisor Prof. Rui L. Reis who has supported and inspired me the most during these years. I was fortunate to have a supervisor who I would walk into his office, deeply worried about some matter, and leave full of hope, eager to attack to problem, whatever it was. Thank you for your unlimited understanding and support.

I acknowledge Prof. Erhan Pişkin who always encourage and guide me in my scientific life. I can not overstate the importance of his involvement in my graduate career.

Special thanks go to my friend Marina for her ability to convert my bad moments to good ones with her positive energy. It was always nice to see the happiness and brightness in her face when I shared a good news about myself. I would like to thank her with a Turkish word which she can pronounce perfectly “Teşekkürler”.

I would like to thank Iva whom I shared my home and many good moments in last five years. Thank you for all your friendship, support and being my sixth sister in Portugal.

I am very grateful to Helena Azevedo and Ricardo Silva whom I started to work in the group at the same time. I am proud to record that I had opportunity to work with scientists and friends like them. Working with them made those experiments not only more efficient but also more enjoyable.

I would like to thank Erkan Türker Baran whom I learned to combine the words “design, architecture and construction” with tissue engineering. I was fortunate in working with him and sharing the experience about being abroad.

Many thanks go to “my churries” Marco Antonio, Cristina, Elizabeth and Paula who were always with me and supporting me, even from far. “Muchas Gracias”

To my friend Pınar, I would like to thank her for helping me in my bad moments and sharing nice time with me during her short stay in Portugal. “Thank you Şeker”

I want to thank Manuela, Xana and Belinha for their friendship and sharing the same office with me. I specially thank to Belinha who saved me from the beautiful north rain in the mornings.

To Ricardo Pires, Luciano, Rui Pereira, António Salgado, José Vitor, Ana Martins, Patricia, Ana Leite, Helena Lima, thank you for your friendship and help.

My friends in Turkey, Melisa, Ceyhun, Sevil, Aygül and Güldem, thanks for always being there for me.

I acknowledge to Management Team, Ariana, Tania, Berta, Virginia, Lilliana for their indispensable help dealing with bureaucratic matters as well as their friendship during my stay in Portugal.

I would like to take this opportunity to thank my doctor, Dr. Selim Nalbant, who helped me to have a second chance to live and made me to continue my PhD. I feel this is the right time to answer his question by saying “ the other side was not for me yet”.

I would also like to deeply thank Dr. Juan Garcia for all his effort to make my life easier and more secure here.

Words fail me to express my appreciation to my Mom and my sisters. Thank you all for your love and support as well as for the understanding you show it to me in every circumstance. My biggest thanks go to three little babies, Dilara, Eylül and Ilgaz, who always keep me in good mood by giving me from their unlimited positive energy.

## **ABSTRACT**

Tissue engineering is a new concept emerged as an alternative approach to tissue and organ reconstruction. It differs from organ transplantation by regenerating patient's own tissue and organs avoiding the biocompatibility and low biofunctionality problems as well as severe immune rejection; which are the main problems of organ transplantation. Tissue engineering methods generally require the use of three main components: a porous scaffold that serves as a matrix, cells and growth factors. The architecture of the tissue engineered scaffold is an important factor to take into consideration that can modulate biological response and the clinical success of the scaffold.

Fiber-based scaffolds can provide large surface area and highly interconnective porous structure for cell attachment and ingrowth as well as variety of geometric possibilities that can be regulated depending on the application.

In the works presented in this thesis, we developed different fiber based structures based on two natural origin polymers, chitosan and starch, for use in tissue engineering.

In Chapter III, chitosan fibers and fiber mesh scaffolds were produced by means of wet spinning technique. The tensile strength of produced fibers was around 205 MPa and Ca-P layer formation could be observed on their surfaces after 14 days of immersion in simulated body fluid (SBF). In Chapter IV, these fibers were then used in further studies for the reinforcement of the structure of a composite material which was consisting of microporous coralline origin hydroxyapatite microgranules, chitosan membranes and chitosan fibers. This composite architecture showed 88% (w/w) swelling in one hour and preserved its complex structure upon long-term incubation. Chitosan fiber meshes were obtained by moulding a predetermined amount of wet-spun fibers. After 7 days of culture, it was found that they were able to support osteoblast-like cell attachment and proliferation. A bone-like apatite layer was obtained on these

scaffolds by means of using a simple biomimetic coating process. The apatite formation was determined by different techniques, including SEM, FTIR-ATR, EDS, XRD. The influence of biomimetic coating on osteoblast cell behaviour was also examined by culturing SaOs-2 cells onto scaffolds. The cell population and ALP enzyme activity were found to be higher in the biomimetic coated scaffolds than those in uncoated scaffolds. Furthermore, cell presented more spread and flat morphology when they were seeded on biomimetic coated scaffolds.

Regarding starch-based fiber structures, wet spinning was used in Chapter VI as an alternative method to melt spinning for production of starch/polycaprolactone fiber mesh scaffolds. This method seemed to be a very reproducible way of obtaining the fiber mesh scaffolds, typically with 77% porosity and mean pore size 250 $\mu$ m. The specific surface of the scaffolds was measured around 29 mm<sup>2</sup>/mm<sup>3</sup>, which was very similar to natural bone. The surfaces of the scaffolds were then treated with plasma under Ar atmosphere. Although both treated and untreated scaffolds exhibited ability for osteoblast-like cell attachment and proliferation, DNA content and ALP enzyme activity were higher in plasma treated scaffolds.

Finally, and as a new approach to mimic the natural extracellular matrix (ECM), nano- and micro-fiber combined scaffolds from starch/polycaprolactone blend were designed by means of two step methodology. Electrospinning was used to obtain nanofibers on melt-spun micro-fiber meshes. With regard to the cell culture studies with osteoblast-like cells and rat bone marrow stromal cells, these new architectures showed excellent cell support ability and very promising properties to make them a proper tissue engineering scaffold.

In summary, results from these works showed that the designed fiber-based structures from natural origin polymers could successfully serve as a scaffold for tissue engineering.

## RESUMO

Engenharia de tecidos é um conceito novo que emergiu como uma abordagem alternativa para a reconstrução de tecidos e órgãos. Difere da transplantação de órgãos na medida em que gera os tecidos e órgãos do próprio doente melhorando desta forma a biocompatibilidade e funcionalidade, assim como reduzindo o risco de rejeição pelo sistema imunitário, que são os principais problemas associados à transplantação de órgãos. Geralmente os métodos de engenharia de tecidos requerem o uso de três componentes principais: um suporte poroso que serve de matriz, células e factores de crescimento. A arquitectura do suporte é um aspecto importante a ter em consideração que pode modular a resposta biológica e o sucesso clínico do mesmo a longo prazo.

Suportes à base de fibras podem dar origem a uma grande área superficial e a uma estrutura porosa interconectada para a adesão migração celulares, assim como uma variedade de possibilidades geométricas que podem ser adaptadas dependendo da aplicação.

No trabalho apresentado nesta tese foram desenvolvidas, para uso em engenharia de tecidos, diferentes estruturas à base de fibras produzidas a partir de dois polímeros de origem natural, sendo estes o quitosano e o amido. Fibras de quitosano e suportes à base de fibras foram produzidos pela técnica de “wet spinning”. A resistência à tracção das fibras produzidas foi em média 204.9 MPa e a formação da camada Ca-P foi observada nas suas superfícies após 14 dias de imersão em “simulated body fluid” (SBF). Estas fibras foram usadas em estudos posteriores para o reforço da estrutura do material compósito, que consiste em microgrânulos de hidroxiapatite de origem coralina microporosa, membranas e fibras de quitosano. Esta arquitectura compósita apresentou 88% (p/p) de inchamento ao fim de uma hora e manteve a sua estrutura complexa em incubações prolongadas. Suportes à base de fibras de quitosano foram obtidos moldando uma quantidade pré-determinada de fibras produzidas por “wet-spinning”. Após 7 dias de cultura, verificou-se que eram capazes de suportar a

adesão e proliferação de osteoblastos. Uma camada de apatite idêntica ao osso foi obtida nestes suportes através de um processo simples de revestimento biomimético. A formação de apatite foi determinada por diferentes técnicas, tais como: SEM, FTIR-ATR, EDS e XRD. A influência do revestimento biomimético foi também examinada na actividade celular dos osteoblastos, cultivando células SaOs-2 nos suportes. Observou-se que a população celular e a actividade da enzima ALP é maior nos suportes com revestimento biomimético do que nos suportes sem revestimento. Além disso, células semeadas nos suportes com revestimento biomimético apresentam-se mais espalhadas e com uma morfologia plana.

Relativamente às estruturas de fibras à base de amido, a técnica de “wet spinning” é utilizada como uma alternativa à técnica de “melt spinning” para produção de suportes à base de fibras de amido/policaprolactona. Este método permite obter de uma forma reprodutível suportes à base de fibras com 77% de porosidade e tamanho médio de poro de 250  $\mu\text{m}$ . A superfície específica dos suportes é de aproximadamente 29  $\text{mm}^2/\text{mm}^3$ , que é em muito semelhante ao osso natural. As superfícies dos suportes foram então tratadas com plasma em atmosfera árgon. Embora ambos os suportes tratados e não tratados por plasma tenham exibido capacidade para adesão e proliferação dos osteoblastos, o conteúdo de DNA e a actividade da enzima ALP foram maiores em suportes tratados.

Numa nova abordagem para mimetizar a matriz extracelular natural (ECM), foram concebidos, por uma metodologia em duas etapas, suportes combinados de nano- e micro-fibras a partir de uma mistura de amido/policaprolactona. A técnica de “electrospinning” é utilizada para produzir nano-fibras no topo de malhas de micro-fibras sendo estas obtidas por “melt-spun”. No que diz respeito a estudos de culturas celulares com osteoblastos e células da medula óssea de rato, estas novas arquitecturas mostraram uma excelente capacidade de suporte celular como uma estrutura de engenharia de tecidos.

Em resumo, os resultados destes trabalhos demonstraram que as estruturas à base de fibras, concebidas a partir de polímeros naturais, podem servir com êxito como suporte para engenharia de tecidos.





## TABLE OF CONTENTS

Acknowledgments.....	i
Abstract.....	iii
Resumo .....	v
Table of Contents.....	viii
List of abbreviations.....	xv
List of Figures .....	xvii
List of Tables .....	xxii
Short <i>Curriculum Vitae</i> .....	xxiii
List of Publications .....	xxiv

## CHAPTER I

### GENERAL INTRODUCTION

<b>BIODEGRADABLE POLYMERIC FIBER STRUCTURES IN TISSUE ENGINEERING.....</b>	<b>1</b>
<b>Abstract .....</b>	<b>2</b>
<b>1. Definition .....</b>	<b>3</b>
<b>2. Fiber Structures .....</b>	<b>4</b>
<b>3. Applications in Tissue Engineering .....</b>	<b>4</b>
3.1. Soft Tissue Engineering .....	5
<i>Skin Replacement</i> .....	5
<i>Vascular Grafts</i> .....	7
<i>Prosthetic heart valves</i> .....	8
<i>Stents</i> .....	8
<i>Nerve Tissue Regeneration</i> .....	9
3.2. Hard Tissue Engineering.....	10
<i>Articular Cartilage</i> .....	10
<i>Bone</i> .....	13

<i>Anterior Cruciate Ligament</i> .....	16
<b>4. Conclusions and Future Aspects</b> .....	18
<b>References</b> .....	19
<b>CHAPTER II</b>	
<b>MATERIALS&amp;METHODS</b> .....	29
<b>I. Materials</b> .....	30
A. Chitosan.....	30
B. Starch/Polycaprolactone Blend.....	30
C. Bioglass® .....	32
<b>II. Production Methods</b> .....	32
A. Wet Spinning.....	32
B. Electrospinning .....	35
C. <i>In vitro</i> Bioactivity Testing and Biomimetic Coating .....	36
C. 1. <i>In vitro</i> Bioactivity .....	36
C. 2. Biomimetic Coating .....	37
D. Plasma Treatment .....	38
<b>III. Characterization Methods for Developed Structures</b> .....	39
A. Morphology .....	39
B. Surface Analysis .....	40
B. 1. Energy Dispersive Spectroscopy (EDS) .....	40
B. 2. Fourier Transform Infrared Attenuated Total Reflectance Spectroscopy (FTIR-ATR) .....	40
B. 3. Thin film X-Ray Diffraction (TF-XRD) .....	40
B. 4. X-Ray Photoelectron Spectroscopy (XPS) .....	41
C. Inductively Coupled Plasma- Optical Emission Spectroscopy (ICP-OES) .....	41
D. Swelling test.....	41
E. Mechanical Analysis .....	42
E. 1. Tensile test.....	42

E. 2. Dynamical Mechanical Analysis (DMA) .....	42
<b>IV. <i>In Vitro</i> Cytotoxicity and Cell Culture Studies .....</b>	<b>43</b>
A. Cell type .....	43
A.1. Cell lines: Mouse lung fibroblast cell line (L929) and a human osteoblast-like cell line (SaoS-2) .....	43
A. 2. Rat Bone Marrow Stromal Cells (isolation) .....	43
B. Indirect Cytotoxicity Evaluation .....	44
C. Cell seeding and culture on the developed scaffolds .....	46
D. Characterization .....	47
D. 1. Cell Morphology .....	47
D. 2. Cell viability and proliferation .....	47
D. 2. 1. MTS .....	47
D. 2. 2. DNA .....	48
D. 3. ALP Enzyme Activity .....	48
<b>References .....</b>	<b>50</b>

### **CHAPTER III**

## **PRODUCTION AND CHARACTERIZATION OF CHITOSAN FIBERS AND 3-D FIBER MESH SCAFFOLDS FOR TISSUE ENGINEERING APPLICATIONS .....**

<b>Abstract .....</b>	<b>53</b>
<b>1. Introduction .....</b>	<b>54</b>
<b>2. Experimental .....</b>	<b>55</b>
2.1. Materials .....	55
2.2. Methods .....	55
2.2.1. Chitosan fiber preparation .....	55
2.2.2. Chitosan fiber meshes preparation .....	56
2.3. Characterization .....	56
2.3.1. Chitosan fiber .....	56
2.2.2. Chitosan fiber meshes .....	59

<b>3. Results and discussion</b> .....	61
3.1. Chitosan fibers .....	61
<i>Scanning Electron Microscopy</i> .....	61
<i>Mechanical Properties</i> .....	61
<i>Swelling Tests</i> .....	61
<i>Bioactivity Tests</i> .....	62
<i>Cytotoxicity Test</i> .....	64
<b>3.2. Chitosan fiber meshes</b> .....	65
<i>Scanning Electron Microscopy</i> .....	65
<i>Mechanical Properties</i> .....	66
<i>Swelling Tests</i> .....	70
<i>Cytotoxicity and Biocompatibility: Direct Contact Test with Osteoblast-like Cells</i> .....	71
<b>4. Conclusions</b> .....	72
<b>References</b> .....	73

## CHAPTER IV

### MULTICHANNEL MOULD PROCESSING OF 3D STRUCTURES FROM MICROPOROUS CORALLINE HYDROXYAPATITE GRANULES AND CHITOSAN SUPPORT MATERIALS FOR GUIDED TISSUE REGENERATION/ENGINEERING .....

76

#### Abstract .....

77

#### 1. Introduction .....

78

#### 2. Materials&Methods .....

79

##### 2.1. Preparation of coralline origin HA reinforced composite material .....

80

##### 2.1. 1. Chitosan fiber preparation.....

80

##### 2.1.2. Chitosan membrane preparation .....

80

##### 2.1.3. Assembly of coralline origin HA granules, chitosan fibers, and membrane.....

80

##### 2.2.Cytotoxicity assays.....

82

##### 2.2.1. Cell culture.....

82

2.2.2. MEM extraction test (72 hours) .....	82
2.3. Swelling test .....	84
<b>3. Results and discussion</b>	
3.1. Coralline origin HA/chitosan composite material preparation .....	84
3.2. Cytotoxicity assays .....	85
3.3. Swelling test .....	86
<b>4. Conclusions</b> .....	87
<b>References</b> .....	88

## CHAPTER V

<b>FORMATION OF BONE-LIKE APATITE LAYER ON CHITOSAN FIBER MESH SCAFFOLDS BY A BIOMIMETIC SPRAYING PROCESS</b> .....	91
<b>Abstract</b> .....	92
<b>1. Introduction</b> .....	93
<b>2. Materials&amp;Methods</b> .....	95
2.1. Production of Chitosan Fiber Mesh Scaffolds.....	95
2.2. Biomimetic Coating .....	95
2.3. Characterization of Ca-P Coated Scaffolds .....	96
2.4. Cell Culture Studies with Osteoblasts .....	96
<i>Cell viability</i> .....	97
<i>Alkaline Phosphatase (ALP) Activity</i> .....	97
<b>3. Results&amp;Discussion</b> .....	98
3.1. Biomimetic Coating .....	98
3.2. Cell Culture Studies with Osteoblasts .....	102
<b>4. Conclusions</b> .....	105
<b>References</b> .....	107

## CHAPTER VI

### A NEW ROUTE TO PRODUCE STARCH-BASED FIBER MESH SCAFFOLDS BY WET SPINNING AND THE IMPROVEMENT IN CELL ATTACHMENT AND PROLIFERATION BY TAILORING THEIR SURFACE PROPERTIES ..... 111

<b>Abstract</b> .....	112
<b>1. Introduction</b> .....	113
<b>2. Materials&amp;Methods</b> .....	114
2.1. Materials.....	114
2.2. Wet Spinning Process .....	114
2. 3. Plasma Surface Treatment.....	115
<i>X-ray Photoelectron Spectroscopy (XPS)</i> .....	116
2. 4. Cell Culture Studies.....	117
<i>Morphological Analysis</i> .....	117
<i>Cell Proliferation-DNA Assay</i> .....	117
<i>Alkaline Phosphatase (ALP) Activity</i> .....	118
<i>Statistical Analysis</i> .....	118
<b>3. Results and Discussion</b> .....	118
3.1. Morphology of the scaffolds.....	118
3.2. Plasma Treatment .....	119
3.3. Cell Culture.....	122
<i>Morphological Analysis</i> .....	122
<i>Cell Viability</i> .....	124
<i>ALP activity</i> .....	125
<b>4. Conclusions</b> .....	125
<b>References</b> .....	127

## CHAPTER VII

### **NANO- AND MICRO-FIBER COMBINED SCAFFOLDS: A NEW ARCHITECTURE FOR BONE TISSUE ENGINEERING** .....

<b>Abstract</b> .....	132
<b>1. Introduction</b> .....	133
<b>2. Materials&amp;Methods</b> .....	135
2.1. Materials.....	135
2.2. Electrospinning Process.....	135
<i>Morphological Analysis</i> .....	135
2.3. Cell Culture.....	135
<i>Morphological Analysis</i> .....	136
<i>Cell proliferation Assay</i> .....	137
<i>Alkaline Phosphatase (ALP) Activity</i> .....	137
<b>3. Results&amp;Discussion</b> .....	138
3.1. Nano- and micro fiber combined scaffolds .....	138
3.2. Cell Culture.....	138
<i>Morphological Analysis</i> .....	138
<i>Cell viability</i> .....	142
<i>ALP Activity</i> .....	143
<b>4. Conclusions</b> .....	144
<b>References</b> .....	146

## CHAPTER VIII

### **GENERAL CONCLUSIONS**

General Conclusions.....	150
Final Remarks/Future Research .....	152





## LIST OF ABBREVIATIONS

### A

**$\alpha$ -MEM**-  $\alpha$ -Minimum Essential Medium  
**ACL**- anterior cruciate ligament  
**ALP** - Alkaline Phosphatase

### B

**bFGF**- Basic fibroblast growth factor  
**BMP** - Bone Morphogenetic Protein  
**BSA** - Bovine Serum Albumin

### C

**Ca-P**- Calcium Phosphate  
**CNS**- Central Nervous System

### D

**DMA**- Dynamical Mechanical Analysis  
**DMEM** - Dulbecco's Modified Eagle's Medium  
**dsDNA** – Double stranded DNA

### E

**ECM** - Extracellular Matrix  
**EDC**- Carbodiimide (EDC)  
**EDS** - Energy Dispersive Spectroscopy

### F

**FBS**- Foetal bovine serum  
**FTIR- ATR** - Fourier Transformed Infrared Spectroscopy – Attenuated Total Reflectance

### G

**GTR**- Guided tissue regeneration (GTR)

### H

**HA** - Hydroxyapatite

### I

**ICP-OES** Inductively coupled plasma atomic emission spectrometry  
**ISO** - International Standards Organization

### M

**$\mu$ CT**- Micro-computed tomography  
**MEM** - Minimal Essential Medium  
**MSCs** - Mesenchymal Stem Cells  
**MTS** – (3-(4,5-dimethylthiazol-2-yl)-5-(3-carboxymethoxyphenyl)-2(4-sulfophenyl)-2H tetrazolium)

**P**

**PBS** - Phosphate Buffered Solution

**pNP** - p-Nitrophenol

**pNPP** - p-Nitrophenyl Phosphate

**PNS**- Peripheral nervous system

**R**

**RBMC** - Rat bone marrow stromal cells

**RF**- Radio frequency

**S**

**SEM** - Scanning Electron Microscopy

**SMCs**- Smooth muscle cells

**SPCL** - Blend of corn starch/poly( $\epsilon$ -caprolactone)

**T**

**TCP** - Tricalcium Phosphate

**TCPS** - Tissue Culture Polystyrene

**TF-XRD** - Thin film X-ray diffraction

**U**

**UHMWPE**- Ultra High Molecular Weight Polyethylene

**X**

**XPS** - X-ray photoelectron spectroscopy

**XRD** - X-Ray Diffraction

## LIST OF FIGURES

### CHAPTER II

**Figure 1.** Chemical structure of chitosan

**Figure 2.** Chemical structure of starch.

**Figure 3.** Chemical structure of polycaprolactone.

**Figure 4.** Schematic diagram of wet-spinning process.

**Figure 5.** Schematic representation of the production of chitosan fibers and fiber mesh scaffolds.

**Figure 6.** Experimental set-up for electrospinning of SPCL nano-fibers onto SPCL micro-fiber meshes.

**Figure 7.** Schematic representation of a novel biomimetic coating process using Bioglass/water suspension.

**Figure 8.** The mechanism of Ca-P formation on chitosan fiber meshes immersed in SBF solution after Bioglass spraying.

### CHAPTER III

**Figure 1.** SEM micrographs of chitosan fibers; a) x360, b) x3000.

**Figure 2.** Swelling ratio vs. time for chitosan fibers.

**Figure 3.** Sem micrographs of chitosan fibers; A) before, B) after 30 days of immersion in SBF (x1000), C) after 30days of immersion in SBF (x3000).

**Figure 4.** SEM mşcrograph of commercial available polyamide fibers after 30 days immersion in SBF (x1000).

**Figure 5.** EDS spectra of the Ca-P coatings on the surface of chitosan fibers (after 30 days in SBF).

**Figure 6.** Evolution of the Ca and P elemental concentrations in the SBF as a function of immersion time of chitosan fibers in SBF.

**Figure 7.** SEM micrographs of the structure of the developed chitosan fibers meshes; A)x33.4, B) x50, C) x250

**Figure 8.** Evolution of the strain of a dry chitosan mesh after it was immersed at 37 °C (symbols). The solid line corresponds to the best fit of the data according to Eq. (2).

**Figure 9.** Creep (60 min) followed by a recovery stage (60 min) and, finally, a second short creep run performed at 37 °C in the immersed chitosan mesh. The inset graphics shows the viscoelastic component of the first creep run, in a log time scale.

**Figure 10.** Storage and loss moduli ( $E'$  and  $E''$ ) as a function of frequency ( $f$ ) at 37 °C of the immersed chitosan mesh. The inset graphics shows the frequency dependence of the loss factor.

**Figure 11.** Swelling ratio vs. time for the developed 3-D chitosan fiber meshes.

**Figure 12.** Osteoblast-like cells A) adhering to chitosan based fibres after 1 day of culture, B) proliferating over chitosan based fibres after 7 days of culture.

## CHAPTER IV

**Figure 1.** Schematic representation of the preparation method of coralline origin HA-chitosan fiber composite using a multichannel mould (A); Principle of production of thicker scaffolds by clasp fixing of TCP/HA replica complexes (B, C).

**Figure 2.** Light transmission microphotographs of HA granules (white cylinder bodies) and chitosan fibers (indicated by arrows) over chitosan membrane: (A) Front view of complex and (B) back view of complex.

**Figure 3.** Cell viability of L929 cells after incubation with test and control extracts over a period of 72h. Results based on optical measurements.

**Figure 4.** Swelling curve of coralline HA-chitosan composite in physiological saline (pH 7.4)

## CHAPTER V

**Figure 1.** Schematic representation of a novel biomimetic Ca-P coating process using a simple spray

**Figure 2.** Chitosan fiber mesh scaffolds produced by wet spinning

**Figure 3.** SEM micrographs of chitosan fiber mesh scaffolds; A) x15, B) x200

**Figure 4.** SEM micrographs of the developed coated scaffolds, exhibiting a fine and homogenous Ca-P layer onto chitosan fiber meshes surfaces; A) x100, B) x300, C) 500, D) x5000

**Figure 5.** EDS spectra of Ca-P coated chitosan fiber mesh scaffolds.

**Figure 6.** FTIR spectra of Ca-P coated sample and uncoated sample.

**Figure 7.** Thin-film XRD patterns of the chitosan fiber meshes immersed in SBF for 7 days.

**Figure 8.** Human osteoblast like cells seeded on A) Ca-P coated (x2000), B) Ca-P coated (x3000) and C) uncoated (x2000) chitosan fiber mesh scaffolds after 2 weeks of culture.

**Figure 9.** Human osteoblast like cells (SaOs-2) seeded on A) Ca-P coated (x1000), B) Ca-P coated (x4000) and C) uncoated (x1000) chitosan fiber mesh scaffolds after 3 weeks of culture.

**Figure 10.** Cell viability and proliferation of human osteoblast like cells determined by MTS after 3 weeks of culture. Error bars represent means  $\pm$  SD for n=3.

**Figure 11.** The ALP activity of human osteoblast like cells seeded on Ca-P coated scaffolds and control (uncoated scaffolds). Error bars represent means  $\pm$  SD for n=3

## CHAPTER VI

**Figure 1.** Morphology of the wet-spun SPCL fiber mesh scaffolds analysed by; A)  $\mu$ CT, showing thin section of sample, B) SEM

**Figure 2.** The surface of the SPCL fiber mesh scaffolds; A) before (x3000) and B) after Ar plasma treatment (x3000).

**Figure 3.** C1s core level spectra for wet-spun SPCL fiber meshes A) before and B) after Ar plasma treatment

**Figure 4.** SEM micrographs of osteoblast-like cells seeded on SPCL fiber mesh scaffolds after 3 days of culture; A) untreated, B) Ar plasma treated scaffold

**Figure 5.** SEM micrographs of osteoblast-like cells seeded on; A) untreated and B) Ar plasma treated SPCL fiber mesh scaffolds after 7 days of culture (Pictures at right show the cells on the surface with higher magnification, (x1000))

**Figure 6.** SEM micrographs of osteoblast-like cells seeded on SPCL fiber mesh scaffolds after 3 days of culture; A) untreated, B) Ar plasma treated scaffold

**Figure 7.** Cell viability and proliferation of human osteoblast like cells determined by DNA. Error bars represent means  $\pm$  SD for n=3.

**Figure 8.** The ALP activity of human osteoblast like cells seeded on untreated and Ar plasma treated wet-spun SPCL fiber meshes. Error bars represent means  $\pm$  SD for n=3.

## CHAPTER VII

**Figure 1.** Microscopic images of the scaffolds. Fig.B presents a detailed view of nanofibers as observed by SEM.

**Figure 2.** Human osteoblast like cells (SAOS-2) seeded on nano- and micro-fiber combined scaffolds and control (scaffolds without nanofibers);A) after 7 days, B), C) and D) after 14 days of culture

**Figure 3.** Human osteoblast like cells on control scaffolds after 14 days of culture

**Figure 4.** Rat bone marrow stromal cells (RBMSC) seeded on nano- and micro-fiber combined scaffolds and control (scaffolds without nanofibers); A) after 7 days, B) and C) after 14 days of culture. D) Rat bone marrow stromal cells on control scaffolds after 7 days of culture.

**Figure 5.** Cell viability and proliferation of human osteoblast like cells determined by MTS. Error bars represent means  $\pm$  SD for n=3.

**Figure 6.** Cell viability and proliferation of rat bone marrow stromal cells determined by MTS. Error bars represent means  $\pm$  SD for n=3.

**Figure 7.** The ALP activity of human osteoblast like cells seeded on SPCL nano- and micro-fiber combined scaffolds and control (scaffolds without nanofibers). Error bars represent means  $\pm$  SD for n=3.

**Figure 8.** The ALP activity of rat bone marrow stromal cells seeded on SPCL nano- and micro-fiber combined scaffolds and control (scaffolds without nanofibers). Error bars represent means  $\pm$  SD for n=3.



## **LIST OF TABLES**

### **CHAPTER II**

**Table 1.** Ion concentrations of human blood plasma and SBF.

**Table 2.** Quantitative and qualitative scores used in the cytotoxicity tests.

**Table 3.** Different cytotoxicity indexes used to classify the reactivity of tested samples

**Table 4.** The parameters used in cell culture experiments for different scaffolds.

### **CHAPTER III**

**Table 1.** Quantitative and qualitative scores used in the cytotoxicity tests

**Table 2.** Different cytotoxicity indexes used to classify the reactivity of tested samples

**Table 3.** Results comparing fibroblasts cytotoxic response and reactivity to chitosan materials and controls.

### **CHAPTER IV**

**Table 1.** Quantitative and qualitative scores used in the cytotoxicity tests.

**Table 2.** Cytotoxicity index.

### **CHAPTER VI**

**Table 1.** XPS data for wet spun SPCL scaffolds before and after modification

## **Short Curriculum Vitae**

Kadriye Tuzlakoglu was born in 1976 in Sakarya, Turkey. She has been a researcher of the 3B's Research Group- Biomaterials, Biodegradables and Biomimetics, since September 2001.

She has graduated in Chemical Engineering in Hacettepe University in Turkey; MSc in Chemical Engineering in the same university. She also started and finished all the courses of PhD in Chemical Engineering in Hacettepe University before restart her PhD in Portugal.

During her master, she worked in the biomaterials field, focusing her work on the development of biodegradable synthetic membranes for guided tissue regeneration in periodontology. In 2001, she joined the 3B's Research Group, where she has been working on the design of fiber-based scaffolds from different natural origin polymers for tissue engineering applications.

As a results of her research work, she has attended the most relevant conferences in her research field. Presently she is the author of 17 papers in international refereed journals (10 published, 1 *in press*, 6 submitted), 5 book chapters (3 published, 2 *in press*) and 28 abstracts in international conference proceedings.

**This thesis is based on the following publications:**

**Papers in international refereed journals:**

1. E. T. Baran, **K. Tuzlakoglu**, A. J. Salgado, R. L. Reis, "Multichannel mould processing of 3D structures from microporous coralline hydroxyapatite granules and chitosan support materials for guided tissue regeneration/engineering" Journal of Materials Science: Materials in Medicine, 15, (2003), 161-165.
2. **K. Tuzlakoglu**, C. M. Alves, J. F. Mano, R. L. Reis; "Production and Characterization of Chitosan Fibers and 3D Fiber Mesh Scaffolds for Tissue Engineering Applications", Macromolecular Bioscience, (2004), 4:8, 811-819.
3. **K. Tuzlakoglu**, N. Bolgen, A. J. Salgado, M. E. Gomes, E. Piskin, R. L. Reis, "Nano- and micro-fiber combined scaffolds: A new architecture for bone tissue engineering", Journal of Materials Science: Materials in Medicine, 16 (2005), 1099 – 1104.
4. **K. Tuzlakoglu**, R. L. Reis, "Formation of bone-like apatite layer on chitosan fiber mesh scaffolds by a biomimetic spraying process", Journal of Materials Science: Materials in Medicine, 18 (2007) 1279-1286.
5. **K. Tuzlakoglu**, I. Pashkuleva, M. R. Rodrigues, M. E. Gomes, G. H. van Lenthe, R. Müller, R.L. Reis "A New Route to Produce Starch-based Fiber Mesh Scaffolds by Wet Spinning and Subsequent Surface Modification as a Way to Improve Cell Attachment and Proliferation", Biomacromolecules, (2007), *submitted*
6. **K. Tuzlakoglu**, R. L. Reis, "Biodegradable polymeric fiber structures in tissue engineering", Tissue Engineering: Reviews, (2007), *submitted*.

### **Book Chapters:**

1. **K. Tuzlakoglu**, R.L. Reis, "Processing and Biomedical Applications of Degradable Polymeric Fibers", In: *Biodegradable Systems in Medical Functions: Design, Processing, Testing and Applications*, ed, RL Reis, J San Román, CRC Press LLC, Florida, USA (2004), 163-174
2. **K. Tuzlakoglu**, R. L. Reis, "Chitosan-based scaffolds in orthopaedic applications", In: *Handbook of Natural-based Polymers for Biomedical Applications*, Woodhead Publishing, *in press*.

### **Communications in International Conferences:**

1. E.T. Baran, **K. Tuzlakoglu**, A.J. Salgado, R.L. Reis, Processing of 3D Architectures Based on HA Porous Particles/Chitosan Fibres/Chitosan Membranes For Guided Tissue Regeneration Using a Multichannel Mold, 5<sup>th</sup> International Meeting of the Tissue Engineering Society International (TESI), Kobe, Japan, (2002).
2. **K. Tuzlakoglu**, C. M. Alves, A. J. Salgado, J. F. Mano, R. L. Reis, "Development, Dynamical-Mechanical Properties and Biological Performance of Novel 3-D Chitosan Fiber Mesh Scaffolds", 29<sup>th</sup> Annual Meeting of the Society for Biomaterials, Reno, USA, (2002).
3. **K. Tuzlakoglu**, E. Piskin, R.L. Reis, "Development of Novel 3-D Chitosan/Hydroxyapatite Composite Fiber Mesh Scaffolds for Tissue Engineering applications", 10<sup>th</sup> International Symposium on Biomedical Science and Technology, Northern Cyprus, (2003).
4. **K. Tuzlakoglu**, E.T. Baran, A.J. Salgado, O.P. Coutinho, R.L. Reis, "*In Vitro* Evaluation of Microporous Coralline-Chitosan Composite Materials for Bone Tissue Engineering", NATO/ASI Learning from Nature How to Design New Implantable Biomaterials: From Biomineralization Fundamentals to Biomimetic Materials and Processing Routes, Alvor, Portugal, (2003).
5. **K. Tuzlakoglu**, R.L. Reis, "Biomimetic Apatite Coating of Chitosan Fiber Mesh Scaffolds and Starch/polycaprolactone Porous Structures for Bone Tissue Engineering Applications "Joint Meeting of the Tissue Engineering Society

International (TESI) and the European Tissue Engineering Society (ETES), Lausanne Switzerland, (2004).

**6. K. Tuzlakoglu**, A.J. Salgado, R.L. Reis, "Development of Silk fibroin-coated Chitosan Fiber Mesh Scaffolds for Bone Tissue Engineering", 6th International Symposium on Frontiers in Biomedical Polymers, Granada, Spain (2005).

**7. K. Tuzlakoglu**, A.J. Salgado, R.L. Reis, "Formation of Ca-P Layer on Chitosan Fiber Mesh Scaffolds by a Biomimetic Process and Its Effect on Osteoblast Cell Morphology and Viability", European Congress on Advanced Materials and Processes (Euromat 2005), Prague, Czech Republic (2005).

**8. K. Tuzlakoglu**, S. Egri, A.J. Salgado, M. E. Gomes, E. Piskin, R.L. Reis, "Nano- and Micro-fiber Combined Scaffolds: A New Architecture for Bone Tissue Engineering", 19<sup>th</sup> European Conference on Biomaterials, Sorrento, Italy (2005).

**9. M. I. Santos, K. Tuzlakoglu**, M. E. Gomes, S. Fuch, R. E. Unger, R. L. Reis, C. J. Kirkpatrick, "Nano- and Micro-fiber Combined Scaffolds: An Innovative Design for Improving Endothelial Cell Migration in Bone Tissue Engineering" 8<sup>th</sup> International Meeting of the Tissue Engineering Society International (TESI), , Shanghai, China (2005).

**9. K. Tuzlakoglu**, I. Pashkuleva, M.T. Rodrigues, M. E. Gomes, R.L. Reis, "A New Route to Produce Starch-based Fiber Mesh Scaffolds by Wet Spinning and the Improvement in Cell Attachment and Proliferation by Tailoring Their Surface Properties", 32<sup>nd</sup> Annual Meeting of the Society for Biomaterials, Chicago, USA (2007).

**10. K. Tuzlakoglu**, M. I Santos, N. Neves, R. L. Reis, "A New Scaffold Design Approach to Mimic the Physical and Chemical Structure of Natural Extracellular Matrix", 4<sup>th</sup> European Symposium on Biopolymers, Kusadasi, Turkey, (2007).

**What is a scientist after all? It is a curious man looking through  
a keyhole, the keyhole of nature, trying to know what's going on.  
Jacques Yves Cousteau**





## **CHAPTER I**

### **GENERAL INTRODUCTION**

# **BIODEGRADABLE POLYMERIC FIBER STRUCTURES IN TISSUE ENGINEERING**



## **Abstract**

Tissue engineering offers a promising new approach to create biological alternatives to repair or restore function of damaged or diseased tissues. In order to obtain three-dimensional tissue constructs, stem/progenitor cells must be combined with a highly porous three-dimensional scaffold. However, so far, many of the structures purposed for tissue engineering can not meet all the criteria required by an adequate scaffold due to the lack of mechanical strength and interconnectivity as well as poor surface characteristics. Fiber-based structures represent a wide range of morphological and geometric possibilities that can be tailored for each specific tissue engineering application. The present article overviews the research data in tissue engineering therapies based on the use of biodegradable fiber architectures as a scaffold.

## 1. Definition

Fibers are the fundamental units of textile and fabrics. They can be directly supplied from nature or produced from synthetic polymers. Both natural and synthetic fibers and fiber-based structures, so-called biotextiles, have been widely used for biomedical applications.

“Biotextiles” has been defined as a “structure composed of textile fibers and designed for used in a specific biological environment (e.g. surgical implant), where its performance depends on its interactions with cells and biological fluids as measured in terms of its biocompatibility and biostability” [1].

Polymeric fibers that are used in medicine can be manufactured by three main techniques; melt spinning [2], dry spinning and wet spinning [3]. All those techniques are based on an extrusion of a polymer melt or solution. The final properties of the produced fibers can be controlled by using different finishing methods for instance stretching [4] or drying treatments with different solvents [5]. Besides those main techniques, some special methods such as electrospinning [6], gel spinning [7] were also used in fiber processing. As we will discuss below, due to the structural similarity of electrospun polymeric mats to the natural extracellular matrix, the electrospinning process has attracted a great deal of attention in scaffold processing for tissue engineering [8]. In a brief, this process is based on the generation of an electrical field between a polymeric solution (or a polymer melt) placed in a capillary tube with a pipette or needle of small diameter and a metal collector. When the electrical field reaches its critical value, repulsive electrostatic force overcomes the surface tension of the polymer solution and a charged jet is produced. This charged polymeric jet then undergoes a stretching process which is accompanied by the rapid solvent evaporation and results the formation of long and thin nano fibers. Electrospinning have been used to fabricate nanofibrous structures from a number of both natural synthetic polymers, such as collagen[9], chitosan [10] , chitin[11] , silk fibroin[12], hyaluronic acid [13] and poly(DL-lactide-co-glycolide) [14], poly(L-lactide) [15], and polycaprolactone [16], among many others. Within last few years, these nanofibrous structures have been used as a scaffold in many different tissue engineering applications.

## **2. Fiber Structures**

Fibers can be manufactured as monofilaments or multifilaments, they find, for instance, application as a suture in surgery. Sutures are the oldest and simplest example of the textiles used in medicine. They are made of both biodegradable and non-degradable polymers, either natural or synthetic origin. Dexon® (polyglycolide; multifilament), Dexon Plus® (polyglycolide, braided), Vicryl® (poly[glycolide-L-lactide]; multifilament), Maxon® (poly[glycolide-co-trimethylene carbonate]; monofilament), Biosyn® (poly[glycolide-co-L-lactide-co-trimethylene carbonate]), and PDS® (poly-*p*-dioxanone; monofilament) are the some examples for commercially available biodegradable sutures [17, 18].

For more complex applications, fibers can also be formed in 3D structures such as knitted, braided, woven, and non-woven. The orientation of fibers into these structures may range from highly regular to completely random. The final structure of the fibers affects the behaviors of the fibers when they are applied. For example, woven structures show more stable and porous structure than the other fiber structures. As a disadvantage, they can be unraveled at the edges when they cut squarely or obliquely for implantation. However, knitted structures have inherent ability to resist unraveling when they cut. Moreover, they are very flexible and porous. But sometimes their flexibility is reduced when the additional yarns are used to interlock the loops in order to obtain more stable structures. Additionally, difficulties of reducing their high porosity below a certain value are another clear disadvantage for some applications. Braided structures are mostly used as a suture. They can be designed using several different patterns, either with or without core. The spaces between the yarns, which cross each other, make them porous and help the fluid flow during the healing process. Non-woven structures may have a wide range of porosity. Their isotropic structure provides good mechanical and thermal stability. They can easily compress and expand. These advantages make them a suitable material for many tissue engineering applications.

## **3. Applications in Tissue Engineering**

Tissue engineering offers a promising new approach to create biological alternatives for regenerating different tissues. It involves typically the use of stem/progenitor

cells seeded in a scaffold which can guide the cell growth and tissue formation in three dimensions. Several requirements must be considered in the design of tissue engineering scaffolds, including high porosity, large surface area, adequate pore size, and uniformly distributed interconnected porous structures throughout the matrix [19-21].

Biodegradable polymeric fiber structures can provide a large surface area, and a relatively large porosity which can be optimized for specific applications. Besides these, many tissues, such as nerve, muscle, tendon, ligament, blood vessel, bone, and teeth, have tubular or fibrous bundle architectures and anisotropic properties. Therefore, fiber-based structures find a number of applications in tissue engineering, including soft tissue repair, vascular prostheses, bone and cartilage scaffolds, nerve guides, among others. On the other hand, many parameters must be considered in the design of fiber architectures, such as optimal fiber diameter and linear density, overall porosity and pore size distribution, influence of fiber orientation on cellular response and influence of degradation on the properties of the structures.

### **3.1. Soft Tissue Engineering**

#### *Skin Replacement*

Skin is a complex organ and mainly consisting of a superficial and an inner layer which are called epidermis and dermis, respectively. It is well known that most wounds can heal naturally. However, the replacement becomes a serious problem when it is irreversibly damaged by burns, trauma or disease. The most common approach for skin replacement is the use of autografts or allografts [22-24]. But they have many limitations including the creation of a donor site, risk of infection and slow healing. Over the past two decades, tissue engineering approach have been studied to construct a three dimensional skin architecture using a temporary scaffold combined with fibroblast, keratinocytes and endothelial cells [25, 26].

Biodegradable fiber-based structures have been proposed to use for healing or dermal or epidermal injuries. The most successful fiber-based dermal equivalents are the commercialized products Dermagraft® and Dermagraft-TC®. Dermagraft® is a structure consisting of fibroblasts, extracellular matrix and a biodegradable fiber mesh [27]. In this product, polyglactin (PLGA) mesh is used as a scaffold for fibroblasts. The fibroblast proliferated into the scaffolds secrete human dermal

collagen, matrix proteins, growth factors and cytokines and create a dermal substitute. It has been already applied clinically to the patients with diabetic foot ulcers. It was found that healing was faster and better in patients with Dermagraft® treatment compared to the control patients (debridement and moist wound healing) [28, 29]. Dermograft-TC® is a Silastic covered form of Dermagraft® and act as a non-biodegradable form due to that covering. It has been also approved by FDA to use as a dermal substitute. More recently, the PLGA knitted mesh has been combined with collagen microsponges for three-dimensional culturing of skin fibroblast [30]. In this new hybrid approach, the PLGA knitted mesh serves as a scaffold to support the forming tissue while collagen microsponges help the new and homogenous dermal tissue formation.

Besides those commercialized synthetic fiber structures, natural fibers, such as chitin, chitosan, alginate and a benzyl ester of hyaluronic acid (Hyaff 11®), are also proposed for wound healing due to their wound healing ability [31]. For instance, Hirano et al. [32] developed a new biocompatible dressing material made of wet spun chitin-acid glycosaminoglycan fibers that released a portion of the glycosaminoglycan in the body. Softness and easy handling of these fibers could be useful to heal epidermal tissue injuries.

Engineering of dermal tissue with using a non-woven scaffolds based on a benzyl ester of hyaluronic acid has been studied by many researchers [29, 33-35]. In order to obtain a nonwoven mesh structure hyaluronan benzyl ester thread is produced by phase separation extrusion technology, then cut, carded and needle-punched. For instance, Tonello et al. [34] studied the co-culturing of fibroblast and endothelial cells into a hyaluronan-based fiber mesh to create microcappillary like structures in a dermal graft. Such structure could benefit the healing of deeper lesions where the tissue vascularization is clearly needed.

Electrospun nanofibrous mats have been also investigated as novel wound dressing material. Nanofiber matrices show high oxygen permeability due to their high surface area (ranging 5-100m<sup>2</sup>/g) which also allows fluid accumulation at the wound site. On the other hand, their pore size is small enough to prevent bacterial penetration and making them a promising candidate for wound dressing. For instance, Katti et al. [36] used electrospinning method to produce antibiotic loaded Poly(lactide-co-glycolide) nanofibrous membranes for wound healing. Collagen-

based electrospun mats were also studied for using in tissue engineering applications including wound healing [37].

### *Vascular Grafts*

Biomedical textiles can find an application in the cardiovascular area namely as vascular grafts. In order to mimic the soft and flexible structure of natural blood vessels, they have been used in woven, knitted, or microporous tubular structures. Early attempts to develop a vascular graft focused on the use of bypass grafts made of nondegradable or degradable synthetic materials. Most used non-biodegradable synthetic polymeric fiber structures for this purpose are Dacron® and Teflon® [38-40]. Later, fiber structures made of biodegradable polymers were applied as a temporary scaffold for the regeneration of blood vessels. The first proposed totally biodegradable vascular graft was Polyglactin 910 knitted mesh (Vicryl® ) in 1979. The woven PGA structures have been also evaluated in a rabbit model, as a vascular graft [41].

After many studies based on directly implantation of biodegradable grafts, tissue engineering approaches have been started to be applied to the cardiovascular system for namely in the development of a blood vessel substitute. For example, Kim et al. [42] studied the use of nonwoven PGA matrices, which were coated with PLLA in order to eliminate stability lack of PGA mesh, to design tissue engineering constructs. The smooth muscle cells (SMCs) seeded onto these matrices has showed high cellular viability and produced high amount of extracellular matrix proteins. Others have attempted to utilize surface hydrolyzed nonwoven PGA scaffolds for culturing smooth muscle cells [43]. In another study, Shum-Tim et al.[44] created a new vascular graft combined of nonwoven PGA mesh and biodegradable polyhydroxyalkanoate (PHA) as a inner and outer layer, respectively. After one week of culturing a mixed cell population of endothelial cells, smooth muscle cells and fibroblasts in these tubular structures, the final construct have been implanted into a lamb. It has been observed that these tissue engineered constructs could resemble the native aorta and be used as vascular substitutes. In a later study , tubular scaffolds have been designed from nonwoven PGA fabrics which were coated with a poly(L-lactide-co-caprolactone) (50/50) porous membrane. The autografts made of these scaffolds and mixed cells have shown no occlusion or

aneurismal formation when they were implanted in dogs. Moreover, a line of endothelial cells has been observed at the luminal surface of each autograft. More recently, these scaffolds with bone marrow cells have been successfully implanted into patients [45].

In order to mimic natural structure of blood vessels, Xu et al. [46] suggested the use of aligned nanofibrous poly(L-lactide-co- $\epsilon$ -caprolactone) scaffolds produced by electrospinning, and proposed these systems to use for blood vessel engineering. They have reported that nanofibers could provide aligned attachment migration of smooth muscle cells along the axis of nanofibers. In addition, it has been also found that distribution and organization of smooth muscle cytoskeleton proteins inside SMCs were parallel to the direction of the nanofibers.

#### *Prosthetic heart valves*

The other application of biodegradable polymeric fibers in the cardiovascular field is on the tissue engineered of heart valves. The clinically used prosthetic heart valves include xenograft valve, mechanical valve and homograft valve. But there are limitations as to the long term benefits of these valve prostheses such as poor durability, foreign body reaction, infection, anticoagulation problem or donor scarcity. Recently, many studies have been undertaken to determine if tissue engineering principles could be used to develop valve tissue substitutes. Seeding of human fibroblasts, endothelial cells or marrow stromal cells on biodegradable fiber mesh is a new approach for the creation of human autologous tissue engineered heart valves. Polyglycolide (PGA) non-woven scaffolds are the most widely used materials for this purpose [47-49]. In order to improve cell attachment and proliferation, PGA and PLA non-woven fiber mesh structures have been coated with poly-4-hydroxybutyrate and their performance have been tested under dynamical conditions [50].

#### *Stents*

Biodegradable fiber structures have also been proposed for using as a stent [51-54]. A stent is a expandable mesh tube which mechanically supports vessels against elastic recoil and reduces the restenosis rate in percutaneous coronary interventions [52]. Biodegradable stents are only used when a temporary airway stenting is

needed. For instance, Paclitaxel loaded melt extruded poly-L-lactide fibers have been tried as a temporary stent [52]. Furthermore, Saito et al. [54] studied a biodegradable knitted stent made by poly-L-lactide in rabbit airways. The results have showed that the knitted tubular PLLA stents could be used like commercially available silicone stents. Nuutinen et al. [51] developed a biodegradable stent from PLLA fibers using a braiding technique. These stents showed the similar radial pressure stiffness as compared to commercial metallic stents. They have also studied the mechanical properties and in vitro degradation of biodegradable knitted stents made of polylactide, poly(L-lactide-co-DL-lactide) and pol(L-lactide-co-glycolide) fibers [53]. It has been shown that different chemical composition of these fiber structures provided for different degradation rates which can be tailored for specific applications.

### *Nerve Tissue Regeneration*

The nervous system is a complex, sophisticated system that regulates and coordinates body activities. It has two major divisions: central nervous system (CNS) and peripheral nervous system (PNS). The central nervous system consists of the brain and the spinal cord, while the peripheral nervous involves all the nerves that branch off from the spinal cord to the extremities. Neurons in central nervous system have different characteristics and cannot regenerate by themselves. Therefore, restoring their function is a major challenge in neurology. Recently, engineering of neural tissue by means of using scaffolds with or without cells become an alternative to traditional transplantation methods. For example, Yang et al.[15] developed highly porous and fibrous PLLA scaffolds prepared by liquid-liquid phase separation methods to be used on nerve tissue engineering. These nanofibrous scaffolds showed an ability to support nerve stem cell differentiation and neurite outgrowth.

In peripheral nervous system, injuries generally affect axons and can be regenerated by a variety of methods, depending on how far the stumps are apart from each other. To avoid the problems of the autografts and allografts, artificial nerve guidance channels have been developed. A nerve guide can be defined as a conduit that bridges the gap between the nerve stumps and directs and supports nerve regeneration. Most of nerve guides reported in literature have a rigid solid structure. Recently, nerve guides based on biodegradable fibers have been studied.



For instance, Bini et al. [55] fabricated a nerve guide from microbraided poly(L-lactide-co-glycolide) fibers, which allowed for a good nutrient transfer due to its microbraided structure. They observed a successful regeneration in rats after one month of implantation. Later, they used the same approach to produce microbraided chitosan conduits [56]. However, chitosan based conduits did not show the same success as poly(L-lactide-co-glycolide) conduits due to the swelling characteristic of chitosan. A nerve guide from poly(L-lactide-co-glycolide) was also fabricated by using an electrospinning method [57].

A nerve guide made of collagen filaments has been proposed as an alternative to the tube type nerve conduits [58]. The collagen conduits consisting of two thousand collagen filaments showed better regeneration than the collagen tubes (as a control) in regeneration of rat static nerve. In another study, synthetic biodegradable fibers made of poly-L-lactide have been examined using dorsal root ganglia in vitro [59]. PLLA filaments oriented the growth of Schwann cells and neuritis along the longitudinal axis of the filament. In addition, it has been observed better neurite growth when the filaments were coated with laminin [59]. Steuer et al. [60] also studied in vitro axonal outgrowth using polylactide filaments coated with rat Schwann cells. They demonstrated that axonal outgrowth on polylactide sheets coated with Schwann cells (+SC) was 15-fold better than that on sheets without Schwann cells (-SC).

As another engineering approach, Cheng et al. [61] have also reported a successful axonal regeneration in rats as a result of implantation of a construct consisting of Schwann cells seeded on polyglactin 910 fiber scaffolds and biomembrane.

### **3.2. Hard Tissue Engineering**

#### *Articular Cartilage*

Articular cartilage of the knee is a highly specialized connective tissue responsible for cushioning and lubricating. It is an avascular, aneural, alymphatic tissue and contains only one cell type, chondrocytes. Due to this avascular and low cellular nature, self-healing capacity of articular cartilage is very limited. Various techniques for repairing cartilage defects have been developed, including abrasion [62], drilling [63], microfracture [64], osteochondral grafting [65] and transplantation of tissue

engineering constructs [66-68]. Many different types of polymeric matrices with/without cells have been tested in vitro, as well as in experimental animals, and in human patients for their ability to promote articular cartilage repair. Recent trends are toward to use of fiber based structures for engineering of articular cartilage. Most used biodegradable fiber structures are made by poly- $\alpha$ -hydroxy acids and hyaluronic acid. In embryonic tissue, hyaluronan is the main component of extracellular matrix and plays an important role in chondrogenic condensation during limb formation [69]. It has been shown that HA can affect the differentiation of chondrocytes [70]. However, HA can not form easily without any modification and usually can be modified by means of esterification. As it was previously described, Hyaff® is a derivative of HA and is being investigated as a scaffold for articular cartilage repair. For example, Brun et al. [71] have compared Hyaff® 7 and Hyaff® 11 nonwoven meshes which have the same fiber thickness, 20 $\mu$ m, but different in vitro and in vivo degradation rates. Chicken embryo chondrocytes seeded in both structures maintained their phenotype and secrete ECM for up to 3 weeks of in vitro culture. On the other hand, Hyaff®11 nonwoven scaffolds with a slower degradation rate promoted a higher cell proliferation rate. They latter reported on the use of Hyaff® 11 non-woven scaffolds as a support for mesenchymal progenitor cells which produced the main extracellular matrix molecules, accompanied by an occasional synthesis of mature type II collagen [72]. Moreover, when those structures were implanted in the rabbit knees, with or without cells, there was no inflammatory response and they degraded within 4 months after implantation. Other studies with human chondrocytes and mesenchymal stromal cells also confirmed that Hyaff® 11 nonwoven meshes could promote the growth and differentiation of chondrocyte and production of collagen type II, aggrecan and downregulate the production of collagen type I [73-75].

Poly- $\alpha$ -hydroxy acid based fibrous matrices have been widely investigated to serve as cartilage grafts. For instance, Freed et al. [76-79] have performed several studies where they used PGA fiber meshes and freshly isolated chondrocytes to investigate the influence of scaffold properties as well as seeding and culture methods on the development of cartilage constructions. Ma et al. [80] have also investigated ways to engineer the cartilage tissue by seeding articular chondrocytes onto polyglycolic acid non-woven scaffolds. They reported that after the aggregate

modulus of the engineered cartilage reached 179±9 kPa after 20 weeks of in vitro cultivation, which was 40% that of natural articular cartilage.

In order to provide the ability of the cells to suspend and making it possible to distribute cells within the polymeric mesh, synthetic non woven mesh structures have been combined with some natural derived materials such as alginate, collagen, and fibrin. Using this approach, Ameer et al. [81] have prepared a composite, which was composed by a polyglycolide non-woven mesh coated by fibrin gel, for use them in meniscal surgery. At 4 weeks in culture, glycosaminoglycan (GAG) content in fibrin coated PGA mesh scaffolds has been found to be better than the uncoated PGA mesh scaffolds. In another similar study, PLGA meshes with two different compositions which are slower resorbing 47.5/52.5 PGA-PLA and faster resorbing 90/10 PGA-PLA have been combined with chondrocyte suspended alginate gel and tested in vitro and in vivo. Both types of coated copolymer pads have shown uniform cell distribution and same performance regarding expression of aggrecan, type I collagen and type II collagen [82]. However, the construct consisting of 47.5/52.5 PGA-PLA, alginate and chondrocytes have exhibit a better performance when they have been implanted to osteochondral defects of rabbits. It has been also shown that alginate stimulates the chondrogenic phenotype of the transplanted chondrocytes and prevents cells from floating out of the defects. Other researchers have used type I collagen for chondrocyte encapsulation and tried to combine this gel with a nonwoven polylactide (PLLA) scaffolds [83]. This method allowed for encapsulating a high number of chondrocytes into the scaffolds, quite homogeneously.

More recently, collagen type I has been also used to create a web-like structures within the PLGA knitted meshes in order in order to achieve a uniform cell distribution [84]. The bovine chondrocytes seeded on these scaffolds have shown a homogenous distribution, maintained their phenotype and regenerated cartilaginous matrix filling the void spaces in the scaffolds. To obtain thicker scaffolds, the cell/composite constructs have been laminated or rolled after 1 day of culture and implanted subcutaneously in the dorsum of athymic nude mice. In vivo results have demonstrated the formation of articular cartilage after 12 weeks of implantation. These new approaches have promised to generate structurally regular cartilage.

The use of bioreactors is a great challenge to obtain a homogenous scaffold/cell construct for cartilage and bone regeneration. Such systems can provide a good nutrient transfer throughout the porosity of the scaffolds which results

in a better cell migration and production of extracellular matrix at interior part of the scaffolds. These systems have been successfully applied for creating a tissue engineered cartilage construct by using fiber based scaffolds. Davisson et al. [85] have been reported the positive effect of perfusion on cell content and extracellular matrix production of bovine articular cartilage cultured polyglycolic acid scaffolds. The synthesis of sulphated glycosaminoglycan has been found to be 40% higher when compared with static conditions. Griffon et al. [86] compared two different dynamic culturing techniques for culturing porcine chondrocytes on a scaffold composed of polyglycolic acid mesh or chitosan sponge. A better and uniform cell attachment has been found where PGA scaffolds used in the vacuum-reactor system.

Finally, within the last few years, biodegradable non-woven nanofibers, which are produced by electrospinning, have been started to be used as scaffolds for regeneration of cartilage. 3D matrix made of polycaprolactone nanofibers with diameter of 700 nm have been proposed as a scaffold for cartilage tissue engineering [87]. The primary chondrocytes that were seeded onto these scaffolds proliferated and efficiently maintained their differentiated phenotype, as indicated by the expression of cartilage-associated genes. In a latter study [88], the same authors demonstrated that PCL nanofibrous scaffolds could significantly enhanced the chondrogenic differentiation of human mesenchymal stem cells (MSC) compared to the cell pellet culture system, which is a widely used culture protocol for studying chondrogenesis of MSC. Collagen based nanofibrous scaffolds have been also purposed for cartilage tissue engineering. It is well known that collagen is a naturally occurring polymer and one of the major components of extracellular matrix of animal tissues. It is found in ECM as fibrillar form with a diameter of 50-300nm. It has been shown that collagen type II could be electrospun in a nonwoven mats with a fiber diameter between 110nm-1.8 $\mu$ m and use as a scaffold for chondrocyte seeding [89].

### *Bone*

Bone is a complex, dynamic and highly vascular tissue with a large amount of extracellular matrix and limited cell population. As in all tissue engineering fields, many researches [90-94] have been carried out to recreate complexity, stability, and biologic function of bone tissue. The most common strategy for engineering of bone

is to use a scaffold combined with osteoblast or the cells that can mature/differentiate into osteoblasts and regulating factors that promote cell attachment, differentiation and mineralized bone formation [95]. The requirements for the design and production of an ideal scaffold for bone regeneration are very complex and not yet fully understood. It is generally agreed that it must be a biocompatible, porous (more than 90% and pore sizes between 100-350 $\mu$ m), interconnected, and permeable structure to in order permit the ingress of cells and nutrients. Clearly, the structures designed with biodegradable fibers can meet all these criteria and serve as a scaffold for the engineering of bone. Many different fiber-based polymeric matrices have been tested with different cell types to create a bone construct. For instance, bone marrow cells seeded in a nonwoven HA polymeric scaffold (Hyaff 11) in a mineralizing medium, and basic fibroblast growth factor (bFGF) have shown mineralization through the expression of the markers Ca, alkaline phosphatase, osteopontin, bone sialoprotein and collagen I [96, 97]. Recently, Mikos and co-workers [90, 98] have been reported a study where they used biodegradable fiber mesh scaffolds to create bone substitutes in dynamic culture conditions. In this study, rat bone marrow cells were seeded onto nonwoven poly(L-lactic acid) scaffolds which was with a thickness of 1.7mm, a volumetric porosity of 99% and a fiber diameter of 17mm [90]. These constructs have been cultured either in a flow perfusion bioreactor or under static conditions. It has been found that nonwoven PLLA scaffolds could support the attachment, growth and differentiation of rat bone marrow cells. Moreover, it has been reported that flow perfusion could accelerate calcified matrix deposition and provide a homogenous cell distribution though the interior part of the scaffold. Gomes, Reis et al. [98] used the same approach to culture rat bone marrow cells in starch-based fiber mesh scaffolds. They have observed an increased osteogenic differentiation of bone marrow stromal cells when they culture on starch-based fiber mesh scaffolds under dynamic conditions. They also reported that fiber-based structures were more advantageous than extruded porous structures due to their highly interconnected structure which provides a homogenous tissue formation.

Also in our group, we developed chitosan based non-woven structures as bone tissue engineering scaffolds, using a traditional wet spinning technique [99].

We demonstrated that chitosan non-woven scaffolds had an ability to support osteoblast cell attachment.

As a new trend in the tissue engineering field, nanofibrous scaffolds produced by electrospinning process have been also suggested for bone tissue engineering. For example, non-woven polycaprolactone nanofibrous scaffolds have been tested with mesenchymal stem cells derived from the bone marrow of neonatal rats under dynamic culture conditions [16]. After 4 weeks of culture, it has been found that at least the surfaces of the cell-polymer constructs were covered with cell multilayers. Additionally, it has been shown that these structures could support mineralization and production of type I collagen under dynamic culture conditions. However, colonization by cells of 3D electrospun scaffolds is a major problem due to the pore size of the scaffolds which is typically less than average cell size. Li et al. [100] have presented the next step in such nanofibrous PCL scaffolds by culturing human mesenchymal stem cells that can differentiate adipogenic, chondrogenic, and osteogenic lineage in the same matrix. This very promising result underscores the potential of using both stem cell and nanofibers in bone tissue engineering. More recently, Jin et al [101] used the electrospinning technique to produce nanofibrous fiber mats with average fiber diameter  $700\pm 50\text{nm}$  from silk fibroin with PEO. In vitro culture studies with human bone marrow stromal cells have shown that these matrices, especially after PEO extraction, could support initial cell attachment and ingrowth.

Tuzlakoglu, Reis et al. [102] have suggested a new approach to design a structure which combines polymeric micro and nanofibers in the same construct. This novel structure is aimed to serve as a scaffold and mimic the physical structure of ECM for bone tissue regeneration, but simultaneously still providing the macro support that cells do require. Nano and micro fiber combined scaffolds have been originally produced from starch based biomaterials by means of a fiber bonding and a electrospinning, two step methodology. The cell culture studies with SaOs-2 human osteoblast-like cell line and rat bone marrow stromal cells demonstrated that presence of nanofibers influenced cell shape and cytoskeletal organization of the cells on the nano/micro combined scaffolds as well as cell viability and ALP activity.

Besides the use of polymeric fiber structures as a scaffold, they also find an application for a special kind of bone regeneration in dentistry, as a membrane for guided tissue regeneration (GTR). These barrier membranes prevent epithelial

migration and promote the regeneration of new connective tissue attachment. Vicryl® periodontal mesh and Gore Resolut® (composed by polyglycolide fiber and trimethylene carbonate) are successfully used for this application [103, 104]. A PLA coated knitted PGA mesh was developed and suggested for using as a barrier membrane in GTR [105]. Another GTR membrane composed of polycaprolactone and calcium carbonate has been developed by Fujihara et al. [106], using again a electrospinning process.

### *Anterior Cruciate Ligament*

Ligaments are bands or sheets of fibrous connective tissue between two or more bones, being responsible for providing the motion and stability of joints and transmitting the tensile loads in the musculoskeletal system. Ligaments are mainly consisting of collagen fibers which are formed into large bundles with specific orientation. The anterior cruciate ligament (ACL) connects the femur to the tibia and acts as a primary stabilizer of the knee motion. A rupture of the ACL can not heal and a surgically reconstruction is required to restore normal joint function. Tissue engineering offers a potential technique to design ligament replacement grafts by using a biodegradable scaffold with/without cells. An ideal scaffold for ACL must provide a high degree of mechanical strength initially and loose its strength by gradually degradation while a new tissue is remodelling. Due to the natural structure of ACL, collagen-based fiber scaffolds are widely used for ACL replacement [107, 108]. The mechanical strength and the control of degradation rate of collagen scaffolds could be improved by crosslinking for instance with UV or carbodiimide (EDC) [108]. However, it has been shown that both crosslinking methods had different advantages on with regards to the final mechanical strength and the correspondent cell attachment. Silk is another natural polymer that has been proposed for tissue engineering of anterior cruciate ligaments[109]. When they are properly prepared, silk fiber matrices, which have good mechanical properties as well as biocompatibility and slow degradation, can serve as a suitable matrices to support adult stem cell differentiation toward ligament lineages. Hyaluronic acid based fibers are another natural origin alternative for ACL replacement. Cristino et al. [110] have designed a prototype scaffold with a multilayered knitted cylindrical array of Hyaff 11 fibers oriented in two directions. They indicated that mesenchymal

stem cells grown on these scaffolds could express collagen type I, type III, laminin, fibronectin, and actin which are the characteristic markers for the ligament tissue.

Alternative biodegradable materials in anterior cruciate ligament reconstructions are the synthetic polymers, namely polydioxanone, polylactide, polyglycolide and their copolymers. These materials have been purposed either as an implant for using directly or a scaffold for creating three-dimensional tissue engineering constructs. Based on the first approach, commercially available polydioxanone (PDS®) has been suggested for ACL replacement [111]. However, this material shows very fast degradation that can be a problem for this application. It has been reported that PDS loose the half of its tensile strength in about 4-6 weeks, whereas the process for replacements can take up to 12 months [112]. A similar problem has occurred when braided polyglycolide (Dexon®) ligaments were used for the replacement. For example, Cabaud et al. [113] used braided polyglycolide (Dexon®) ligaments, which showed 828N max. linear load at 22.6% strain, for the repair of ACL of dogs. Although they showed high initial strength, degradation time was not long enough to protect the repaired ligament. In a later study, Laitinen et al. [114] tested the mechanical properties of braided poly(L-lactide) implants in vitro and after subcutaneous implantation in rabbits. These implants have shown a better mechanical strength and slower degradation rate than PDS and PGA that would be advantageous for reconstruction of ACL. Within the last few years, biodegradable synthetic fibers have been formed into 3-D scaffolds for engineering of ACL. Cooper et al. have developed a new braiding procedure to create 3-D scaffolds with a desired pore diameter, porosity, mechanical properties and geometry from different polyesters, namely PLLA, PGA and PLAGA [115, 116]. Although PGA scaffolds have showed a highest tensile strength, they have supported lowest level of ACL cell attachment and growth compared to PLAGA and PLA due to their fast degradation time and released degradation product during cell culture. On the other hand, fibronectin coated PLLA scaffold have provide for a better cell viability than PGA and PLAGA and maintained their structural integrity and high mechanical properties over culturing period [115]. These results confirm that tissue engineering of ACL using fiber based scaffolds and ACL cells is a promising approach for ACL reconstruction.



#### **4. Conclusions and Future Aspects**

Tissue engineering is a relatively new approach that purposes the regeneration of tissues by using stem/progenitor cells and scaffolds or artificial extracellular matrices. The design of an ideal scaffold still remains as a problem in most of the tissue engineering fields. Although it is specific for each tissue, it is generally agreed that biocompatibility, biodegradability, porosity and interconnectivity, as well as surface properties are main requirements for an ideal scaffold. Fiber-based architectures described in this review seem to be quite promising scaffolds in many different tissue engineering applications due to their highly porous and interconnected pore structures as well as mechanical strength and structural integrity, combined with a large surface area. However, there are still many issues to be addressed, including the choice of a proper material, the combination and diameter of fibers (distinct for different applications and cell sources), and scaffold geometry for each specific application.

## References

1. King, M.W., Designing fabrics for blood vessel replacement. *Canadian Textile Journal*, 1991. 108: p. 24-30.
2. Fambri, L., Bragagna, S., and Migliaresi, C., Biodegradable fibers of poly-L,DL-lactide 70/30 produced by melt spinning. *Macromol. Symp.*, 2006. 234: p. 20-25.
3. Ellis, M.J. and Chaudhuri, J.B., Poly(lactic-co-glycolic acid) hollow fibre membranes for use as a tissue engineering scaffold. *Biotechnol. and Bioeng.*, 2007. 96: p. 177-187.
4. SolarSKI, S., Ferreira, M., and Devaux, E., Thermal and mechanical characteristics of polylactide filaments drawn at different temperatures. *J. Textile Institute*, 2007. 98(3).
5. Knaul, J., et al., Improvements in the drying process for wet-spun chitosan fibers. *J. Appl. Polymer Sci.*, 1998. 69: p. 1435-1444.
6. Sell, S., et al., Extracellular matrix regenerated: Tissue engineering via electrospun biomimetic nanofibers. *Polymer International*, 2007. 56: p. 1349-1360.
7. Kim, S.-H., et al., Fabrication of a new tubular fibrous PLCL scaffold for vascular tissue engineering. *J. Biomater. Sci.: Polym. Ed.*, 2006. 17: p. 1359-1374.
8. Ashammakhi, N., et al., Biodegradable nanomats produced by electrospinning: expanding multifunctionality and potential for tissue engineering. *J. Nanosci. and Nanotech.*, 2007. 7: p. 862-882.
9. Matthews, J.A., et al., Electrospinning of collagen nanofibers. *Biomacromolecules*, 2002. 3: p. 232-238.
10. Ohkawa, K., Cha, D., Kim, H., Nishida, A., Yamamoto, H., Electrospinning of chitosan. *Macromol. Rapid Commun.*, 2004. 25: p. 1600-1605.
11. Min, B.M., et al., Chitin and chitosan nanofibers: electrospinning of chitin and deacetylation of chitin nanofibers. *Polymer*, 2004. 45: p. 7137.
12. Jin, H.J., et al., Electrospinning of bombyx mori silk with poly(ethylene oxide). *Biomacromolecules*, 2002. 3: p. 1233-1239.
13. Um, I.C., et al., Electro-spinning and electro-blowing of hyaluronic acid. *Biomacromol.*, 2004. 5: p. 1428-1436.

14. Li, W., et al., Electrospun nanofibrous structure:a novel scaffold for tissue engineering. *J. Biomed. Mater. Res.*, 2002. 60: p. 613-621.
15. Yang, F., et al., Fabrication of nano-structured porous PLLA scaffold intended for nerve tissue engineering. *Biomaterials*, 2004. 25: p. 1891-1900.
16. Yoshimoto, H., et al., A biodegradable nanofiber scaffold by electrospinning and its potential for bone tissue engineering. *Biomaterials*, 2003. 24: p. 2077-2082.
17. Bourne, R.B., et al., In-vivo comprasion for four absorable sutures:Vicryl, Dexon Plus, Maxon and PDS. *Can. J. Surg.*, 1988. 31: p. 43-45.
18. Hong, J.-T., et al., Biodegradable studies of poly(trimethylenecarbonate-ε-caprolactone)- block-poly(p-dioxanone), poly(dioxanone), and poly(glycolide-ε-caprolactone) (monocryl®) monofilaments. *J. Appl. Polymer Sci.*, 2006. 102: p. 737-743.
19. Mikos, A.G. and Temenoff, J.S., Formation of highly porous biodegradable scaffolds for tissue engineering. *Electronic J. Biotechol.*, 2000. 3: p. 114-119.
20. Gomes, M.E., Malafaya, P.B., and Reis, R.L., Fiber Bonding and Particle Aggregation as Promissing Methodologies For The Fabrication Of Biodegradable Scaffolds For Hard-Tissue Engineering, in *Biodegradable Systems for Tissue in Engineering and Regenerative Medicine*, R.L.R.a.J.S. Roman, Editor. 2004, CRC Press: Boca Raton. p. 53-65.
21. Ikada, Y., Challenges in Tissue Engineering. *J. R. Soc. Interface*, 2006. 3: p. 589-601.
22. Gibbs, S., et al., Autologous full-thickness skin substitute for healing chronic wounds. *British J. of Dermatology*, 2006. 155: p. 267-274.
23. Cuono, C., Langdon, R., and Mcguire, J., Use of cultured epidermal autografts and dermal allografts as skin replacement after burn injury. *Lancet*, 1986. 1: p. 1123-1124.
24. Leigh, I.M., et al., Treatment of chronic venous ulcers with sheets of cultured allogenic keratinocytes. 1987. 117: p. 591-597.
25. Schulz, J.T., Tompkins, R.G., and Burke, J.F., Artificial skin. *Annu. Rev. Med.*, 2000. 51: p. 231-244.
26. Bello, Y.M., Falabella, A.F., and Eaglstein, W.H., Tissue-engineered skin: Current status in wound healing. 2001. 2: p. 305-313.

27. Kirsner, S.K., Falanga, V., and Eaglstein, W.H., The development of bioengineered skin. *Trends in Biotech.*, 1998. 16: p. 246-249.
28. Edmons, M.E., Foster, A.V., and Mccolgan, M., "Dermagraft": a new treatment for diabetic foot ulcers. *Diabet. Med.*, 1997. 14: p. 1010-1011.
29. Zacchi, V., et al., In vitro tissue engineering of human skin-like tissue. *J. Biomed. Mater. Res.*, 1998. 40: p. 187-194.
30. Chen, G., et al., Culturing of skin fibroblasts in a thin PLGA-collagen hybrid mesh. *Biomaterials*, 2005. 26: p. 2559-2566.
31. Mirafteb, M., et al., Fibers for wound dressing based on mixed carbohydrate polymer fibres. *Carbohydrate Polym.*, 2003. 53: p. 225-231.
32. Hirano, S., Zhang, M., and Nakagawa, M., Release of glycosaminoglycans in physiological saline and water by wet-spun chitin acid glycosaminoglycan fibers. *J. Biomed. Mater. Res.*, 2001. 56: p. 556-561.
33. Gallasi, G., et al., In vitro reconstructed dermis implanted in human wounds: degradation studies of the HA-based supporting scaffold. *Biomaterials*, 2000. 21: p. 2183-2191.
34. Tonello, C., et al., In vitro reconstruction of human dermal equivalent enriched with endothelial cells. *Biomaterials*, 2003. 24: p. 1205-1211.
35. Caravaggi, C., et al., HYAFF 11-based autologous dermal and epidermal grafts in the treatment of noninfected diabetic plantar and dorsal foot ulcers: a prospective, multicenter, controlled, randomized clinical trial. *Diabetes Care*, 2003. 26: p. 2853-2859.
36. Katti, D.A., et al., Bioresorbable nanofiber-based systems for wound healing and drug delivery: optimization of fabrication parameters. *J. Biomed. Mater. Res. Part B: Appl. Biomater.*, 2004. 70B: p. 286-296.
37. Huang, L., et al., Engineered collagen-PEO nanofibers and fabrics. *J. Biomater. Sci.: Polym. Ed.*, 2001. 12: p. 979-995.
38. Sipehia, R., et al., Enhanced attachment and growth of human endothelial cells derived from umbilical veins on ammonia plasma modified surfaces of PTFE and ePTFE synthetic vascular graft biomaterials. *Biomater. Artif. Cells Immobil. Biotechnol.*, 1993. 21: p. 465-468.
39. Vohra, R.K., et al., Fibronectin coating of expanded polytetrafluoroethylene (ePTFE) grafts and its role in endothelial seeding. *Artif. Org.*, 1990. 14: p. 41-45.

40. Schmidt, S.P., et al., Endothelial cell-seeded four-milimeter Dacron vascular grafts: effects of blood flow manipulation through the grafts. *J. Vasc. Surg.*, 1984. 1: p. 434-441.
41. Greisler, H.P., et al., Arterial regenerative activity after prosthetic implantation. *Arch. Surg.*, 1985. 120: p. 315-323.
42. Kim, B. and Mooney, D.J., Engineering smooth muscle tissue with a predefined structure. *J. Biomed. Mater. Res.*, 1998. 41: p. 322-332.
43. Gao, J., Niklason, L., and Langer, R., Surface hydrolysis of poly(glycolic acid) meshes increases the seeding density of vascular smooth muscle cells. *J. Biomed. Mater. Res.*, 1998. 42: p. 417-424.
44. Shum-Tim, D., et al., Tissue engineering of autologous aorta using a new biodegradable polymer. *Ann. Thorac. Surg.*, 1999. 68: p. 2298-2035.
45. Matsumura, G., et al., Successful application of tissue engineered vascular autografts: clinical experience. *Biomaterials*, 2003. 24: p. 2303-2308.
46. Xu, C.Y., et al., Aligned biodegradable nanofibrous structure: a potential for blood vessel engineering. *Biomaterials*, 2004. 25: p. 877-886.
47. Zund, G., et al., Tissue engineering: A new approach in cardiovascular surgery; seeding of human fibroblasts followed by endothelial cells on resorbable mesh. *Eur. J. Cardiothorac. Surg.*, 1998. 13: p. 160-164.
48. Zund, G., et al., The in vivo construction of a tissue engineered bioprosthetic heart valve. *Eur. J. Cardiothorac. Surg.*, 1997. 11: p. 493-497.
49. Hoerstrup, S.P., et al., Tissue engineering of functional trileaflet heart valves from human marrow stromal cells. *Circulation*, 2002. 106: p. 1143-1149.
50. Engelmayer, G.C., et al., A novel bioreactor for the dynamic flexural stimulation of tissue engineered heart valve biomaterials. *Biomaterials*, 2003. 24: p. 2523-2532.
51. Nuutinen, J.P., et al., Mechanical properties and in vitro degradation of bioabsorbable self-expanding braided stents. *J. Biomater. Sci.: Polym. Ed.*, 2003. 14: p. 255-266.
52. Nguyen, K.T., et al., In vitro hemocompatibility studies of drug-loaded poly-(L-lactic acid) fibers. *Biomaterials*, 2003. 24: p. 5191-5201.
53. Nuutinen, J.P., et al., Mechanical properties and in vitro degradation of bioresorbable knitted stents. *J. Biomater. Sci.: Polym. Ed.*, 2002. 13: p. 1313-1323.

54. Saito, Y., et al., New tubular bioabsorbable knitted airway stent: biocompatibility and mechanical strength. *J. Thorac. Cardiovasc. Surg.*, 2002. 123: p. 161-167.
55. Bini, T.B., et al., Peripheral nerve regeneration by microbraided poly(L-lactide-co-glycolide) biodegradable polymer fibers. *J. Biomed. Mater. Res. PartA*, 2004. 68: p. 286-295.
56. Bini, T.B., et al., Development of fibrous biodegradable polymer conduits for guided nerve regeneration. *J. Mater. Sci.: Mater. Medic.*, 2005. 16: p. 367-375.
57. Bini, T.B., et al., Electrospun poly(L-lactide-co-glycolide) biodegradable polymer nanofibre tubes for peripheral nerve regeneration. *Nanotech.*, 2004. 15: p. 1459-1464.
58. Yoshii, S. and Oka, M., Peripheral nerve regeneration along collagen filament. *Brain Res.*, 2001. 2001: p. 158-162.
59. Rangappa, N., et al., Laminin-coated poly(L-lactide) filaments induce robust neurite growth while providing directional orientation. *J. Biomed. Mater. Res.*, 2000. 15: p. 625-630.
60. Steuer, H., et al., Biohybrid nerve guide for regeneration: degradable polylactide fibers coated with rat Schwann cells. *Neurosci. Lett.*, 1999. 277: p. 165-168.
61. Cheng, B. and Chen, Z., Fabrication autologous tissue to engineering artificial nerve. *2002*, 2002. 22: p. 133-137.
62. Friedman, M.J., Berasi, C.C., and Fox, J.M., Preliminary results with abrasion arthroplasty in the osteoarthritic knee. *Clin. Orthop.*, 1984. 4: p. 200-2005.
63. Dzioba, R.B., The classification and treatment of acute articular cartilage lesions. *Arthroscopy*, 1988. 4: p. 72-80.
64. Blevins, F.T., Steadman, J.R., and Rodrigo, J.J., Treatment of articular cartilage defects in athletes: an analysis of functional outcome and lesion appearance. *Orthopedics*, 1998. 21: p. 761-768.
65. Bobic, V., Autologous osteo-chondral grafts in the management of articular cartilage lesions. *Orthopedics*, 1999. 28: p. 19-25.
66. Vacanti, C.A., et al., Synthetic polymers seeded with chondrocytes provide a template for new cartilage formation. *Plast. Reconstr. Surg.*, 1991. 88: p. 753-759.

67. Zwingmann, J., et al., Chondrogenic differentiation of human articular chondrocytes differs in biodegradable PGA/PLA scaffolds. *Tissue Eng.*, 2007. 13: p. 2335-2343.
68. Banu, N., et al., Biodegradable polymers in chondrogenesis of human articular chondrocytes. 2005. 8: p. 184-191.
69. Solchaga, L.A., et al., Repair of osteochondral defects with hyaluronan- and polyester-based scaffolds. *Osteoarthritis Cartilage*, 2005. 13: p. 297-309.
70. Cortivo, R., et al., Hyaluronic acid promotes chick embryo fibroblast and chondroblast expression. *Cell. Biol. Int. Rep.*, 1990. 14: p. 111-112.
71. Brun, P., et al., Chondrocyte aggregation and reorganization into three-dimensional scaffolds. *J. Biomed. Mater. Res.*, 1999. 46: p. 337-346.
72. Radice, M., et al., Hyaluronan-based biopolymers as delivery vehicles for bone-marrow-derived mesenchymal progenitors. *J. Biomed. Mater. Res.*, 2000. 50: p. 101-109.
73. Grigolo, B., et al., Evidence for redifferentiation of human chondrocytes grown on a hyaluronan-based biomaterial (HYAFF 11): molecular, immunohistochemical and ultrastructural analysis. *Biomaterials*, 2002. 23: p. 1187-1195.
74. Lisignolli, G., et al., Cellular and molecular events during chondrogenesis of human mesenchymal stromal cells grown in a three-dimensional hyaluronan based scaffold. *Biomaterials*, 2005. 26: p. 5677-5686.
75. Aigner, J., et al., Cartilage tissue engineering with novel nonwoven structures biomaterial based on hyaluronic acid benzyl ester. *J. Biomed. Mater. Res.*, 1998. 42: p. 172-181.
76. Blunk, T., et al., Differential effects of growth factors on tissue engineered cartilage. *Tissue Eng.*, 2002. 8: p. 73-84.
77. Freed, L.E., et al., Tissue engineering of cartilage in space. *Proc. Natl. Acad. Sci. USA* 94, 1997. 94: p. 13885-1389.
78. Vunjak-Novakovic, G., et al., Bioreactor cultivation conditions modulate the composition and mechanical properties of tissue-engineered cartilage. *J. Orthop. Res.*, 1999. 17: p. 130-138.
79. Obradovic, B., et al., Integration of engineered cartilage. *J. Orthop. Res.*, 2001. 19: p. 1089-1097.

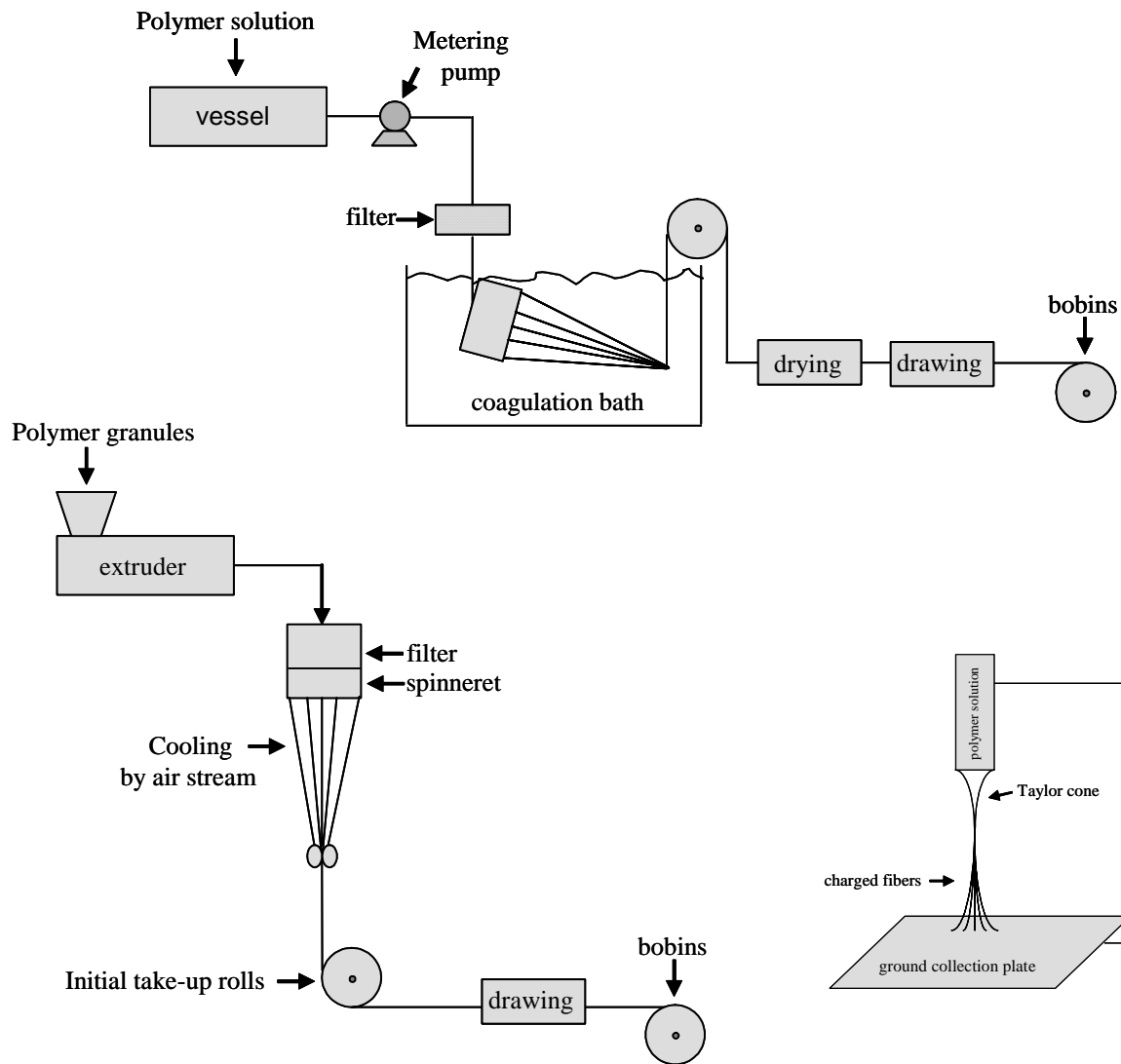
80. Ma, P.X., et al., Development of biomechanical properties and morphogenesis of in vitro tissue engineered cartilage. *J. Biomed. Mater. Res.*, 1995. 29: p. 1587-1595.
81. Ameer, G.A., Mahmood, T.A., and Langer, R.A., A biodegradable composite scaffold for cell transplantation. *J. Orthop. Res.*, 2002. 20: p. 16-19.
82. Cohen, S.B., et al., The use of absorbable co-polymer pads with alginate and cells for articular cartilage repair in rabbits. *Biomaterials*, 2003. 24: p. 2653-2660.
83. Ushida, T., et al., Three-dimensional seeding of chondrocytes encapsulated in collagen gel into PLLA scaffolds. *Cell Transplantation*, 2002. 11: p. 489-494.
84. Chen, G., et al., The use of a novel PLGA fiber/collagen composite web as a scaffold for engineering of articular cartilage with adjustable thickness. 2003: p. 1170-1180.
85. Davisson, T., Sah, R.L., and Ratcliffe, A., Perfusion increases cell content and matrix synthesis in chondrocyte three-dimensional culture. *Tissue Eng.*, 2002. 8: p. 807-816.
86. Griffon, D.J., et al., Evaluation of vacuum and dynamic cell seeding of polyglycolic acid and chitosan scaffolds for cartilage engineering. *Am. J. of Vet. Res.*, 2005. 66: p. 599-605.
87. Li, W.J., et al., Biological response of chondrocytes cultured in three-dimensional nanofibrous poly( $\epsilon$ -caprolactone) scaffolds. *J. Biomed. Mater. Res.*, 2003. 67A: p. 1105-1114.
88. Li, W.J., et al., A three-dimensional nanofibrous scaffold for cartilage tissue engineering using mesenchymal stem cells. *Biomaterials*, 2005. 26: p. 599-609.
89. Matthews, J.A., et al., Electrospinning of collagen type II: A feasibility study. *J. Bioact. Compat. Polym.*, 2003. 18: p. 125-134.
90. Sikavitsas, V., et al., Flow perfusion enhances the calcified matrix deposition of marrow stromal cells in biodegradable nonwoven fiber mesh scaffolds. *Ann. Biomed. Eng.*, 2005. 33: p. 63-70.
91. Salgado, A.J., et al., In vivo response to starch-based scaffolds designed for bone tissue engineering applications. 2007. 80: p. 983-989.
92. Morgan, S.M., Tilley, S., Perera, S., Ellis, M.J., Kanczler, J., Chaudhuri, J.B., Oreffo, R.O.C., Expansion of human bone marrow stromal cells on poly-(dl-



- lactide-co-glycolide) (PDLLGA) hollow fibres designed for use in skeletal tissue engineering. *Biomaterials*, 2007. 28: p. 5332-5343.
93. Jiang, T., Abdel-Fattah, W.I., and Laurencin, C.T., In vitro evaluation of chitosan/poly(lactic acid-glycolic acid) sintered microsphere scaffolds for bone tissue engineering. *Biomaterials*, 2006. 27: p. 4894-4903.
  94. Tuzlakoglu, K. and L., R.R., Formation of bone-like apatite layer on chitosan fiber mesh scaffolds by a biomimetic spraying process. *J. Mater. Sci.: Mater. Med.*, 2007. 18: p. 1279-1286.
  95. Liu, X. and Ma, P.X., Polymeric scaffolds for bone tissue engineering. *Annal. Biomed. Eng.*, 2004. 32: p. 477-486.
  96. Lisignolim, G., et al., Basic fibroblast growth factor enhances in vitro mineralization of rat bone marrow stromal cells grown on non-woven hyaluronic acid based polymer scaffold. *Biomaterials*, 2001. 22: p. 2095-2105.
  97. Lisignolim, G., et al., Osteogenesis of large segmental radius defects enhanced by basic fibroblast growth factor activated bone marrow stromal cells grown on non-woven hyaluronic acid-based polymer scaffold. 2002, 2003. 23: p. 1043-1051.
  98. Gomes, M.E., et al., Effect of flow perfusion on the osteogenic differentiation of bone marrow stromal cells cultured on starch-based three-dimensional scaffolds. *J. Biomed. Mater. Res. PartA*, 2003. 67A: p. 87-95.
  99. Tuzlakoglu, K., et al., Production and characterization of chitosan fibers and 3-D fiber mesh scaffolds for tissue engineering applications. *Macromol. Biosci.*, 2004. 4: p. 811-819.
  100. Li, W.J., et al., Multilineage differentiation of human mesenchymal stem cell in a three-dimensional nanofibrous scaffold. *Biomaterials*, 2005. 26: p. 5158-5166.
  101. Jin, H.J., et al., Human bone marrow stromal cell responses on electrospun silk fibroin mats. *Biomaterials*, 2004. 25: p. 1039-1047.
  102. Tuzlakoglu, K., et al., Nano- and micro-fiber combined scaffolds: A new architecture for bone tissue engineering. *J. Mater. Sci.: Mater. Med.*, 2005. 16: p. 1099-1104.
  103. Taddei, P., Monti, P., and Simoni, R., Vibrational and thermal study on the in vitro and in vivo degradation of a bioresorbable periodontal membrane: Vicryl periodontal (polyglactin 90). *J. Mater. Sci.: Mater. Med.*, 2002. 13: p. 59-64.

104. Soncini, M., et al., Experimental procedure for the evaluation of the mechanical properties of the surrounding dental implants. *Biomaterials*, 2002. 23: p. 9-17.
105. Park, Y.J., et al., Porous poly(L-lactide) membranes for guided tissue regeneration and controlled drug delivery: membrane fabrication and characterization. *J. Control Rel.*, 1997. 43: p. 151-160.
106. Fujihara, K., Kotaki, M., and Ramakrishna, S., Guided bone regeneration membrane made of polycaprolactone/calcium carbonate composite nano-fibers. *Biomaterials*, 2005. 26: p. 4139-4147.
107. Chvapil, M., et al., Collagen fibers as a temporary scaffold for replacement of ACL in goats. *J. Biomed. Mater. Res.*, 1993. 27: p. 313-325.
108. Caruso, A.B. and Dunn, M.G., Changes in mechanical properties and cellularity during long-term culture of collagen fiber ACL reconstruction scaffolds. *J. Biomed. Mater. Res.*, 2005(73A): p. 388-397.
109. Altman, G.H., et al., Silk matrix for tissue engineered anterior cruciate ligaments. *Biomaterials*, 2002. 23: p. 4131-4141.
110. Cristino, S., et al., Analysis of mesenchymal stem dimensional HYAFF 11 (R)-based cells grown on a prototype ligament scaffold. *J. Biomed. Mater. Res.*, 2005. 73A: p. 275-283.
111. Puddu G, C.M., Cerullo G, Franco V, Gianni E, Anterior cruciate ligament reconstruction and augmentation with PDS graft. *Clin. Sports Med.*, 1993. 12: p. 13-24.
112. Buma, P., et al., Augmentation in anterior cruciate ligament reconstruction-a histological and biomedical study on goats. *Int. Orthoped.*, 2004. 28: p. 91-96.
113. Cabaud, H.E., Feagin, J.A., and Rodkey, W.G., Acute anterior cruciate ligament injury and repair reinforced with a biodegradable intraarticular ligament: experimental studies. *Am. J. Sports Med.*, 1982. 10: p. 259-264.
114. Laitinen, O., et al., Mechanical properties of biodegradable ligament augmentation device of poly(L-lactide) in vitro and in vivo. *Biomaterials*, 1992. 13: p. 1012-1016.
115. Lu, H.H., et al., Anterior cruciate ligament regeneration using braided biodegradable scaffolds: in vitro optimization studies. *Biomaterials*, 2005. 26: p. 4805-4816.

116. Cooper, J.A., et al., Fiber-based tissue-engineered scaffold for ligament replacement: design considerations and in vitro evaluation. *Biomaterials*, 2005. 26: p. 1523-1532.



**No amount of experimentation can ever prove me right;  
a single experiment can prove me wrong.**

**Albert Einstein**



## **CHAPTER II**

### **MATERIALS&METHODS**

## I. Materials:

The materials used in the studies described in the present thesis were the following:

### A. Chitosan

The chitosan used in the studies of the present thesis was a medium molecular weight with a deacetylation degree of 87%. It was obtained from Aldrich Chemical Co.

Chitosan is a deacetylated derivative of chitin which is the second most abundant natural biopolymer after cellulose, being commonly found in shells of marine crustaceans and cell walls of fungi [1]. It is a linear polysaccharide, composed of glucosamine and N-acetyl glucosamine linked in a  $\beta(1-4)$  manner. (Figure 1).

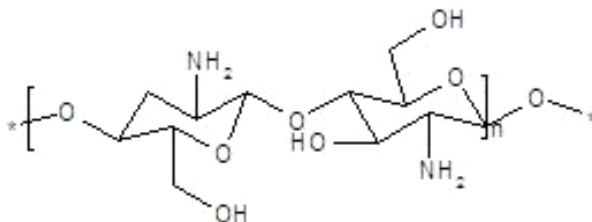


Figure 1. Chemical structure of chitosan

The degree of deacetylation of chitosan refers to the ratio between glucosamine and N-acetyl glucosamine. Depending on the source and preparation procedure, its molecular weight may range from 300 to over 1000kDa with the degree of deacetylation from 30% to 95%. Chitosan is typically not soluble in aqueous solutions above pH 7. However, chitosan solutions can be obtained in dilute acids which protonates amino groups on glucosamine, rendering the polymer positively charged. Above the pH 6.2, the chitosan solution shows a gel-like precipitation due to the neutralization of free amine groups and the consequent removal of repulsive interchain electrostatic forces which allows for hydrogen bonding and hydrophobic interaction between chains. This

behaviour of the chitosan allows for the wet spinning (which is based on solution/precipitation) of the polymer

## B. Starch/Polycaprolactone Blend

In the present studies, a starch/polycaprolactone (30/70 wt/wt) blend was used for the production of the fibers.

Starch is a natural polymer which occurs widely in plants such as corn, potato and rice. It consists of two types of molecules, amylose and amylopectin (Figure 2). Amylose is a linear polymer and makes up about 20% wt of the starch. The other component, amylopectin, has a branched structure and made up about 80% of the starch. The relative proportions of amylose to amylopectin depend on the source of the starch [2].

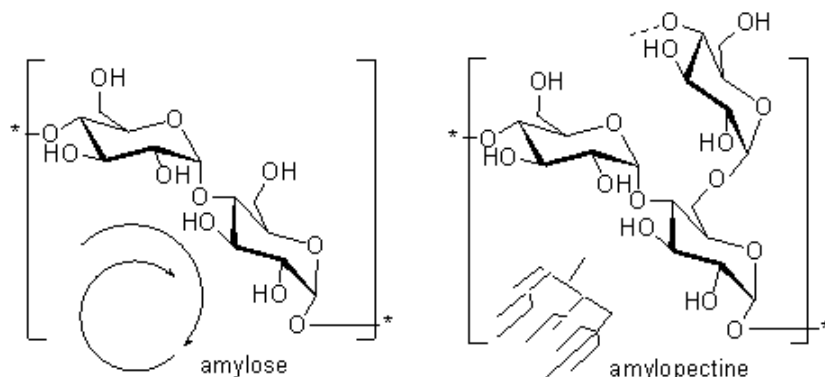


Figure 2. Chemical structure of starch.

Starch is an inexpensive, totally biodegradable polymer found in a wide variety of environments and used in many industrial applications, mainly as a raw material for packaging. However, starch itself has poor mechanical properties and it is difficult to process. Moreover, pure starch articles and even those derived from the so-called thermoplastic starch (starch with disrupted granular structure), are usually brittle and moisture sensitive, thus strongly limiting their potential fields of application. To overcome this problem, starch can be blended with different polyesters such as polycaprolactone, polylactide, etc [3, 4].



In the present studies, the synthetic part of the used blend was polycaprolactone which is a biodegradable polyester synthesized by a ring opening polymerization of a cyclic lactone monomer (i.e.  $\epsilon$ -caprolactone) (Figure 3).

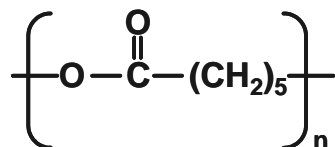


Figure 3. Chemical structure of polycaprolactone.

It is a hydrophobic and a semicrystalline polymer with a glass transition temperature about  $-60^\circ\text{C}$ . High permeability of polycaprolactone to various substances makes it capable for long-term implantable drug delivery applications. However, it shows slower in vivo degradation than poly( $\alpha$ -hydroxy acids). It has been reported that the biodegradation rate of PCL can significantly increase in the presence of starch [5].

### **C. Bioglass®**

Bioglass® with a particle size of  $5\mu\text{m}$  was supplied by US Biomaterials Corp. (Florida, USA), being used in biomimetic coating studies as a nucleation-inducing agent.

## **II. Production Methods**

### **A. Wet Spinning**

Wet spinning is the oldest method of fiber spinning. This process is based on solution/precipitation. Basically, the polymer is dissolved in a suitable solvent. After passing through the spinneret, the solution enters into a coagulation bath. Either the bath reacts chemically to coagulate the polymer, or it draws out the solvent from the polymer stream so that the filament can harden. In most cases, the second liquid is aqueous. A main difference between wet spinning and either

melt or dry spinning is that one is spinning into a fluid with a much higher viscosity. Due to this higher viscosity, higher shearing stress occurs on fiber surfaces which introduce very high tension into the filaments. Figure 4 shows the schematic presentation of the production of wet spun fibers in large scale.

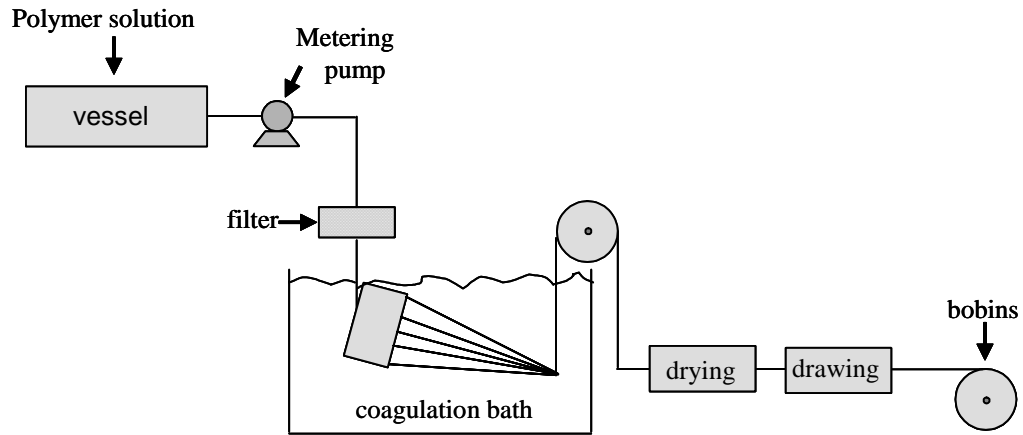


Figure 4. Schematic diagram of wet-spinning process.

The extrusion may be out directly into the coagulating liquid or through a small air-gap. In the second case it is known as dry-jet wet spinning or air-gap wet spinning.

Wet spinning method is mostly used to produce fibers from natural polymers, such as chitin and chitosan fibers which can not be formed by either melt or dry spinning methods. The strong inter-chain forces as derived from the hydroxyl, acetamido and amino groups, raise the melting point of chitin and chitosan to well above their thermal degradation temperatures. Therefore, melt spinning is typically not possible for chitin and chitosan. Besides that, these two natural polymers can only be dissolved in polar solvents which have high boiling points. As a consequence, dry spinning is also not practical for producing chitin and chitosan fibers.

In the studies described in present thesis, the wet spinning technique was used to produce chitosan fibers and fiber mesh scaffolds, as well as SPCL fiber

mesh scaffolds. Figure 5 shows the schematic representation of the production of chitosan fibers and fiber mesh scaffolds.

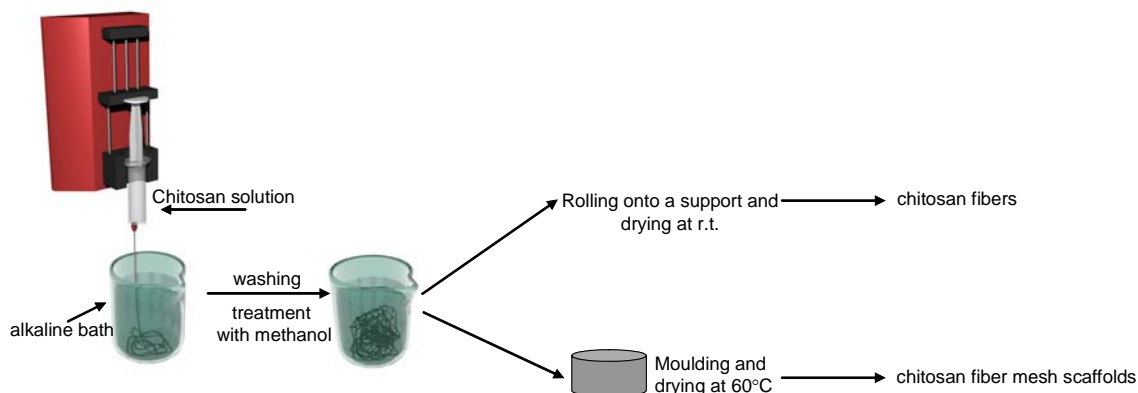


Figure 5. Schematic representation of the production of chitosan fibers and fiber mesh scaffolds.

Briefly, chitosan was dissolved in aq. 2% (v/v) acetic acid solution in 5% (w/v) concentration at room temperature overnight. Methanol was added to dilute the viscous solution for easy injection until reaching 3% (w/v) final concentration. Glycerol was used as a plasticizer (2.5% (w/w)). After filtration with a cloth filter, the solution was placed in an ultrasonic bath to remove the air bubbles. The clear solution was injected into a coagulation bath (30% 1N  $\text{Na}_2\text{SO}_4$ , 10% 1N NaOH and distilled water) by using a syringe pump (Word Precision Instruments, UK). The formed fibers were kept in this coagulation medium for one day and then washed several times with distilled water. In the case of chitosan fibers, they were suspended in an aq. 30% methanol for 4-5h and subsequently in aq. 50% methanol overnight. The filaments are then wounded onto a cylindrical mould and dried at room temperature. In order to obtain fiber meshes, the suspended fibers were treated with aq. 50% methanol and 100% methanol for 1 and 3 h respectively. The fibers were then put in a plastic cylindrical mould and dried at 60°C overnight.

The fiber mesh scaffolds from SPCL were also prepared by wet spinning technique. In this case, the polymer solution with a high viscosity (40% (w/v))

was prepared by dissolving SPCL in chloroform. The homogenous polymer solution was subsequently extruded into the coagulation bath containing methanol. The high viscosity of the polymer solution and high extrusion rate were chosen to provide the fall of the polymer solution stream to the bottom of the bath. This approach allowed to form 3-D scaffolds in the bottom of the coagulation bath by means of a random movement. The scaffolds were kept in the bath until coagulation is completed and dried at room temperature to remove the remaining solvents

## **B. Electrospinning**

Electrospinning is another fiber processing method which allows to obtain submicron size fibers (below 3 $\mu$ m) from a polymer solution or melt. This process is based on an electrostatic potential (typically up to 30kV) that is applied between a spinneret and a collector [6]. Both the spinneret and the collector must be electrically conductive and separated at a distance of around 10-25cm. In a typical electrospinning process, a fluid is slowly pumped through the spinneret. This fluid is usually a solution, whereby the solvent can evaporate during the spinning process. The spinning of the polymeric melt is more complicated due to the fast solidification process under a dynamic spinning condition at high temperatures and usually does not allow for the forming of uniform submicron-sized fibers. The electrical charge is subjected to the spinneret tip that contains the fluid droplet held by its own surface tension. As the intensity of electrical charge increases, the polymer droplet becomes as a conical shape, known as the Taylor cone [7]. When the surface tension of the fluid can be overcome, the droplet becomes unstable and charged jet fluid is ejected from the tip. This charged jet then goes to a stretching process that leads the formation of nano-size fiber by evaporation of the solvent. In the case of polymer melt the discharged jet solidifies during the travel in the air. The final fiber diameter depends on various parameters, including applied voltage, the distance between the tip and the collector, used solvent, concentration of the polymer solution, etc [8]

In the present thesis, electrospinning was used for the development of nano- and micro-fiber combined scaffolds as described in detail in Chapter VI. In brief, the polymeric solution with a concentration of 10% was prepared by dissolving starch/polycaprolactone (SPCL, 30/70) in a solvent system consisting of chloroform and dimethylformamide (DMF) with a ratio of 7/3, respectively. Dimethylformamide was used to enhance the conductivity of the polymer solution for this process. Electrospinning apparatus used in the study is presented schematically in Figure 6.

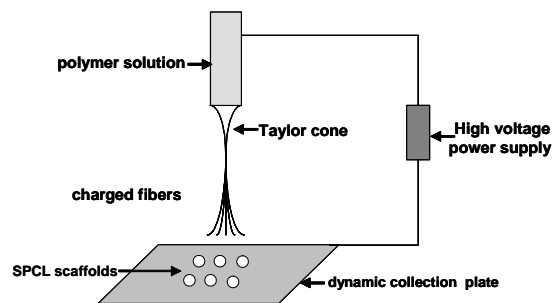


Figure 6. Experimental set-up for electrospinning of SPCL nano-fibers onto SPCL micro-fiber meshes.

The polymer solution was vertically placed in a simple capillary tube. SPCL scaffolds produced by fiber bonding method were put onto a special design metal collector which is movable through the electrospun polymeric jets. The distance between the tip of capillary and collector was adjusted to 10 cm. A high voltage of 15kV was applied by a high voltage supplier (Gamma High Voltage, USA) for 10s. The time was selected by considering the proportion between the spinning time and the amount of electrospun nano-fibers. The final constructs were allowed to dry overnight at room temperature.

## C. *In vitro* Bioactivity Testing and Biomimetic Coatings

### C. 1. *In vitro* Bioactivity

*In vivo* bioactivity of a material can be predicted by assessing the bone-like apatite formation on its surface in simulated body fluid (SBF) *in vitro*. The

bioactivity test for the chitosan fibers was carried out with the use of standard *in vitro* procedure described by Kokubo et al. [9]. The ion concentrations of SBF solution used in this study were similar to human blood plasma as presented in Table 1.

Table 1. Ion concentrations of human blood plasma and SBF.

Solution	Concentrations (mM)							
	Na <sup>+</sup>	K <sup>+</sup>	Ca <sup>+</sup>	Mg <sup>2+</sup>	Cl <sup>-</sup>	HCO <sup>3-</sup>	HPO <sub>4</sub> <sup>2-</sup>	SO <sub>4</sub> <sup>2-</sup>
Human plasma	142	5	2.5	1.5	103	27	1.0	0.5
SBF (1.0x)	142	5	2.5	1.5	142.8	4.2	1.0	0.5

In order to perform the bioactivity test, chitosan fibers were immersed in SBF solution and incubated at 37°C during 30 days. The fibers were removed and washed carefully with distilled water at different time intervals (3, 7, 14, 30 days). They were then dried at room temperature before analysis.

### C. 2. Biomimetic Coating

When a material is not bioactive or showing delayed bioactivity, a biomimetic coating approach can be used to obtain a bone-like apatite layer on its surface before *in vivo* implantation. Different functional groups can be introduced on to the materials surfaces, such as Si-OH, Ti-OH and carboxyl or carboxylate [10]. In the present thesis, Bioglass® was used to introduce functional Si-OH groups on the chitosan fiber mesh scaffolds.

Regarding the biomimetic coating experiments, an innovative and simple Bioglass® spraying method was developed in order to obtain Ca-P layers on the scaffolds. The spraying approach was chosen to have a homogenous distribution of the Bioglass® particles on the complex fiber mesh structure. Figure 7 presents schematically the experimental procedure followed in this study. In brief, the Bioglass® particles were suspended in ultra-pure water and the suspension was placed into a simple container with a spray. The chitosan scaffolds were wet with

this suspension in all sides and dried under air flow before immersion in SBF(x) solution in polyethylene tubes at 37°C. The solution and the tubes were renewed the following day. After 7 days of immersion, the samples were removed from the solution, washed several times with distilled water and dried at room temperature before analysis.

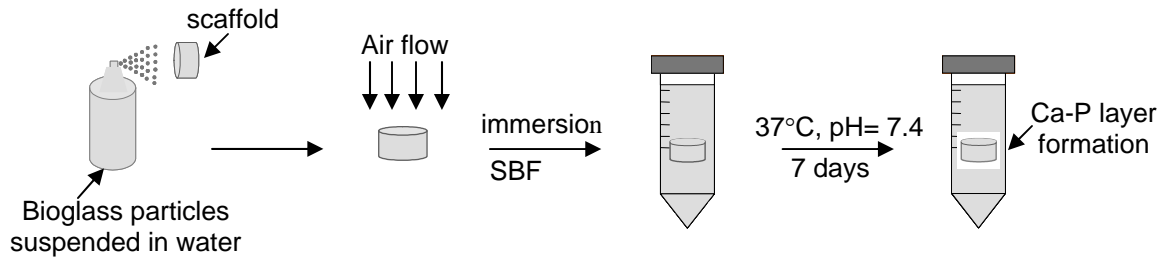


Figure 7. Schematic representation of a novel biomimetic coating process using Bioglass/water suspension.

The mechanism of Ca-P formation by this method is given in Figure 8.

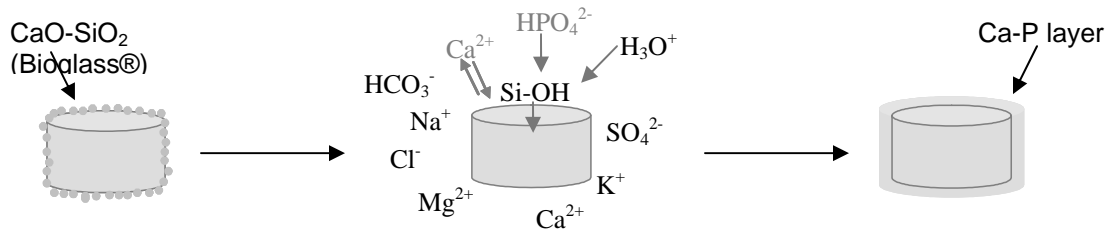


Figure 8. The mechanism of Ca-P formation on chitosan fiber meshes immersed in SBF solution after Bioglass spraying.

#### D. Plasma Treatment

Plasma treatment, using different inert gases or monomers, is one of the most commonly used techniques for surface modification of the materials. As it is discussed in Chapter V, Ar plasma treatment was applied to wet-spun SPCL fiber mesh scaffolds to enhance the cell attachment and proliferation capability on them. The plasma reactor (Gala Instrument GmbH, Germany) used in this study allows for a fully automated process and has a control reactor with a chamber

size of 15 cm diameter and 31 cm length (5L). The scaffolds were hanged onto a metal wire with a distance of 1cm between them and then placed into the chamber. The air present in the system was first displaced with argon, by flushing argon through the reactor. The outlet was then closed, and the reactor was filled with argon with a controlled pressure of 0.18 mbar. The power of the plasma was set at 30W and the scaffolds were exposed to plasma for 15 min. In the end of this period, they were kept at ambient conditions before using in further studies.

### **III. Characterization Methods for the Developed Structures:**

#### **A. Morphology**

Morphologies of the scaffolds developed in the studies were analyzed under an optical microscope and a scanning electron microscope (SEM). In order to examine the nanofiber amount and distribution on the developed nano- and micro-fiber combined scaffolds, both sides of the samples were observed under an optical microscope (Olympus, MIC-D). Light transmission microscopy images were taken for HA/chitosan multichannel structures in order to see the placement of the components within the structure. SEM (Leica Cambridge S360 microscope) was used for all developed scaffolds to analyze the overall structure as well as the surfaces. All the samples were sputtered coated with gold and the analysis were performed at an accelerating voltage 15 kV and magnifications between 15-5000 times.

In the case of wet spun starch-based fiber meshes, a  $\mu$ CT imaging system ( $\mu$ CT40, Scanco Medical AG, Bassersdorf, Switzerland) with a nominal resolution of 12  $\mu$ m was also used to determine the mean pore size, total porosity, surface-to volume ratio, mean fiber diameter of the wet-spun SPCL fiber mesh scaffolds. The reconstructed images were filtered using a constrained 3D Gaussian filter to partially suppress noise in the volumes ( $\sigma = 1.2$  voxel, support = 1 voxel), and binarized using a global threshold. Standard 3D morphometry as developed for trabecular bone was used to assess structural parameters for the scaffolds. Pore



size and fiber thickness were determined using the distance transformation method. In this method, each pore (fiber) is filled with a non-redundant set of maximal spheres. Mean pore (fiber) size was then calculated as the volume-averaged diameter of all spheres making up the pore (fiber).

## **B. Surface Analysis**

### **B. 1. Energy Dispersive Spectroscopy (EDS):**

Energy Dispersive Spectroscopy (EDS) is an analytical technique that is used to identify the elemental composition of the specimen. It is based on utilization of x-rays that are emitted from the specimen when bombarded by the electron beam of SEM. In the present thesis, EDS technique was employed to determine Ca and P elements on the surface of the samples after either bioactivity test or biomimetic coating. All the samples were coated with carbon by ion sputtering before analysis.

### **B. 2. Fourier Transform Infrared Attenuated Total Reflectance Spectroscopy (FTIR-ATR):**

Fourier transform infrared attenuated total reflectance spectroscopy (FTIR-ATR) was used to evaluate the presence of Ca-P bioactive layer on chitosan fiber mesh scaffolds after biomimetic coating. FTIR spectra were recorded at least at 32 scans with a resolution of  $2\text{cm}^{-1}$  in a FTIR spectrophotometer (Perkin Elmer System 1600) with an attenuated total reflectance device from SPECAC (MKII Golden Gate, diamond crystal, penetration depth  $20\mu\text{m}$ , active area  $0.8\text{ mm}^2$ ).

### **B. 3. Thin film X-Ray Diffraction (TF-XRD)**

X-ray diffraction technique (XRD) is used to provide information on structure, phases, crystal orientation and other structural parameters such as crystallinity, strain, and crystal defects for the crystalline materials. In this thesis, TF-XRD (Philips X'Pert MPD, The Netherlands) was utilized for identifying the crystalline phases present, and characterizing the crystalline/amorphous nature of the

formed Ca-P layer on chitosan fiber mesh scaffolds after biomimetic coating. The data collection was performed by  $2\theta$  scan method with  $1^\circ$  as incident beam angle using  $\text{CuK}\alpha$  X-ray line and a scan speed of  $0.05^\circ/\text{min}$  in  $2\theta$ .

#### **B. 4. X-Ray Photoelectron Spectroscopy (XPS)**

XPS is used in major and minor elemental identification and chemical bonding information at the surface. It provides information about elemental composition of the surface approximately the top  $100 \text{ \AA}$ .

In Chapter V, XPS analysis was performed to determine the chemical changes on the surface of SPCL wet-spun fiber mesh scaffolds after plasma treatment, using an 250 iXL ESCA instrument (VG Scientific) equipped with two X-Ray sources: a source with Al  $\text{K}\alpha_{1,2}$  monochromatized radiation at  $1486.92 \text{ eV}$  and another one (Dual) equipped with two anodes: Mg and Al. Further details of the analysis are discussed in Chapter V.

#### **C. Inductively Coupled Plasma- Optical Emission Spectroscopy (ICP-OES)**

One possible way to follow Ca-P layer formation during bioactivity test is to measure the changes in Ca and P ion concentration of SBF solution. In the case of bioactivity test for chitosan fibers, the immersion solutions were analyzed after each time interval by Inductively Coupled Plasma- Optical Emission Spectroscopy (ICP-OES, JY 70 plus, Jobin Yvon, France).

#### **D. Swelling test**

The swelling ratios of samples were determined in  $0.154\text{M}$  NaCl aqueous isotonic saline solution ( $\text{pH}=7.4$ ) at  $37^\circ\text{C}$ . The immersed samples were taken out from the solution at various time intervals, and wet weight of the samples were determined by blotting them with filter paper to remove the excess water on the surface and then immediately weighing on an analytical balance. The experiment was continued until reaching of an equilibrium value. The equilibrium swelling percentage of samples was calculated as follows:

$$S\% = (m_w - m_i) / m_i \times 100$$

where  $S\%$  is the percentage of swelling,  $m_w$  donates the swollen weight of the samples and  $m_i$  is the initial weight of the sample. Five samples were used for each experiment and the average values were taken as the swelling percentage.

## **E. Mechanical Analysis**

### **E. 1. Tensile test**

The stress-strain curve of developed chitosan fibers was recorded on a Universal Mechanical Testing machine (Lyloyd Instruments, LR %K Serensworth Fareham, England) at room temperature and under room humidity. The measurements were performed with a 500N load cell. The crosshead speed and the gauge length were set to be 20mm/min and 20mm, respectively. Average values of tensile strength and maximum strain were determined after repeating the test for five samples.

### **E. 2. Dynamical Mechanical Analysis (DMA)**

Dynamical Mechanical Analysis (DMA) provides information about the stiffness and damping properties of the materials. DMA is the most sensitive technique for monitoring relaxation event as the mechanical properties change dramatically when relaxation behaviour is observed.

In the present thesis, this technique was used to analyze short-time swelling, creep and rheological behaviour of chitosan fiber mesh scaffolds. All the experiments were carried out while the samples were in an isotonic saline solution in a DMA7e Perkin-Elmer apparatus, in compression mode, using parallel plates with 10mm diameter. The details for each kind of measurements are given in Chapter III.

## **IV. *In Vitro* Cytotoxicity and Cell Culture Studies**

### **A. Cell type**

#### **A.1. Cell lines: Mouse lung fibroblast cell line (L929) and a human osteoblast-like cell line (SaoS-2)**

Cell lines can be easily maintained in culture and employed in the experiments which are conducted outside of the living system or the host body. In the present studies, mouse lung fibroblast cell line (L929) was selected for use in cytotoxicity tests. Cell culture studies on the developed scaffolds were performed by using a human osteoblast-like cell line (SaoS-2).

#### **A. 2. Rat Bone Marrow Stromal Cells (isolation)**

Although the cell lines are quite useful to test the tissue engineering scaffolds *in vitro*, they have major limitations for the use *in vivo*. The use of primary cells appears to be a more realistic approach for tissue engineering.

Based on this fact, rat bone marrow stromal cells were also used in some part of the cell culture studies. Rat bone marrow stromal cells were isolated from 4 weeks-old male Wistar rats (Charles River, Spain). Surgical procedure was as follows: The rats were euthanized by placing them in a plastic bag in CO<sub>2</sub> atmosphere. Their femurs and tibia were excised under aseptic conditions and washed within  $\alpha$ -MEM (Eagle, Sigma, St. Louis, MO) containing 10 times more amount of normal antibiotics concentrations. Soft tissues were removed from the bones and their epiphyses were cut off and the marrow residing in the midshaft was flushed out with 5ml of complete medium ( $\alpha$ -MEM containing 10% foetal bovine serum (FBS, Biochrome), 50  $\mu$ g/ml ascorbic acid (Sigma), 50  $\mu$ g/ml gentamycin, 1% antibiotics, 100mM  $\beta$ -glycerolphosphate (Sigma) and 10<sup>-8</sup> M dexamethasone (Sigma) using a syringe and collected in a 50 ml sterile centrifuge tube. Then, the cells were put in a culture flask and cultured at 37°C in a humidified atmosphere containing 5% CO<sub>2</sub>. These primary cultures were incubated for 2 days. After 2 days of incubation, hematopoietic and other

unattached cells were removed from the flasks by repeated washes with PBS and the complete medium of the flasks was renewed every other day until reaching confluency.

## **B. Indirect Cytotoxicity Evaluation**

Cytotoxicity test is a first step towards screening the biocompatibility of a biomaterial. Indirect cytotoxicity tests are a rapid, standardized, sensitive, and inexpensive method to determine whether a material contains significant quantities of biologically harmful extracts.

In the present thesis, a mouse lung fibroblast cell line (L929) was used in the cytotoxicity assessment to comply with the ISO/EN 10993-5 standard test method [11]. This standard test method is based on exposing the cells to the fluid extract of the test material and control materials. Ultra High Molecular Weight Polyethylene (UHMWPE) and latex rubber were used as negative and positive control, respectively. The extracts were obtained by placing the test and control materials ( $n=3$ ) in cell culture medium ( $2.5\text{cm}^2/\text{ml}$  or  $0.2/\text{ml}$ ) for 24 hours at  $37^\circ\text{C}$  under constant agitation. In the end, the extract fluids were filtered ( $45\mu\text{m}$  of pore size). Each fluid extract obtained were then applied to cultured-cell monolayer, replacing the medium that had nourished the cells to that point, and incubated for 72h at  $37^\circ\text{C}$  in a humidified atmosphere containing 5% of  $\text{CO}_2$ . Cells were then observed morphologically under a light microscope in response to the test and control materials' extraction fluids. A score for confluency of the monolayer, degree of floating cells and change of cellular morphology was then calculated based on the values given in Table 1.

Table 2. Quantitative and qualitative scores used in the cytotoxicity tests.

Score	<u>Confluency</u> (%)	<u>Floating cells</u> (%)	Change of cellular morphology	<u>Inhibition of cell growth</u> (%)
0	100	0	No changes during test period	0-10
1	90-100	0-5	Slight changes, few cells affected	10-30
2	60-90	5-10	Mild changes, some cells round/spindle shaped	30-50
3	30-60	10-20	Moderate changes, many cells round/spindle	50-70
4	0-30	> 20	Severe changes, about all cells show morphological changes	70-100

In the end of the test, cells were trypsinized and the percentage of growth inhibition was determined through trypan blue exclusion test. The final cytotoxic indexes of the samples were then obtained by combining all the scores. The scores used in the test are given in Table 3.

Table 3. Different cytotoxicity indexes used to classify the reactivity of tested samples.

Cytotoxic Response	Reactivity	Pass/Fail
0-1	None	Pass
1-3	Slight	Pass
3-5	Mild	Retest
5-7	Moderate	Fail
7-8	Severe	Fail

### C. Cell seeding and culture on the developed scaffolds

In order for a scaffold to be considered successful, it should support to cells which are already seeded into the scaffolds prior the implantation, as well as the cells that might migrate into the scaffolds from the host.

To evaluate the cell supporting ability of the scaffolds developed in this thesis, a direct contact method was used. The parameters for the different scaffolds were given in Table 4. All the scaffolds were incubated with a culture medium without serum overnight prior to cell seeding. The determined number of cells was suspended in a low amount of culture medium (50-300 $\mu$ l) and the suspension was then dropped over the scaffolds carefully. After 1.5h incubation, 1-3 ml (depending on the culture well used) of medium was added up to each well. All the experiments were performed at 37°C with 5% CO<sub>2</sub> in humidified atmosphere with medium changes every 2-3 days.

Table 4. The parameters used in cell culture experiments for different scaffolds.

Scaffold	Dimensions	Cell type	Number of cells seeded per scaffold	Culture Medium	Culturing time intervals (days)
SPCL nano- and micro- fiber combined	$\phi$ = 0.8cm, h= 1.5 mm	SaOs-2	$3 \times 10^5$	<b>DMEM low glucose</b> with 10% FBS, 1%antibiotics/antimicotics	7 and 14
		RBMSc	$3 \times 10^5$	<b><math>\alpha</math>-MEM</b> with 10% FBS, 1%antibiotics/antimicotics $10^{-8}$ dexamethasone, 10mM $\beta$ glycerophosphate	7 and 14
Ca-P coated chitosan fiber meshes	$\phi$ = 1 cm, h= 1 cm	SaOs-2	$2 \times 10^6$	<b>DMEM low glucose</b> with 10% FBS, 1%antibiotics/antimicotics	14 and 21
Wet-spun SPCL fiber meshes	$\phi$ = 0.8 cm, h= 1mm	SaOs-2	$3 \times 10^5$	<b>DMEM low glucose</b> with 10% FBS, 1%antibiotics/antimicotics	7 and 14

## **D. Characterization**

### **D. 1. Cell Morphology**

The morphology of the cells cultured on the developed scaffolds were examined with scanning electron microscopy (SEM, Leica Cambridge S360) at 15 V. After each time interval, cell/scaffold constructs were fixed with 2.5% glutaraldehyde for 30 min and washed excessively with PBS. They were then dehydrated through graded series of ethanol, dried and mounted onto brass stubs. Before the analysis, all the samples were sputtered coated with gold.

### **D. 2. Cell viability and proliferation**

#### **D. 2. 1. MTS**

MTS (3-(4,5-dimethylthiazol-2-yl)-5-(3-carboxymethoxyphenyl)-2(4-sulfophenyl)-2H tetrazolium) is a substrate that is converted by NADPH or NADP produced by dehydrogenase enzymes in metabolically active cells to yield a brown formazan product . The intensity of the colour is directly related to the number of viable cells, and thus their proliferation *in vitro*. Cell viability on the scaffolds after different time intervals was determined by using Cell Titer 96® Aqueous One Solution Cell Proliferation Assay kit (Promega, USA). According to the standard procedure, the triplicates of the samples were washed with sterile PBS and placed in new culture wells. Fresh medium without phenol red and MTS reagent were added to each well in 5/1 ratio. The reaction was carried out by incubating the cell/scaffold constructs with this medium for 3h at 37°C in a humidified atmosphere containing 5% of CO<sub>2</sub>. In the end of the reaction, 100 µl of incubated medium was transferred to 96-well plate and optical density was read at 490nm in a micro-plate reader (Synergy HT, Bio-tek). The results are expressed as the average absorbance of triplicate samples.



### **D. 2. 2. DNA**

DNA assay is one of the most used measurements to evaluate cell proliferation by quantifying DNA content of cells cultured on the scaffolds. In order to determine the cell proliferation on wet-spun SPCL fiber mesh scaffolds, PicoGreen dsDNA kit (Molecular Probes, USA) was used. PicoGreen dsDNA Quantitation Reagent is an ultra-sensitive fluorescent nucleic acid stain for quantitative analysis of double-stranded DNA (dsDNA) in solution.

For the assay, the samples were prepared by rinsing with sterile PBS and incubated with sterile ultra pure water at 37°C for 1h. They were then frozen at -80°C and thawed. Before starting the assay, they were sonicated 15min in an ultrasonic bath. An aliquot of each sample was transferred to the 96-well plate. A certain ratio of Tris-EDTA buffer and PicoGreen reagent prepared in the same buffer was added to the each well. The fluorescence was read at 485nm and 528nm excitation and emission, respectively. The DNA amount of each samples was then calculated using a standard curve.

### **D. 3. ALP Enzyme Activity**

Alkaline phosphatase, an ectoenzyme produced by osteoblasts, is believed to involve in the degradation of inorganic pyrophosphate to provide a sufficient local concentration of phosphate or inorganic pyrophosphate for mineralization to proceed. Among the various biological functions of osteoblasts, secretion of alkaline phosphatase (ALP) is an important indicator determining the activity of the cells on a scaffold.

In order to determine the extent of osteoblast phenotype expression, amount of alkaline phosphatase produced by the cells were determined. ALP activity of the cultured cells on the scaffolds was analyzed by either in weekly collected supernatant (culture medium) of the samples or lysed cells. In both experiments, the enzyme activity determination was based on the specific conversion of p-nitrophenyl phosphate (pNPP) into p-nitrophenol (pNP).

To determine the activity of the secreted enzyme in the culture medium, supernatants were collected at each time point and frozen at  $-80^{\circ}\text{C}$  until further analysis. For the assay, the collected supernatant were thawed and mixed with substrate solution (0.2% w/v p-nitrophenyl phosphate (pnPP) in 1M diethanolamine HCl (pH=9.8)) at the ratio of 1/3. The enzyme reaction was carried out by incubation of the mixture at  $37^{\circ}\text{C}$  for 1h and then stopped by adding a solution containing 2M NaOH and 0.2mM EDTA in distilled water. The final mixture was vortexed and dispensed in a 96 well-plate. The absorbance of p-nitrophenol formed was measured at 405nm. A standard curve was made using pNP values ranging from 0-600 $\mu\text{mol/ml}$ . The results were expressed in  $\mu\text{mol}$  of pNP produced/ml/h.

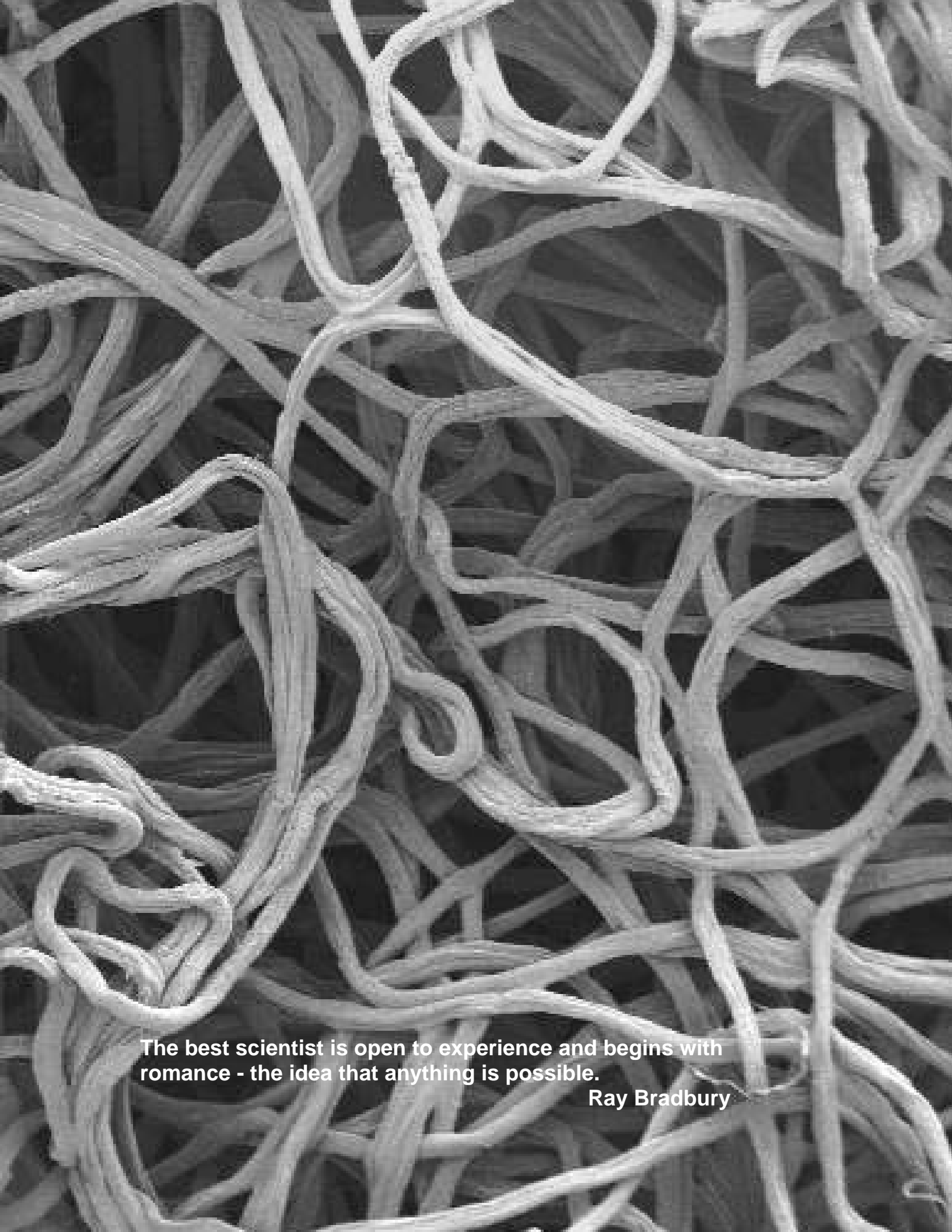
The ALP activity could also be measured in lysed cells. In this case, the determined enzyme is the one which is present in cells at the moment of the test. For this assay, scaffolds seeded with cells were washed three times with PBS and transferred into an eppendorf containing ultra pure water. Then, the samples were frozen and thawed, and sonicated for 15 min . The same reaction procedure was followed. Briefly, an aliquot of 50  $\mu\text{L}$  of each sample was added to 150  $\mu\text{L}$  of p-nitrophenyl phosphate solution at room temperature in the well of a 96-well plate and incubated for 1h at  $37^{\circ}\text{C}$  in the incubator. The absorbance of p-nitrophenol reduced in the presence of alkaline phosphatase was measured at 405nm. Calibration curve of p-nitrophenol at  $37^{\circ}\text{C}$  is used to determine the enzyme activity in units of  $\mu\text{mol}$  substrate converted to product per hour.

## References

1. Majeti, N. V., Kumar, R., A review of chitin and chitosan applications. *Reactive&Functional Polymers*, 2000. 46: p. 1-27.
2. Singh, N., Singh, J., Kaur, L., Singh Sodhi, N. and Singh Gill, B., Morphological, thermal and rheological properties of starches from different botanical sources. *Food Chem.*, 2003. 81: p. 219-231.
3. Gomes, M. E., Godinho, J. S., Tchalamov, D., Cunha, A. M., Reis, R. L., Alternative tissue engineering scaffolds based on starch: processing methodologies, morphology, degradation and mechanical properties. *Materials Science & Engineering C-Biomimetic and Supramolecular Systems*, 2002. 20(1-2): p. 19-26.
4. Salgado, A.J., Coutinho, O. P., Reis, R. L., Novel starch-based scaffolds for bone tissue engineering: Cytotoxicity, cell culture, and protein expression. *Tissue Engineering*, 2004. 10(3-4): p. 465-474.
5. Bastioli, C., Cerruti, A., Guanella, I., Romano, G. C., Tosin, M., Physical state and biodegradation behaviour of starch-polycaprolactone systems. *J. Environ. Polym. Deg.*, 1995. 3: p. 81-95.
6. Huang, Z. M., Zhang, Y.Z., Kotaki, M., Ramakrishna, S., A review on polymer nanofibers by electrospinning and their applications in nanocomposites. *Composites Sci. And Tech.*, 2003. 63: p. 2223-2253.
7. Taylor, G., Electrically Driven Jets. *Proceedings of the Royal Society of London Series a-Mathematical and Physical Sciences*, 1969. 313(1515): p. 453-&.
8. Li, D., Xia, Y., Electrospinning of Nanofibers: Reinventing the Wheel? *Adv. Mater.*, 2004. 16: p. 1151-1170.
9. Kim, H. M., Furuya, T., Kokubo, T., Miyazaki, T., Nakamura, T. in *Bioceramics 14*. 2001. USA: Palm Springs.
10. Oyane, A., Uchida, M., Choong, C., Triffitt, J., Jones, J., Ito, A, Simple surface modification of poly(e-caprolactone) for apatite deposition from simulated body fluid. *Biomaterials*, 2005. 26: p. 2407-2413.

11. 10993-5, I.E., Biological evaluation of medical devices-Part 5: Tests for cytotoxicity, in-vitro methods:8.2 tests on extracts.





The best scientist is open to experience and begins with  
romance - the idea that anything is possible.

Ray Bradbury



## **Chapter III**

### **PRODUCTION AND CHARACTERIZATION OF CHITOSAN FIBERS AND 3-D FIBER MESH SCAFFOLDS FOR TISSUE ENGINEERING APPLICATIONS**



## **Abstract**

This study reports on the production of chitosan fibers and 3-D fiber meshes for using as tissue engineering scaffolds. Both structures were produced by means of a wet spinning technique. Maximum strain at break, and tensile strength of developed fibers were found to be 8.5%, 204.9 MPa, respectively. After 14 days of immersion in simulated body fluid (SBF); scanning electron microscopy (SEM), energy dispersive spectroscopy (EDS), and inductively-coupled plasma emission (ICP) spectroscopy analyses showed that a bioactive Ca-P layer was formed on the surface of the fibers, meaning that they exhibit a bioactive behaviour. The samples showed around 120% max. swelling in physiological conditions.

The pore sizes of 3-D chitosan fiber mesh scaffolds were observed to be in the range of 100-500 $\mu$ m by SEM. The equilibrium-swelling ratio of the developed scaffolds was found to be around 170% (w/w) in NaCl solution at 37°C. Besides that, the limit swelling strain was less than 30%, as obtained by mechanical spectroscopy measurements in the same conditions. The viscoelastic properties of the scaffolds were also evaluated by both creep and dynamic mechanical tests.

By means of using short-term MEM extraction test both types of structures (fibers and scaffolds) were found to be non-cytotoxic to fibroblasts. Furthermore, osteoblasts directly cultured over chitosan fiber mesh scaffolds presented good morphology and no inhibition of cell proliferation could be observed.

## 1. Introduction

Tissue engineering needs the development of better polymeric scaffolds, which among other characteristics should be biodegradable and biocompatible. The scaffolds can be applied simultaneously as a carrier matrix for bioactive agents and as a support to seed primary undifferentiated cells. A number of natural [1-3] and synthetic polymers are currently in use as tissue scaffolds [4]. Depending on the applications, scaffolds can be presented in different forms, such as for instances membranes, and several types of 3-D architectures. Within the last years, non-woven mesh-like scaffolds have been started to be used in tissue engineering applications due to their highly porous structures. Polyglycolide (PGA) [5, 6], polylactide/polyglycolide (PLA/PGA) [7], and chitosan meshes [8] have been used as a scaffold for different tissue engineering applications.

Chitosan, a (1→4)-2-amino-2-deoxy-β-D-glucose, is derived from chitin, which is found in the exo-skeleton of shellfish like shrimp or crabs. Because of its stable, crystalline structure, chitosan is normally insoluble in aqueous solutions above pH 7. However, in dilute acids, the free amino groups are protonated and the molecule becomes fully soluble below pH 5 [3]. Viscous solutions can be formed into fibers in different coagulation solution with high pH, such as aq. NaOH [9], aq. KOH [10], aq. NaOH-40% methanol [11], and aq. NaOH-NaSO<sub>4</sub> (or AcONa) mixture [12]. Chitosan fiber forming properties have been investigated by several researchers [13]. A number of methods have been tried in order to produce chitosan fibers with good mechanical properties [10, 14, 15].

Chitosan is a well known natural polymer that is biodegradable, biocompatible and nontoxic [16]. It has been shown [3, 17] to aggressively bind to a variety of mammalian and microbial cells. Binding on cells and biodegradability of chitosan may lead to a variety of biomedical applications such as wound dressing [18], carriers for drug delivery systems [19, 20] and space filling implants [21, 22]. Recent studies of chitosan confirm the utility of chitosan for promoting the bone growth [23, 24]. Muzzarelli et al. [23] reported the formation of mineralized bone-like tissue in osseous defects in rats, sheep and dogs when using chitosan plugs.

In the present study, chitosan fibers were produced for being used subsequently to process tissue engineering scaffolds. The developed scaffolds

should ideally combine an adequate porous structure with proper mechanical and degradation properties. Furthermore, this study aimed for the analysis of this materials cytotoxicity as a first screening of its biocompatibility by means of using mouse fibroblast (L929) and human osteoblast (SaOs-2) cell lines.

## **2. Experimental**

### **2.1. Materials**

Medium molecular weight chitosan with an 85% degree of deacetylation was obtained from Sigma-Aldrich. All other chemicals were analytical grade and used as received.

### **2.2. Methods**

#### **2.2.1. Chitosan fiber preparation**

Chitosan fibers were produced by a wet spinning method as described elsewhere [12]. In a typical procedure; chitosan was dissolved in aq. 2% (v./v) acetic acid in 5% (w./v) concentration by stirring at room temperature overnight. The solution was diluted with methanol to reach 3% (w./v) final solution concentration. Glycerol at 2.5% wt/wt concentration was added into this solution as a plasticizer. The solution was filtered through a cloth filter and put in ultrasonic bath to remove the air bubbles. The solution was injected into a coagulation bath at 40°C containing a mixture of 30% 0.5 M Na<sub>2</sub>SO<sub>4</sub>, 10% 1M NaOH and 60% distilled water. The fibers were kept in this coagulation medium for one day and washed several times with distilled water. They were then suspended in aq. 30% methanol for 4/5 h and then in aq. 50% methanol overnight. The chitosan filaments were wounded on the cylindrical support. The fibers were dried at room temperature/humidity conditions for one day.

## **2.2.2. Chitosan fiber meshes preparation**

A similar production method was used to produce 3-D chitosan fiber meshes. However, a different drying method and a thinner needle were used. After fibers were formed in coagulation medium at room temperature, they were kept in this solution overnight. The fibers were then washed several times with distilled water before being suspended in 50% methanol for 1h. Then they were suspended 100% methanol for 3h and put in the oven at 55°C for drying in a mould.

## **2.3. Characterization**

### **2.3.1. Chitosan fiber**

#### *Scanning Electron Microscopy*

The morphology of fibers was visualized by Scanning Electron Microscopy (SEM) in a Leica Cambridge S360 microscope. Samples were sputter coated with gold.

#### *Mechanical Properties*

Tensile tests were performed on a Universal Test Machine (Lyloyd Instruments, LR %K Serensworth Fareham, England), with a 500N load cell, using a cross-head speed of 20mm/min and a gauge length 20mm. Average values of tensile strength and maximum strain were determined after repeating the test five times.

#### *Swelling Tests*

Swelling behaviours of fibers have been investigated in 0.154M NaCl aqueous isotonic saline solution at pH=7.4. Fibers with different glycerol ratios were used, in order to observe the effect of glycerol on swelling ratio. The samples were immersed in the solution, taken out from it at various time intervals, and then weighted with an electronic balance. The experiment was continued until samples reach the equilibrium. Swelling degree was calculated according to the following equation:

$$\%S = (m_w - m_i) / m_i \times 100$$

where %S is the percentage of swelling,  $m_w$  is the weight of the wet sample after immersion in the NaCl solution.

### *Bioactivity Tests*

Chitosan fibers were immersed in 15 ml simulated body fluid (SBF) in a plastic bottle at 37°C. SBF solution was proposed initially by Kokubo et al [25], present an ionic composition similar to human blood plasma, and has been widely used [26, 27] to test the bioactivity of different materials in-vitro. After various periods of incubation (3, 7, 14, 30 days) in SBF, samples were removed from the solution, washed carefully with water and dried at room temperature in a desiccator. The apatite formation on the fiber surface of a calcium-phosphate film was visualized by SEM (Leica Cambridge S360). EDS spectra were obtained after the observation. Changes in concentration of calcium and phosphorus of SBF solution due to soaking of fibers were measured using inductively-coupled plasma emission (ICP) spectroscopy.

### *Cytotoxicity: Short Term MEM Extraction Test using Fibroblast Cells*

To establish the cytotoxic rate of leachables, a MEM Extract test, a cytotoxicity test laid down in European and International standards (ISO/EN 109935 Guidelines) was performed [28]. For this assay, a cell line of mouse lung fibroblasts (L929) was selected. Growth to confluency was performed in controlled atmosphere (37°C, 5% CO<sub>2</sub>, 100% humidity) using Dulbecco's Modified Eagle's Medium (DMEM, Sigma), supplemented with 10% Foetal Bovine Serum (FBS, Biochrome) and 1% antibiotic/antimicotic solution (Sigma). In order to achieve 80% of confluency, cells seeded in cell culture polystyrene plates (10 000 cells/cm<sup>2</sup>) were incubated for 24h. According to ISO/EN 109935 Guidelines, surface area of the different samples was determined and immersion in the correspondent cell culture media volume was performed (37°C, 60 rpm). The same procedure was carried out for a negative control Ultra High Molecular Weight Polyethylene (UHMWPE), and positive control Latex Rubber. After 24 hours, fibroblasts were morphologically analysed, and culture media was replaced by the extraction one. Test samples and controls were incubated in triplicate (n=3). After 24, 48 and 72 h testing, the reaction of cells to extracts was evaluated by means of light microscopy and compared to the positive control and

negative control. A score for confluency of monolayer, degree of floating cells and changes in cellular morphology was calculated based on the scores posted on Table 1. In the end of the test, cell number was measured and the percentage of cell growth inhibition determined. By means of combining the different quantitative and qualitative parameters scores, the obtained cytotoxic index defines if samples fail or pass the cytotoxicity test (used scores can be seen in Table 2).

Table 1. Quantitative and qualitative scores used in the cytotoxicity tests.

Score	<u>Confluency</u> (%)	<u>Floating cells</u> (%)	Change of cellular morphology	<u>Inhibition of cell growth</u> (%)
0	100	0	No changes during test period	0-10
1	90-100	0-5	Slight changes, few cells affected	10-30
2	60-90	5-10	Mild changes, some cells round/spindle shaped	30-50
3	30-60	10-20	Moderate changes, many cells round/spindle	50-70
4	0-30	> 20	Severe changes, about all cells show morphological changes	70-100

Table 2. Different cytotoxicity indexes used to classify the reactivity of tested samples.

Cytotoxic Response	Reactivity	Pass/Fail
0-1	None	Pass
1-3	Slight	Pass
3-5	Mild	Retest
5-7	Moderate	Fail
7-8	Severe	Fail

### **2.2.2. Chitosan fiber meshes:**

#### *Scanning Electron Microscopy*

The mesh structure of chitosan fibers was analysed by Scanning Electron Microscopy (Leica Cambridge S360) again after coating with gold.

#### *Mechanical Properties*

Short-time swelling, creep and dynamic mechanical analysis (DMA) experiments were carried out in a DMA7e Perkin-Elmer apparatus, in the compression mode, using parallel plates with 10 mm diameter. The analysed samples, with cylindrical shape, were typically 2 mm high. All experiments were performed while the samples were immersed in an isotonic saline solution. In order to implement such runs, a metallic cylindrical vessel was fitted into the inner part of the furnace of the apparatus. The vessel was filled with isotonic saline solution. The calibration of the force was performed with the top plate immersed, in order to take into account the impulsion effect of the solution. Before the runs have been carrying out on the samples, the temperature of the bath was stabilised at 37 °C, using the own temperature sensor of the apparatus.

The short-time monitoring of the swelling of the studied mesh was carried out using the thermal mechanical analysis (TMA) mode of the Perkin-Elmer dynamic mechanical analysis (DMA) apparatus. Briefly, the temperature of the dry sample is kept at 37 °C in an external furnace, near the DMA equipment. The sample is quickly positioned between the plates and the furnace with the bath is immediately raised up. The height of the sample starts to be recorded less than 10 seconds after the sample contacts with the liquid. During the experiment a small stress of 10 Pa is imposed to the sample by the top plate, in order to maintain the contact between the sample and the plates.

In the creep experiments, previously swelled samples are positioned between the plates and immersed until the temperature equilibrates at 37°C. The creep stress was 0.1 MPa. A program of creep/recovery was used, where the strain,  $\epsilon$ , was measured against time.

DMA experiments were performed in the immersed samples (with equilibrated water content) at 37 °C. The real (storage modulus),  $E'$ , and the imaginary (loss modulus),  $E''$ , of the complex modulus,  $E^* = E' + iE''$  (with  $i = (-1)^{1/2}$ ), were recorded against frequency, that varied between 0.5 and 10 Hz. A static stress of 36 kPa and a dynamic stress of 30 kPa were used in such experiments.

### *Swelling Tests*

The swelling ratios of the samples were calculated using the same experimental set-up and method that was described above.

### *Cytotoxicity and Biocompatibility: Direct Contact Test with Osteoblast-like Cells*

Cytotoxicity assay was performed for chitosan fiber meshes by following the same methodology as described for chitosan fibers in part 2.2.1.

In order to study cell morphology, attachment and proliferation onto the chitosan fiber meshes scaffolds a human osteoblasts SaOs-2 cell line was selected. Former described culture conditions were also used for osteoblast-like cells. Cells cultured in DME Media (Sigma), enriched with 10% FBS (Biochrome) and 1% antibiotic/antimicrobial solution (Sigma) were seeded directly over samples in a concentration of  $3.3 \times 10^4$  cell/ml. Incubation was performed at 37 °C (5% CO<sub>2</sub>, 100% humidity) for 24 hours and 7 days. Tissue culture grade polystyrene (TCPS) discs were used as control and replicates were always prepared. After each incubation period, samples were washed with Phosphate Buffer Saline (PBS, Sigma) solution and fixed in glutaraldehyde 2.5% (v/v). For Scanning Electronic Microscopy (SEM) observation, samples were previously dehydrated in crescent alcohol concentrations (50%, 70%, 90% and 100%), air-dried and sputter coated with gold.



### 3. Results and discussion

#### 3.1. Chitosan fibers

##### *Scanning Electron Microscopy*

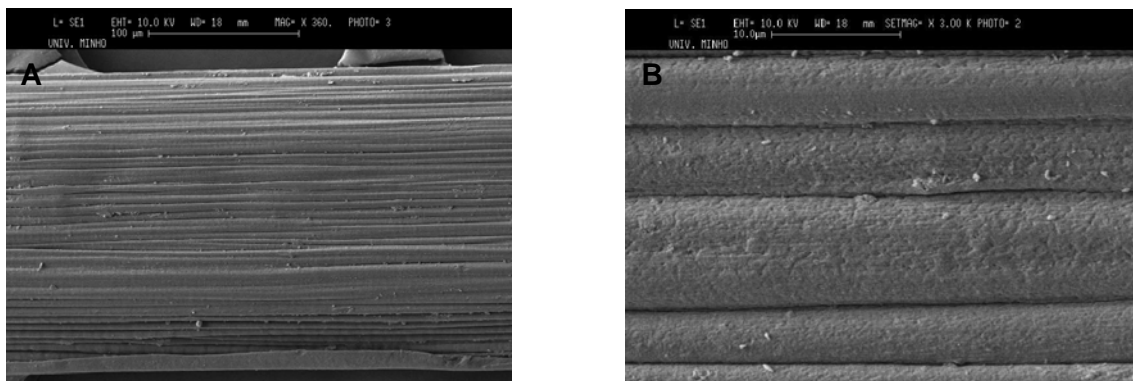


Figure 1. SEM micrographs of chitosan fibers; A) x360, B) x3000.

Figure 1.A and B present SEM images of the developed chitosan fibers. As it can be seen here in, chitosan fibers have been oriented in one direction due to the stretching process. Additionally, the images show that the fibers have a smooth and uniform striated surface even though using drying elements and rolling up the fiber on cylindrical support following a methanol drying bath may damage a fiber surface. For instance, Knaul et al. [15] have reported the effects of different drying elements on chitosan fiber surfaces.

##### *Mechanical Properties*

With regard to tensile tests maximum strain at break, and tensile strength of fibers were found  $8.5 \pm 2.3\%$  and  $204.9 \pm 9.7$  MPa, respectively.

##### *Swelling Tests*

Figure 2 shows the swelling behaviour of produced fibers. As it can be seen in the graph, the fibers showed a rapid swelling in the first 30 minutes, and then they gradually tend to equilibrium that is achieved in about 120 min.

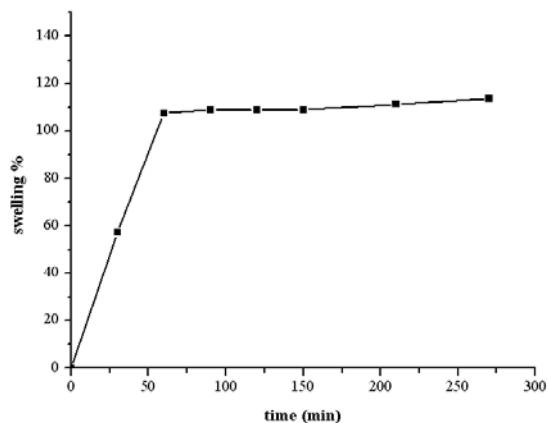


Figure 2. Swelling ratio vs. time for chitosan fibers.

### *Bioactivity Tests*

Figure 3.A, B, C present SEM micrographs of chitosan fibers before (Figure 3.A) and after a bioactivity test for 30 days (Figure B, C). In Figure 3.A it is possible to observe the typical oriented morphology of the fiber. Similar morphology was observed in the first days of immersion in SBF. However, after 14 days of immersion, a number of nucleus started to form on the surface of the fibers, that by EDS analysis were found to correspond to the formation a calcium phosphate (Ca-P) (Data not shown). This nucleus have grown with increasing immersion times and after 30 days a compact and well-defined Ca-P layer could be observed, as presented in Figures 3.B and 3.C For higher magnifications (Figure 3.C) this layer tended to the typical so-called cauliflower like morphology of Ca-P films.

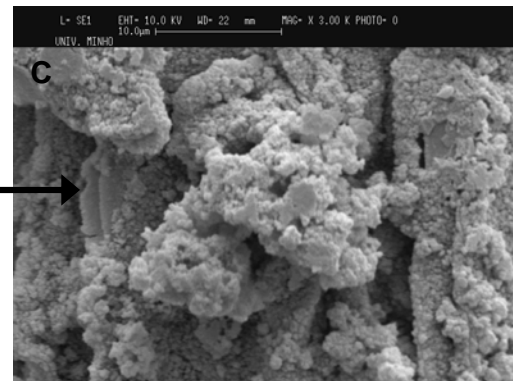
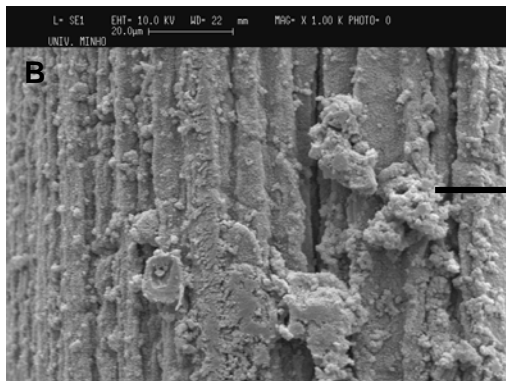
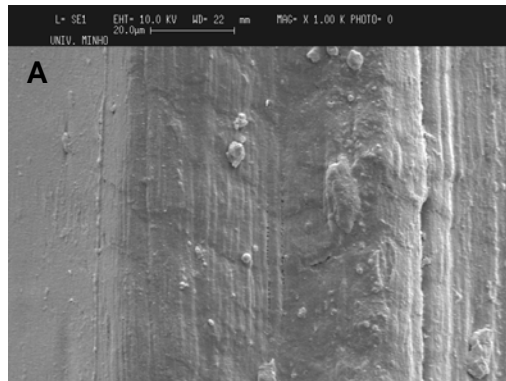


Figure 3. Sem micrographs of chitosan fibers; A) before, B) after 30 days of immersion in SBF (x1000), C) after 30days of immersion in SBF (x3000).

A commercial polyamide fiber was used as a control and for this case no Ca-P film could be observed even after 30 days of immersion in SBF (Figure 4). This clearly indicates the bioactive of the developed fibers, confirming what has been observed by authors such as Muzzarelli in-vivo [25].

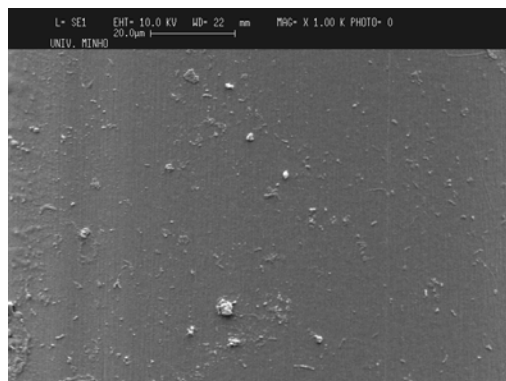


Figure 4. SEM micrograph of commercial available polyamide fibers after 30 days immersion in SBF (x1000).

This result is supported by EDS and ICP analysis (Figure 5 and 6, respectively). Ca and P elements in the formed layers can be clearly seen in EDS spectra. In addition, ICP results showed that there was a decreasing of Ca and P concentration in the SBF solution after 14 days leading to the precipitation and growth of the Ca-P layer that was observed by SEM.

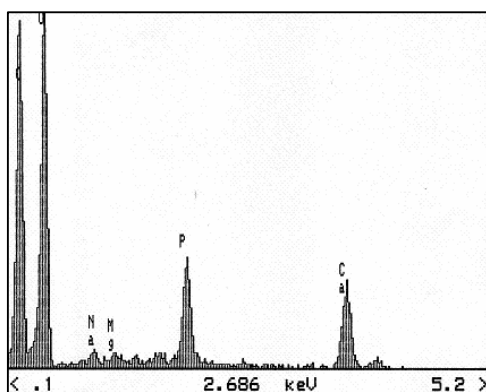


Figure 5 – EDS spectra of the Ca-P coatings on the surface of chitosan fibers (after 30 days in SBF).

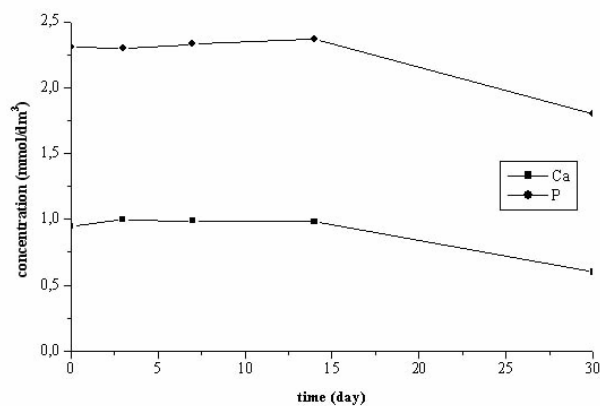


Figure 6 – Evolution of the Ca and P elemental concentrations in the SBF as a function of immersion time of chitosan fibers in SBF.

### Cytotoxicity Test

Regarding the *in vitro* study of the cytotoxic effect of chitosan fibers; results indicate that the material passed the test with a cytotoxic index of 0 (see Table 3). This means that as for tissue culture polystyrene surfaces and UHMWPE, when cell

culture media was replaced by extracts of materials in study good fibroblast proliferation and no cell morphology modifications were observed. This is not typically at all of biodegradable polymers.

**Table 3.** Results comparing fibroblasts cytotoxic response and reactivity to chitosan materials and controls.

Sample	Total Cytotoxic Response	Reactivity	Pass/Fail
Chitosan fiber	0	None	Pass
Chitosan fiber mesh scaffolds	0	None	Pass
UHMWPE	0	None	Pass
TCPS	0	None	Pass
Latex	8	Severe	Fail

### 3.2. Chitosan fiber meshes

#### *Scanning Electron Microscopy*

SEM images of fiber meshes are presented in Figure 7.A, B, C. As it can be seen in the micrographs, the chitosan fibers could be formed into mesh structures having an average pore size in range of 100-500  $\mu\text{m}$ . In addition, it was possible to see that fibers have stucked to each other. This structure gives them good mechanical strength as well as it will enable cell ingrowth, as required for tissue engineering scaffolding applications.

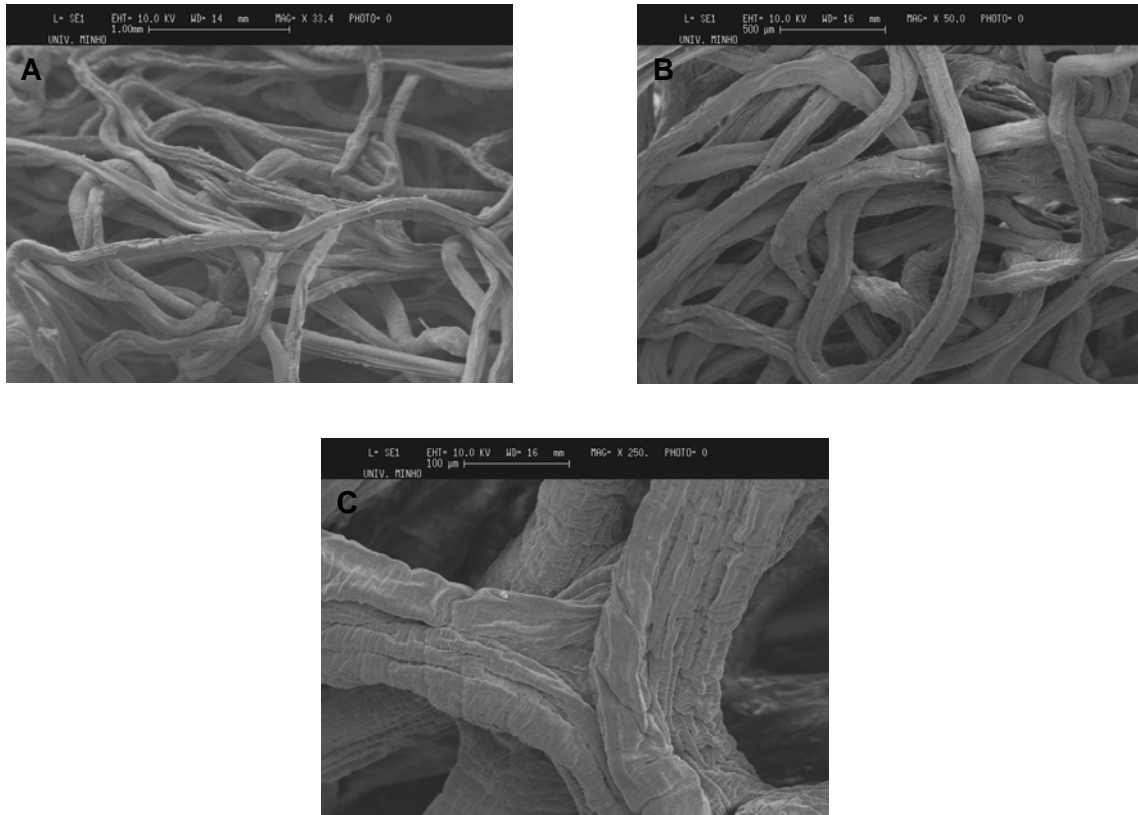


Figure 7 – SEM micrographs of the structure of the developed chitosan fibers meshes; A) x33.4, B) x50, C) x250

### *Mechanical Properties*

Swelling experiments are usually carried out by means of measuring the sample's weight after different periods of immersion. It is then very difficult to access the swelling data during short-time immersion periods, which would be rather relevant for materials having a fast swelling rate. The studied chitosan meshes are among such systems, where the equilibration of water content occurs mostly in the first hour after immersion. The innovative procedure described here in permits to follow this process by continuously monitoring the height of the samples immediately after the moment they are immersed. Obviously, considering an isotropic swelling, the height of the sample is easily correlated with the increase of volume

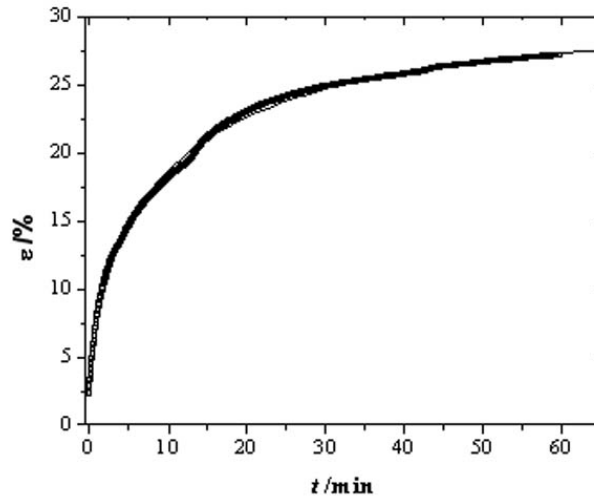


Figure 8 – Evolution of the strain of a dry chitosan mesh after it was immersed at 37 °C (symbols). The solid line corresponds to the best fit of the data according to Eq. (2).

The sample's strain ( $\varepsilon=(h-h_0)/h_0$ , where  $h$  and  $h_0$  are the measured and initial heights of the sample) is measured against time. The results obtained with an initially dry sample with  $h_0=2.351$  mm are shown in Figure 8. The increase of the strain is faster in the first 20 minutes and the limit strain seems to be less than 30%.

The data in Figure 8 was fitted according to the stretched exponential function:

$$\varepsilon(t) = \varepsilon_{\infty} \left[ 1 - \exp\left(-\left(t/\tau\right)^{\beta}\right) \right]$$

where  $\varepsilon_{\infty}$  is the limit swelling strain,  $\tau$  is a characteristic swelling time and  $\beta$  is an exponent parameter that measures the deviation from a first-order swelling kinetics ( $\beta=1$ ). This function appears in this context as an empirical model that may be useful to characterise the strain at equilibrium and the swelling rate. This equation has been often used to follow relaxational processes, i.e., the isothermal evolution to the equilibrium when a system is subjected to an external perturbation (see, for example, ref. [29]); in that case the model has physical significance. The results in Figure 8 were fitted using a Levenberg-Marquard algorithm and the adjusted parameters were:  $\varepsilon_{\infty}= 29,4\pm 0.08\%$ ,  $\tau= 9.8\pm 0.1$  min and  $\beta=0.54\pm 0.003$ .

The meshes may be subjected to static loads if used in different biomedical applications. In polymer-based materials an applied static stress usually results in a continuous, long term deformation under the applied stress, called creep. Such phenomenon may be relevant in the clinical use of the studied meshes, being associated with changes on the mechanical performance of the material and in variations in the dimensions of the implant. In this work creep/recovery of the immersed chitosan mesh was studied in simulated *in-vitro* conditions.

The “instantaneous” increase of the strain is mainly associated with the expulsion of water within the mesh and thus is weakly assigned with the changes of geometry of the chitosan fibres, but rather is to the quantity of water initially in equilibrium and to the original cellular geometry of the sample. Please note that the initial strain value ( $\approx 35\%$ ) is higher than the plateau in the swelling experiments ( $\approx 30\%$ , as suggested by Figure 8). The excess strain ( $\approx 5\%$ ) is then basically due to the deformation of the mesh geometry of the chitosan sample.

After the initial deformation a clear delayed response is observed in the creep experiment (see inset graphics in Figure 9). The approximately linear relationship found in the log time graphics may be in accordance with the power-law for the time dependence found in the viscoelastic creep response found in another system [30]. Therefore, it is possible to assign this delayed creep to the viscoelastic properties of the chitosan fibres.

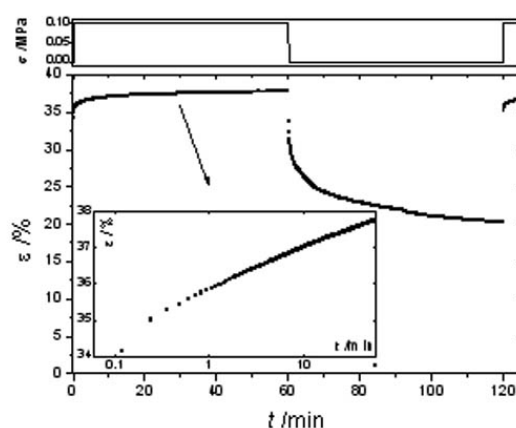


Figure 9 – Creep (60 min) followed by a recovery stage (60 min) and, finally, a second short creep run performed at 37 °C in the immersed chitosan mesh. The inset graphics shows the viscoelastic component of the first creep run, in a log time scale.



The removing of the strain results in a quick decrease of strain that occurs with a similar time-scale of the swelling experiment ( $\tau \approx 10$  min). Therefore, most of the strain recovery is related with the swelling of the mesh. After 1 h of recovery, it is found that the strain is far to converge to 0. This may be an indication that part of the mesh structure was irreversibly transformed during the creep state, leading to a more compact cellular arrangement.

After this creep/recovery experiment the sample was again subjected to the same creep stress. The strain appears to respond similarly to the first creep exposition, being an indication that neither apparent complex memory effects nor drastic structural occurs in the sample.

The rheological behaviour of the immersed mesh was also characterised by DMA. Both storage and loss moduli ( $E'$  and  $E''$ ) were measured at 37 °C in the frequency range 0.5-10 Hz, which are typical frequencies found in physiological stress-variation situations (blood pumping rate, masticatory frequency, time for patient movements...). The results are shown in Figure 10. It is to be noticed that the values may change if the experiment is carried out at different stresses, due to the variation of the water content in equilibrium inside the mesh. Please also note that  $E'$  and  $E''$  may be transformed into other viscoelastic parameters [31], such as compliance,  $D^* = D' - iD'' = 1/E^*$ , shear complex modulus,  $G^* = G' + iG'' = E^*/[2(1+\nu^*)]$ , where  $\nu^*$  is the complex Poisson's ratio, shear compliance,  $J^* = J' - iJ'' = 1/G^*$ , or the real and imaginary components of the dynamic viscosity,  $\eta' = G''/\omega$  and  $\eta'' = G'/\omega$ .

The storage modulus increases with increasing frequency, being  $E'$  typically above 1 MPa. The loss modulus shows the inverse tendency. This results in a decrease of the loss factor,  $\tan \delta = E''/E'$  with increasing frequency (inset graphics in Figure 10). This parameter measures the fraction of the imposed mechanical stress that is dissipated in the form of heat. As  $\tan \delta$  is typically above 0.15 for  $f < 1$  Hz, one may conclude that the damping capability of the system is significant, which may be important for some biomedical application that require dissipation of mechanical energy. It was found that living cells behaves as soft glassy materials existing close to a glass transition, implying that cytoskeletal proteins may regulate cell mechanical properties [32]. This kind of evidences leads one to speculate on the existence of some advantages upon biological functions when the materials of the implant that will

be in contact with living tissues, also present a viscoelastic character, as is the case for the studied chitosan mesh.

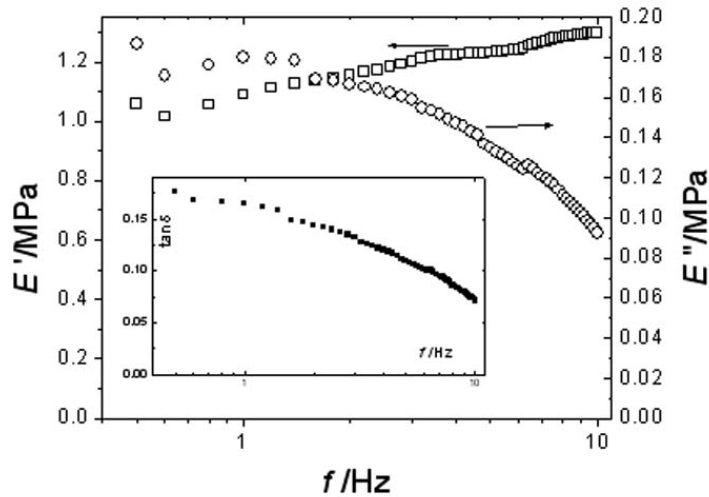


Figure 10 – Storage and loss moduli ( $E'$  and  $E''$ ) as a function of frequency ( $f$ ) at 37 °C of the immersed chitosan mesh. The inset graphics shows the frequency dependence of the loss factor.

### Swelling Tests

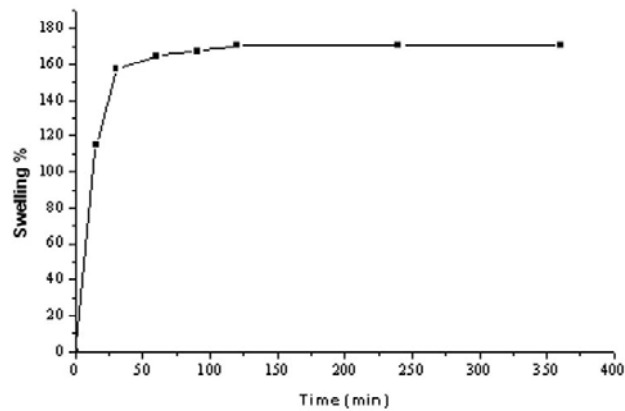


Figure 11 – Swelling ratio vs. time for the developed 3D chitosan fiber meshes.

Figure 11 shows the swelling behaviour of chitosan fiber meshes. In this figure, it is possible to observe the typical swelling behaviour of chitosan scaffolds [7]. Samples reach the equilibrium water uptake ratio, which is around 170% (w/w), after

about 3h in NaCl solution. Although fiber meshes were swelled up to high ratio, they preserved their physical integrity upon incubation in aqueous solution. This property of chitosan fiber meshes may enable for easy handling of the scaffold material in practical clinical applications. This result has been confirmed by DMA tests.

#### *Cytotoxicity and Biocompatibility: Direct Contact Test with Osteoblast-like Cells*

Cytotoxicity test results for chitosan fiber mesh scaffolds can be seen in Table 3. They showed no cytotoxic effect, and behaviour very similar to tissue culture and UHMWPE surfaces

In order to observe cell morphology and proliferation of an osteoblast cell line over chitosan fiber mesh scaffold surfaces SaOs-2 cells were directly cultured and incubated for 1 and 7 days. By means of observing Figures 12.A and B it is possible to verify that scaffolds allowed for very significant cell proliferation from day 1 to day 7, respectively. After 7 days, it was clearly seen that cells have been attaching to the scaffolds and bridging each other by means of filapodia structures which is typical for osteoblast-like cells (Figure 13) [33]. Furthermore, a detailed analysis of osteoblastic-like cells morphology confirmed short-term cytotoxic results performed with fibroblasts, and allowed for observing extensive lamellipodium structure formation.

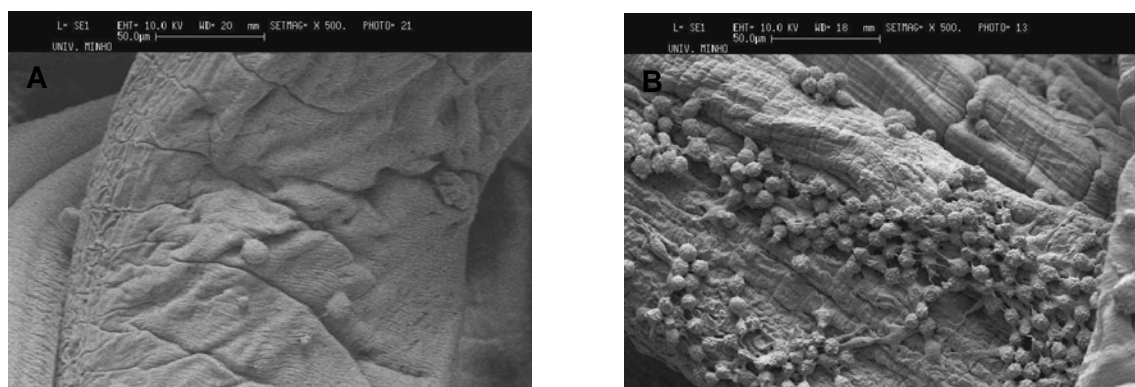


Figure 12 – Osteoblast-like cells A)adhering to chitosan based fibres after 1 day of culture, B) proliferating over chitosan based fibres after 7 days of culture.

#### **4. Conclusions**


In this paper attention has been focused on the preparation and properties of chitosan fiber and fiber meshes for potential use in tissue engineering applications. In the present study, chitosan fibers could be produced by a wet spinning technique. A subsequent drying treatment with methanol was used to improve the mechanical strength of fibers. Mechanical tests showed that the fibers had enough tensile strength to be used to produce scaffolds with good mechanical performance. Unexpectedly, the developed fibers showed a bioactive behaviour, which is also very important for biomaterials aimed to be used for instances in bone tissue engineering scaffolding. Fibers could also be formed into 3D structure aimed to be used as tissue engineering scaffolds. One could observe that mesh structure of the scaffold was suitable for cell ingrowth. This was confirmed by the results obtained on the in-vitro cell culture studies. Both types of samples extracts were comparable to UHMWPE clearly passing the test. In addition, osteoblasts growing over scaffold surfaces presented adequate morphology and good proliferation, proofing that the developed scaffolds might be used for bone tissue engineering applications.

## References

1. Majeti, N.V., Kumar, R., A review of chitin and chitosan applications. *React. Funct. Polym.*, 2000(46): p. 1-27.
2. Lee, C.H., Singla, A., and Lee, Y., Biomedical applications of collagen. *International Journal of Pharmaceutics*, 2001. 221(1-2): p. 1-22.
3. Suh, J.K.F. and Matthew, H.W.T., Application of chitosan-based polysaccharide biomaterials in cartilage tissue engineering: a review. *Biomaterials*, 2000. 21(24): p. 2589-2598.
4. Hayashi, T., Biodegradable Polymers for Biomedical Uses. *Progress in Polymer Science*, 1994. 19(4): p. 663-702.
5. Schaefer, D., et al., In vitro generation of osteochondral composites. *Biomaterials*, 2000. 21(24): p. 2599-2606.
6. Zund, G., et al., Tissue engineering: A new approach in cardiovascular surgery; Seeding of human fibroblasts followed by human endothelial cells on resorbable mesh. *European Journal of Cardio-Thoracic Surgery*, 1998. 13(2): p. 160-164.
7. Klinge, U., Schumpelick, V., and Klosterhalfen, B., Functional assessment and tissue response of short- and long-term absorbable surgical meshes. *Biomaterials*, 2001. 22(11): p. 1415-1424.
8. Denkbas, E.B., Seyyal, M., and Piskin, E., Implantable 5-fluorouracil loaded chitosan scaffolds prepared by wet spinning. *Journal of Membrane Science*, 2000. 172(1-2): p. 33-38.
9. Struszczyk, H., Wawro, D., Nicktaszcwicz, A., *Advances in chitin and chitosan*, ed. P.A.S. C. J. Brinc, J. P. Zikakis. 1992, London: Elsevier. 580.
10. Knaul, J.Z., Hudson, S.M., and Creber, K.A.M., Improved mechanical properties of chitosan fibers. *Journal of Applied Polymer Science*, 1999. 72(13): p. 1721-1732.
11. Urbanczyk, G.W., *Application of chitin and chitosan*, ed. M.F.A. Gooden. 1997, Lancaster: Technomic.
12. Hirano, S., et al., Chitosan staple fibers and their chemical modification with some aldehydes. *Carbohydrate Polymers*, 1999. 38(4): p. 293-298.

13. Agboh, O.C. and Qin, Y., Chitin and chitosan fibers. *Polymers for Advanced Technologies*, 1997. 8(6): p. 355-365.
14. Zheng, H., et al., Preparation and characterization of chitosan/poly(vinyl alcohol) blend fibers. *Journal of Applied Polymer Science*, 2001. 80(13): p. 2558-2565.
15. Knaul, J., et al., Improvements in the drying process for wet-spun chitosan fibers. *Journal of Applied Polymer Science*, 1998. 69(7): p. 1435-1444.
16. VandeVord, P.J., et al., Evaluation of the biocompatibility of a chitosan scaffold in mice. *Journal of Biomedical Materials Research*, 2002. 59(3): p. 585-590.
17. Lahiji, A., et al., Chitosan supports the expression of extracellular matrix proteins in human osteoblasts and chondrocytes. *Journal of Biomedical Materials Research*, 2000. 51(4): p. 586-595.
18. Kratz, G., et al., Heparin-chitosan complexes stimulate wound healing in human skin. *Scandinavian Journal of Plastic and Reconstructive Surgery and Hand Surgery*, 1997. 31(2): p. 119-123.
19. Miyazaki, S., Ishii, K., Nadai, T., The use of chitin and chitosan as drug carriers. *Chemical and Pharmaceutical Bulletin*, 1981. 29: p. 3067-3069.
20. Miyazaki, S., Yamaguchi, H., Takada, M., Hou, W.-M., Takeichi, Y.-I., Yasubuchi, H., Pharmaceutical application of biomedical polymers. XXIX. Preliminary study on film dosage form prepared from chitosan for oral drug delivery. *Acta Pharmaceutica Nordica*, 1990. 2: p. 401-406.
21. Muzzarelli, R., et al., Reconstruction of Parodontal Tissue with Chitosan. *Biomaterials*, 1989. 10(9): p. 598-603.
22. Kuen Yong Lee, W.S.H.a.W.H.P., Blood compatibility and biodegradability of partially N-acylated chitosan derivatives. *Biomaterials*, 1995. 16: p. 1211-1216.
23. Muzzarelli, R.A.A., et al., Stimulatory Effect on Bone-Formation Exerted by a Modified Chitosan. *Biomaterials*, 1994. 15(13): p. 1075-1081.
24. T. Kawakami, M.A., H. Hasegawa, T. Yamagishi, M. Ito and S. Eda, Experimental study on osteoconductive properties of a chitosan-bonded hydroxyapatite self-hardening paste. *Biomaterials*, 1992. 13: p. 759-763.

25. Kim, H.M., Furuya, T., Kokubo, T., Miyazaki, T., Nakamura, T. in *Bioceramics* 14. 2001. Palm Springs, USA.
26. Abe, Y., Kokubo, T., and Yamamuro, T., Apatite Coating on Ceramics, Metals and Polymers Utilizing a Biological Process. *Journal of Materials Science-Materials in Medicine*, 1990. 1(4): p. 233-238.
27. Leonor, I.B., et al., Novel starch thermoplastic/Bioglass((R)) composites: Mechanical properties, degradation behavior and in-vitro bioactivity. *Journal of Materials Science-Materials in Medicine*, 2002. 13(10): p. 939-945.
28. *Biological Evaluation of Medical Devices - Part 5: Tests for Cytotoxicity, I.-V.M.T.o.E.*
29. R. Richert, A.B., *Disorder Effects on Relaxational Processes*. 1994, Berlin: Springer-Verlag.
30. Boesel, L.F., Mano, J.F., and Reis, R.L., Optimization of the formulation and mechanical properties of starch based partially degradable bone cements. *Journal of Materials Science-Materials in Medicine*, 2004. 15(1): p. 73-83.
31. Ferry, J.D., *Viscoelastic Properties of Polymers*. 3rd ed. 1980, New York: Wiley.
32. Fabry, B., et al., Scaling the microrheology of living cells. *Physical Review Letters*, 2001. 8714(14): p. -.
33. Wang, Y.W., Wu, Q.O., and Chen, G.Q.A., Attachment, proliferation and differentiation of osteoblasts on random biopolyester poly(3-hydroxybutyrate-co-3-hydroxyhexanoate) scaffolds. *Biomaterials*, 2004. 25(4): p. 669-675.



**The most exciting phrase to hear in science, the one that heralds new discoveries, is not "Eureka!" (I found it) but "That's funny..."**  
**Isaac Asimov**





## **CHAPTER IV**

### **MULTICHANNEL MOULD PROCESSING OF 3D STRUCTURES FROM MICROPOROUS CORALLINE HYDROXYAPATITE GRANULES AND CHITOSAN SUPPORT MATERIALS FOR GUIDED TISSUE REGENERATION/ENGINEERING**

## **Abstract**

A 3D composite material was produced from microporous coralline origin hydroxyapatite (HA) microgranules, chitosan fibers and chitosan membrane. Cylindrical HA microgranules were oriented along channel direction within multichannel mould space and aligned particles were supported with fibers and a chitosan membrane. The positive replica of mould channels was clasp fixed to produce thicker scaffolds. Light microphotographs of the developed complex structure showed good adhesion between the HA particles, the fibers and the supporting membrane. The composite material showed 88 % (w/w) swelling in one hour and preserved the complex structure of the original material upon long-term incubation in physiological medium. MEM extract test of HA chitosan complex showed no cell growth inhibition and cell viability assay (MTS) indicated over 90 % cell viability.

## 1. Introduction

The new and rapidly developing tissue engineering field is requiring novel processing methods and designs of scaffold and membranes for guided tissue regeneration. The scaffolds have been fabricated using conventional techniques such as fiber bonding, solvent casting, particulate leaching, membrane lamination and melt molding [1-4]. The disadvantage of the above technologies includes the intensive fabrication process, the limitation to thin structures, and residual particles in the polymer matrix, irregularly shaped pores, and insufficient interconnectivity. Recently, rapid prototyping technologies such as fused deposition modelling, laminated object manufacturing, three dimensional printing and 3D plotting have also been applied to process biodegradable and bioresorbable materials with controllable and reproducible porosity and well-defined 3D microstructures [5-8].

Marine skeletal material is usually made of  $\text{CaCO}_3$  in the crystalline form of calcite and aragonite and silicated  $\text{SiO}_2$  materials combined with  $\text{Mg}(\text{OH})_2$ . Organisms from different species of corals and hydrocorals have a wide variety of skeletal architectures and crystalline structures [9]. Coralline carbonate derivatives, mostly coralline hydroxyapatite, are currently being used mostly as bone filler or nonweight-bearing areas and orbital implants [10]. The internal structure of some coral species is very similar to porous structure of bone and replica of porous calcium carbonate can be converted to highly biocompatible and osteogenic tricalcium phosphate and/or hydroxyapatite by a hydrothermal process [11, 12].

Chitin and chitosan are biologically renewable, biodegradable, biocompatible, non-toxic and biofunctional [13]. The use of chitosan together with bioceramics such as calcium phosphate as a scaffold material for tissue engineering applications has been reported previously by a number of researchers [14-16]. The incorporation of bioceramics has been shown to increase osteoconductivity and improved mechanical strength greatly [17, 18].

Chitosan fibers, which can be easily extended into three-dimensional structures of woven, knitted and nonwoven are widely used in a variety of biomedical applications, including sutures, wound dressing, and artificial hair [19, 20]. This interest is mainly derived from the fact that chitosan is a natural

polymer that shows well-known wound acceleration ability and a biological aptitude to stimulate cell proliferation. Depending on the processing conditions, chitosan fibers can present good mechanical properties. Several authors have described the improving the mechanical strength of fibers from chitosan [21-23]. Adequate mechanical properties can make chitosan based materials adequate for the developing of tissue engineering scaffolds that can be used for bone or cartilage regeneration.

The aim this study is the development of a composite material from coralline origin hydroxyapatite (HA) particles and chitosan fibers for use in tissue engineering or in guided tissue regeneration. By orienting the cylindrical coral particles (microchannels run parallel along the particle length) in one direction, an anisotropic material similar to biologic structure of bone can be produced. The bone forming cells osteocytes are known to be arranged in concentric layers called lamellae. In turn, lamellae surrounds central microscopic channels known as haversian canals, through which run capillaries and nerves. Haversian canals and surrounding lamellar structure are oriented parallel to bone structure. It is believed that a scaffold structure mimicking these arrangements can provide a guided bone ingrowth and correct vascularization of biomaterial inside the body.

Since coralline origin HA granules are prone to damage from mechanical stirring or harsh handling procedure, a new processing method was suggested in order to blend cylinder shaped coralline HA particles with chitosan fibers. In this method, semi-cylinder parallel channels (1 mm in width and deep) were prepared in a mould for holding and orienting the particles in one direction. This composite material was reinforced with chitosan fibers along and right angle to channels and finally, a membrane was used to cover the material in the mould. After obtaining a replica of mould channels over the membrane, thicker scaffolds can be produced by physical clamp fixing of subsequent replicas of coralline HA to each other.

## **2. Materials&Methods**

Chitosan (deacetylation degree 87 %), acetic acid, and sodium hydroxide were obtained from Sigma Chemical Co. (St. Louis, USA). Methanol was obtained

from Merck Chemical Co. (Germany). Sodium sulphate was obtained from Aldrich Chemical Co. All the other chemicals used were of analytical grade.

## **2.1. Preparation of coralline origin HA reinforced composite material**

### **2.1. 1. Chitosan fiber preparation**

Chitosan fibers were produced as previously reported [24]. In brief, chitosan was dissolved in aq. 2 % (v/v) acetic acid solution in 5 % (w/v) concentration by stirring magnetically at room temperature overnight. Methanol was added to dilute the viscous solution for easy injection until reaching 3 % (w/v) final concentration. Glycerol was used as a plasticizer (2.5 % (w/w)). After filtration with a cloth filter, solution was placed in an ultrasonic bath to remove the air bubbles. The solution was allowed to remain at room temperature overnight for aging. The clear solution was injected into a coagulation bath at 40 °C, (30 % 1N Na<sub>2</sub>SO<sub>4</sub>, 10 % 1N NaOH and 60 % distilled water). The formed fibers were kept in this coagulation medium for one day and then washed several times with distilled water. They were suspended in aqueous 30 % methanol for 4-5 h and then in aqueous 50 % methanol overnight. The chitosan filaments were wound on the cylindrical support and the fibers were dried at room for one day.

### **2.1.2. Chitosan membrane preparation**

Chitosan membranes were made by a simple solvent casting technique. The chitosan was dissolved in aqueous acetic acid solution (1 % (w/v)), and then was casted onto a plastic petri dishes in a ratio of 0.25g/cm<sup>2</sup>. Membranes were then allowed to dry slowly in an incubator at 37 °C for 3 days.

### **2.1.3. Assembly of coralline origin HA granules, chitosan fibers, and membrane**

A chitosan-coralline origin HA slurry was obtained by careful mixing chitosan solution (3 %, (w/v)) with prewetted HA microgranules in 1/1 ratio (w/w). The slurry was then placed into channel spaces by means of a gentle smear process (Figure 1).

Over the coralline origin HA filled spaces, chitosan fibers were aligned as one set parallel and another set right angle to channel direction to produce a chess like pattern (Figure 2). Finally, a chitosan membrane was placed over the coralline origin HA particles and the fiber network. In order to provide good adhesion between membrane and wet particles, a weight was applied over the membrane and let to act overnight. The assembly with the mould was placed to an oven at 37 °C to dry the material. Special care was given to peel off the composite material from the mould. Released material was stored in desicator until further assembly.

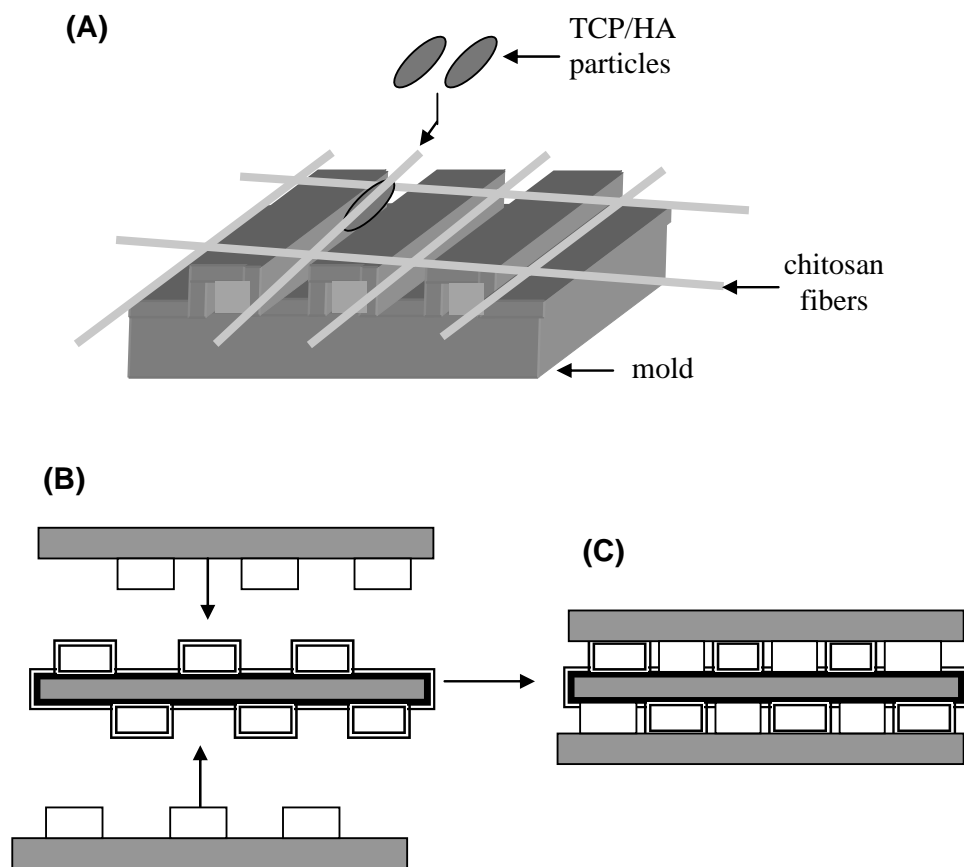


Figure 1. Schematic representation of the preparation method of coralline origin HA-chitosan fiber composite using a multichannel mould (A); Principle of production of thicker scaffolds by clasp fixing of TCP/HA replica complexes (B, C).

## **2.2.Cytotoxicity assays**

The cytotoxicity of leachables of the tested material was evaluated by using cell culture methods, namely short MEM (minimum essential medium) extraction test (72 hours), according to ISO/EN 109935 guidelines [25].

### **2.2.1. Cell culture**

A cell line of mouse long fibroblasts (L929) was selected for all cytotoxicity assays. Cells were grown in Dulbecco's modified eagle medium (DMEM, Sigma), supplemented with 10 % of Foetal Bovine Serum (Biochrome) and 1 % of antibiotics/antimicrobics solution (Sigma) until they reach confluency. Twenty-four hours before the cytotoxicity tests start, cells were trypsinized and seeded (n= 3 per tested condition) on 24 and 96 well plates using a density of  $7 \times 10^4$  cells/cm<sup>2</sup>.

### **2.2.2. MEM extraction test (72 hours)**

The materials (n= 3) were incubated in 10 ml of complete culture medium (2.5 cm<sup>2</sup>/ml) (1) for 24 hours at 37 °C under constant agitation. In the end of the 24 hours the extraction fluids were filtered (45 µm of pore size).

#### *Morphological evaluation*

For morphological evaluation, culture medium present in the 24 well plates was replaced by 2 ml of extraction fluid and incubated for 72 hours at 37 °C in a humidified atmosphere containing 5 % of CO<sub>2</sub>. After 72 hours the reaction of the cells to the extracts was evaluated by means of light microscopy and compared to the negative control (cells incubated with standard culture medium) and positive control (latex rubber). A score for confluency of the monolayer, degree of floating cells and change of cellular morphology was then calculated based on the values posted on Table 1. Cells were also trypsinized, the percentage of growth inhibition was determined through trypan blue exclusion test and a score was obtained after correction for the value of positive and negative controls. The scores were then combined (four parameters have equal weight) resulting in a final cytotoxic response index ranging from 0 to 8 (Table 2).



Table 1. Quantitative and qualitative scores used in the cytotoxicity tests.

Score	<u>Confluency</u> (%)	<u>Floating cells</u> (%)	Change of cellular morphology	<u>Inhibition of cell growth</u> (%)
0	100	0	No changes during test period	0-10
1	90-100	0-5	Slight changes, few cells affected	10-30
2	60-90	5-10	Mild changes, some cells round/spindle shaped	30-50
3	30-60	10-20	Moderate changes, many cells round/spindle	50-70
4	0-30	> 20	Severe changes, about all cells show morphological changes	70-100

Table 2. Cytotoxicity index

Cytotoxic Response	Reactivity	Pass/Fail
0-1	None	Pass
1-3	Slight	Pass
3-5	Mild	Retest
5-7	Moderate	Fail
7-8	Severe	Fail

### *Cell viability assay*

After 24 hours of cell seeding culture medium was replaced by 200  $\mu$ l of extraction fluid and incubated for 72 hours at 37 °C in a humidified atmosphere containing 5 % of CO<sub>2</sub>. After 72 hours cell viability was assessed by using Cell Titer 96<sup>®</sup> One solution Cell proliferation Assay kit (Promega, USA). This test is based on the bioreduction of the substrate, (3-(4,5-dimethylthiazol-2-yl)-5-(3-carboxymethoxyphenyl)-2(4-sulfophenyl)-2H tetrazolium) (MTS), into a brown formazan product by NADPH or NADP produced by dehydrogenase enzymes in

metabolically active cells [26, 27]. For the assay to occur extraction fluids were removed and 100  $\mu$ l of a mixture of culture medium without FBS and MTS in 5:1 ratio were added into each well. Cells were then incubated for three hours at 37  $^{\circ}$ C in a humidified atmosphere containing 5 % of CO<sub>2</sub>, in the end of which optical density was read at 490 nm in a plate reader (Molecular Devices, USA). Results are plotted as percentage of negative control.

### **2.3. Swelling test**

In order to test the swelling behaviour, the scaffold was cut into five small pieces and each piece was immersed in 0.154 M NaCl aqueous isotonic saline solution (pH 7.4). The samples were taken out from solution at various time intervals being weighted with an analytical balance. The experiment was continued until reaching of an equilibrium value.

The swelling ratio of the samples was calculated according to the following equation:

$$\% S = (m_w - m_i) / m_i \times 100 \quad (1)$$

where % S is the percentage of swelling,  $m_w$  is the weight of the wet sample after immersion in the NaCl solution. Average values were used to determine the swelling ratio of scaffold for each of the time points.

## **3. Results and discussion**

### **3.1. Coralline origin HA/chitosan composite material preparation**

Light transmission microscopy analysis of the composite material showed that most of coralline origin HA cylinder bodies were aligned along channel direction. Chitosan microfibers are seen to be running along coralline origin HA granules and making chess structure between coralline origin HA replica and chitosan membrane (Figure 2.B). Chitosan membrane was observed to hold both granules and fibers securely. The strength of composite materials can be increased greatly with the incorporation of fibers. In this respect, the coralline origin HA filled channels were supported by parallel chitosan fibers. A chess-like

structure was produced, so that the load can be distributed evenly over the complex.

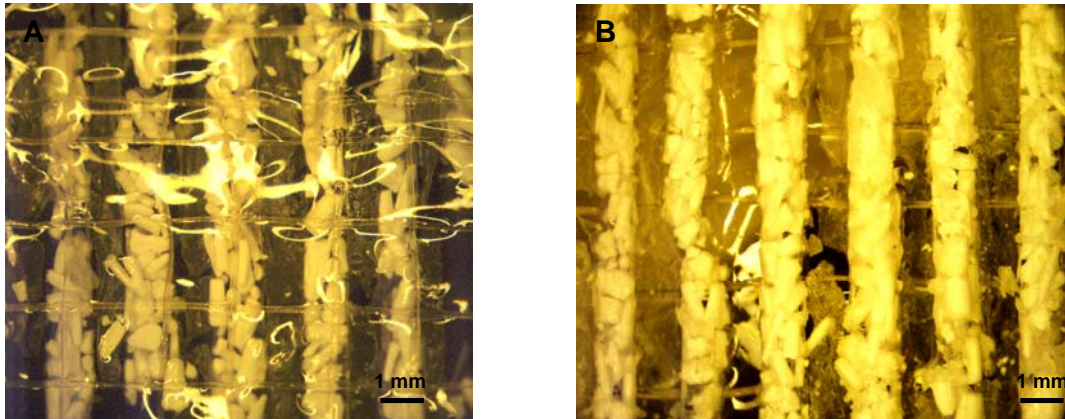


Figure 2. Light transmission microphotographs of HA granules (white cylinder bodies) and chitosan fibers (indicated by arrows) over chitosan membrane: (A) Front view of complex and (B) back view of complex.

The parallel distribution of coralline origin HA particles is especially important because, fine microchannel architecture of cylindrical structures align in longitudinal direction of ceramic structure. By that way, highly oriented channel networks can be created through the composite material. This pattern would mimic the haversian network of natural bone and as a result, a correct remodelling of biomaterial by infiltration of bone tissue and extensive vascularization at implantation site can be expected. This will be analysed in future in-vivo studies.

### 3.2. Cytotoxicity assays

With regard to short-term MEM extract test there was no cell growth inhibition detected after the trypan blue exclusion test ( $0.00 \pm 0.00$ ). Moreover cells revealed similar morphologies and proliferation patterns when compared with the negative control, obtaining a score of 1 in the cytotoxicity index (Table 2) showing in this sense that these materials were non-toxic. This type of result is not typical at all for biodegradable polymers.

Regarding cell viability assay (MTS test), cells produced large amounts of the brown formazan product, which indicates a normal metabolism (Figure 3). L929 cells incubated with composite extracts showed a good incorporation and

metabolization of MTS, displaying only a slight inhibition of the metabolism when compared to negative control.

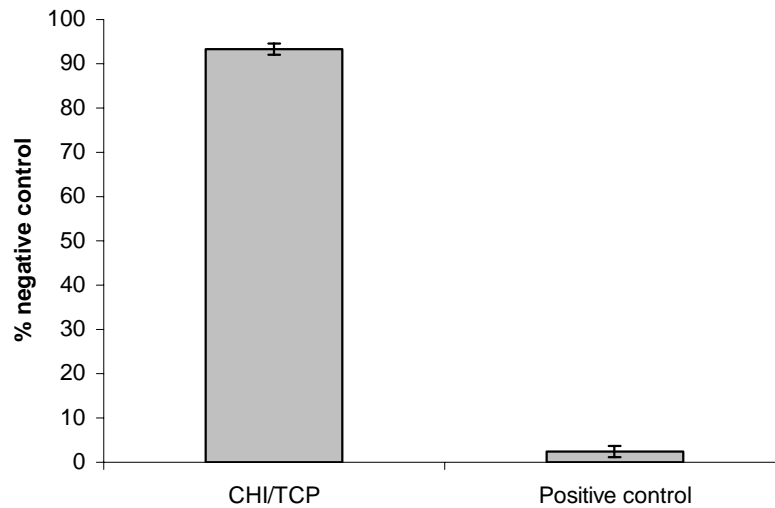


Figure 3. Cell viability of L929 cells after incubation with test and control extracts over a period of 72h. Results based on optical measurements.

As a result of the cytotoxicity experiments it can be said that the chitosan/coralline origin HA scaffolds are non-toxic and hence can be used for further studies within the biomaterials/tissue engineering field.

### 3.3. Swelling test

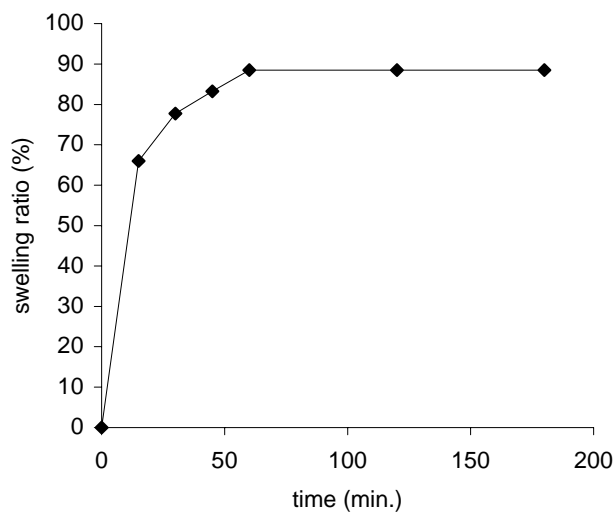


Figure 4. Swelling curve of coralline HA-chitosan composite in physiological saline (pH 7.4).

Figure 4 shows that the composite material was swelled up to 88 % and no further swelling was observed afterwards. Upon long-term incubation of scaffold material in a physiological saline solution, no physical alteration or deformation in coralline origin HA replica or fiber alignment was detected. Chitosan material is known to swell in aqueous solutions and sometimes this property can be used to secure biomaterial inside the implantation space [28], taking advantage of a press-fitting mechanism. The developed composite materials maintain their integrity when immersed in physiological media, even though they showed a brief swelling. Consequently, it can be expected that in implantation site it will show no further change in structure due to swelling.

#### **4. Conclusions**

A 3D composite of coralline origin HA microgranules was obtained by using a multichannel mould processing and chitosan as reinforcing material. The composite material showed parallel orientation of cylindrical coralline origin HA bodies along channel direction and good adhesion of particles to chitosan fibers and the outer chitosan membrane. MEM extraction test indicated no cell growth inhibition as determined by the trypan blue exclusion method. MTS test with the composite showed more than 90 % cell viability compare to negative controls. The cytotoxicity assays confirmed that the composite material is non-toxic. The swelling test in physiological medium indicated 88 % (w/w) swelling in one hour and afterwards no further change was observed. Long-term incubation of the composite in aqueous medium showed no change in integrity of the constituents of the composite material. Consequently the developed complex architectures presents a range of properties that might allow for their use in guided tissue regeneration and as tissue engineering scaffolds.

## References


1. Hutmacher, D.W., Scaffolds in tissue engineering bone and cartilage. *Biomaterials*, 2000. 21(24): p. 2529-2543.
2. Freed, L.E., Vunjak-Novakovic, G., Biron, R.J., Eagles, D.B., Lesnoy, D.C., Barlow, S.K., Langer, R., Biodegradable polymer scaffolds for tissue engineering. *Bio/Technology*, 1994. 12: p. 689-693.
3. Mikos, A.G., et al., Laminated 3-Dimensional Biodegradable Foams for Use in Tissue Engineering. *Biomaterials*, 1993. 14(5): p. 323-330.
4. Mikos, A.G., Temenoff, J.S., Formation of highly porous biodegradable scaffolds for tissue engineering. *Electronic Journal of Biotechnology*, 2000. 3: p. 114-119.
5. Ang, T.H., et al., Fabrication of 3D chitosan-hydroxyapatite scaffolds using a robotic dispensing system. *Materials Science & Engineering C-Biomimetic and Supramolecular Systems*, 2002. 20(1-2): p. 35-42.
6. Agarwala, M.K., Jamalabad, V.R., Langrana, N.A., Safari, A., Whalen, P.J., Danforth, S.C., Structural quality of parts processed by fused deposition. *Rapid Prototyping Journal*, 1996. 2: p. 4-19.
7. Sachs, E., Cima, M., Williams, P., Brancazio, D., Cornie, J., Three dimensional printing. Rapid Tooling and prototypes directly from a CAD model. *Journal of engineering for industry*, 1992. 114: p. 481-488.
8. Cima, L.G., et al., Tissue Engineering by Cell Transplantation Using Degradable Polymer Substrates. *Journal of Biomechanical Engineering-Transactions of the Asme*, 1991. 113(2): p. 143-151.
9. Barnes, D.J., Lough, J.M., Coral skeletons: Storage and recovery of environmental information. *Global Change Biology*, 1996. 2: p. 569-582.
10. Vago, R., et al., Hard tissue remodeling using biofabricated coralline biomaterials. *Journal of Biochemical and Biophysical Methods*, 2002. 50(2-3): p. 253-259.
11. Holmes, R.E., Bone Regeneration within a Coralline Hydroxyapatite Implant. *Plastic and Reconstructive Surgery*, 1979. 63(5): p. 626-633.
12. Vuola, J., et al., Compressive strength of calcium carbonate and hydroxyapatite implants after bone-marrow-induced osteogenesis. *Biomaterials*, 1998. 19(1-3): p. 223-227.

13. Hirano, S., Chitin and chitosan as novel biotechnological materials. *Polymer International*, 1999. 48(8): p. 732-734.
14. Yamaguchi, I., et al., Preparation and mechanical properties of chitosan/hydroxyapatite nanocomposites. *Bioceramics*, 2000. 192-1: p. 673-676.
15. Ito, M., et al., Effect of hydroxyapatite content on physical properties and connective tissue reactions to a chitosan-hydroxyapatite composite membrane. *Journal of Biomedical Materials Research*, 1999. 45(3): p. 204-208.
16. Zhang, Y. and M.Q. Zhang, Microstructural and mechanical characterization of chitosan scaffolds reinforced by calcium phosphates. *Journal of Non-Crystalline Solids*, 2001. 282(2-3): p. 159-164.
17. Reis, R.L., Cunha, A.M., Bevis, M.J., Using Nonconventional Processing Routes to Develop Anisotropic and Biodegradable Composites of Starch-Based Thermoplastics Reinforced with Bone-Like Ceramics. *J. Appl. Med. Polym.*, 1998. 2: p. 49-53.
18. Reis, R.L., et al., Structure development and control of injection-molded hydroxylapatite-reinforced starch/EVOH composites. *Advances in Polymer Technology*, 1997. 16(4): p. 263-277.
19. Muzzarelli, R.A.A., Biochemical Significance of Exogenous Chitins and Chitosans in Animals and Patients. *Carbohydrate Polymers*, 1993. 20(1): p. 7-16.
20. Takanori, M., Takashi, K., Shojiro, H. and J.P. (1991), J. Patent, Editor. 1991.
21. Knaul, J.Z., S.M. Hudson, and K.A.M. Creber, Improved mechanical properties of chitosan fibers. *Journal of Applied Polymer Science*, 1999. 72(13): p. 1721-1732.
22. Knaul, J., et al., Improvements in the drying process for wet-spun chitosan fibers. *Journal of Applied Polymer Science*, 1998. 69(7): p. 1435-1444.
23. Hirano, S., et al., Chitosan staple fibers and their chemical modification with some aldehydes. *Carbohydrate Polymers*, 1999. 38(4): p. 293-298.

24. Tuzlakoglu, K., et al., Production and characterization of chitosan fibers and 3-D fiber mesh scaffolds for tissue engineering applications. *Macromolecular Bioscience*, 2004. 4(8): p. 811-819.
25. 10993-5, I.E., Biological Evaluation - Part 5. Tests for Cytotoxicity: in Vitro Methods. 1992.
26. Cory, A.H., Owen, T.C., Barltrop, J.A., Cory, J.G., *Cancer Commun.*, 1998. 7: p. 207.
27. Salih, V., et al., Development of soluble glasses for biomedical use Part II: The biological response of human osteoblast cell lines to phosphate-based soluble glasses. *Journal of Materials Science-Materials in Medicine*, 2000. 11(10): p. 615-620.
28. Lauto, A., et al., Self-expandable chitosan stent: design and preparation. *Biomaterials*, 2001. 22(13): p. 1869-1874.







**I am among those who think that science has a great beauty. A scientist is a child placed before a natural phenomena which impress him like a fairy tale**

**Marie Curie**



## **CHAPTER V**

### **FORMATION OF BONE-LIKE APATITE LAYER ON CHITOSAN FIBER MESH SCAFFOLDS BY A BIOMIMETIC SPRAYING PROCESS**

## **Abstract**

Bone-like apatite coating of polymeric substrates by means of biomimetic process is a possible way to enhance the bone bonding ability of the materials. The created apatite layer is believed to have an ability to provide a favorable environment for osteoblasts or osteoprogenitor cells.

The purpose of this study is to obtain bone-like apatite layer onto chitosan fiber mesh tissue engineering scaffolds, by means of using a simple biomimetic coating process and to determine the influence of this coating on osteoblastic cell responses. Chitosan fiber mesh scaffolds produced by a previously described wet spinning methodology were initially wet with a Bioglass®-water suspension by means of a spraying methodology and then immersed in a simulated body fluid (SBF) mimicking physiological conditions for one week. The formation of apatite layer was observed morphologically by scanning electron microscopy (SEM). As a result of the use of the novel spraying methodology, a fine coating could also be observed penetrating into the pores, that is clearly within the bulk of the scaffolds. Fourier Transform Infrared spectroscopy (FTIR-ATR), Electron Dispersive Spectroscopy (EDS) and X-ray diffraction (XRD) analysis also confirmed the presence of apatite-like layer. A human osteoblast-like cell line (SaOs-2) was used for the direct cell contact assays. After two weeks of culture, samples were observed under the SEM. When compared to the control samples (unmodified chitosan fiber mesh scaffolds) the cell population was found to be higher in the Ca-P biomimetic coated scaffolds, which indicates that the levels of cell proliferation on this kind of scaffolds could be enhanced. Furthermore, it was also observed that the cells seeded in the Ca-P coated scaffolds have a more spread and flat morphology, which reveals an improvement on the cell adhesion patterns, phenomena that are always important in processes such as osteoconduction.

## 1. Introduction

Bone is a complex, dynamic and highly vascular tissue with a large amount of extracellular matrix. In nanoscale, bone matrix consists of highly organized collagen fibers surrounded by apatite crystals [1]. Due to this very specialized structure, repair or replacement of damaged or traumatized bone still remains as a serious problem in surgery. For many years, autografts and allografts have been used for bone repair. However, there are many limitations and complications in the use of autografts and allografts, including limited supply, donor site morbidity and transfer of diseases.

Engineering of bone tissue is a new approach to recreate complexity, stability, and biologic function of bone tissue. The most common strategy for the tissue engineering of bone is to use a scaffold combined with osteoblast or the cells that can mature/differentiate into osteoblasts and regulating factors that promote cell attachment, differentiation and mineralized bone formation [2]. To serve as a scaffold for bone tissue engineering, the material should be biocompatible, biodegradable, and porous with an interconnective pore structure in order to allow nutrients and metabolites to permeate. Furthermore, it must also be osteoconductive, so that osteoblasts and osteoprogenitor cells can attach and migrate in the scaffold.

Calcium phosphate ceramics and bioactive glasses have been proposed to be used as a scaffold for bone tissue engineering due to their excellent osteoconductivity [3, 4]. It has been shown that they can bind to bone through an apatite layer at the interface or bind directly to bone [5]. However, they can not serve alone as a scaffold because of their brittleness and low resistance against impact loading.

Biodegradable polymers have been proposed as possible alternatives and received much attention as bone replacement materials [6-8]. They can be easily processed into 3-D porous structures with a proper degradation rate and mechanical strength. However, most of them are not show bioactivity without any surface modification. To overcome this problem, the surface of the material can be coated with HA or apatite. A number of methods, such as plasma spraying [9],

ion sputtering [10], laser deposition [11], sol-gel deposition [12], dip coating sintering [13], have been used for apatite coating of the material surfaces. However, these processes need very high temperatures or very high/low pH that can not be applied to the polymeric materials. In addition, the apatite formed by these processes is usually highly crystalline and has different crystal structure than that in natural bone apatite. Another drawback in these processes is the difficulties in obtaining a homogenous and a thin layer of coating on the surface of the material.

Biomimetic coating using simulated body fluid (SBF) has been developed by Kokubo and co-workers as an alternative to the methods discussed above [14]. They have reported that the formed apatite, so-called bone-like apatite, is more similar to natural bone with a low crystallinity and nano-crystal size which is also an important issue in its degradation. Moreover, the conditions that are used in this process are very mild and allow applying a variety of polymeric and non-polymeric surfaces [15, 16]. For instance, Reis et al. [17-19] adapted and used this methodology for starch-based biodegradable polymers. Regarding the mechanism, it has been shown that the functional groups on the polymer surface, such as Si-OH, Ti-OH and carboxyl or carboxylate, are the responsible for the apatite nucleation in SBF. Once the material with a functional surface immersed in SBF, which is already supersaturated with ions that constitute apatite, apatite nuclei starts to form and grow into a dense and uniform bone-like apatite layer [15]. One way to introduce functional Si-OH group on the polymeric surfaces is to face the polymer with Bioglass® particles before immersion in SBF [20].

The objective of the present study is to obtain bone-like apatite layer on chitosan fiber mesh scaffolds by using the biomimetic approach. We developed a new methodology based on a simple spraying process in order to have a homogeneous coating on these complex structures. Moreover, we also tested the scaffolds with human osteoblast-like cell line (SaOs-2) to determine the influence of bone-like apatite coating on cell adhesion and viability.

## **2. Materials&Methods**

Chitosan (deacetylation degree 87 %), was obtained from Aldrich Chemical Co. Bioglass® with particle size of 5µm was kindly supplied by US Biomaterials Corp. (Florida, USA). All the other chemicals used were of analytical grade.

### **2.1. Production of Chitosan Fiber Mesh Scaffolds**

Chitosan fibers were produced as previously reported [21]. In brief, chitosan was dissolved in aq. 2% (v/v) acetic acid solution in 5% (w/v) concentration at room temperature overnight. Methanol was added to dilute the viscous solution for easy injection until reaching 3% (w/v) final concentration. Glycerol was used as a plasticizer (2.5% (w/w)). After filtration with a cloth filter, the solution was placed in an ultrasonic bath to remove the air bubbles. The clear solution was injected into a coagulation bath (30% 1N Na<sub>2</sub>SO<sub>4</sub>, 10% 1N NaOH and distilled water). The formed fibers were kept in this coagulation medium for one day and then washed several times with distilled water. They were then suspended in an aqueous 50% methanol solution for 1h and subsequently in 100% methanol for 3h. The fibers were then put in a plastic cylindrical mould and dried at 60°C overnight.

### **2.2. Biomimetic Coating**

A simple methodology was developed for the biomimetic coating experiments. The method is basically based on spraying a Bioglass®/water suspension on the surface of the scaffolds. This spraying methodology allows for the coating of the bulk of the scaffold. Briefly, a certain amount of Bioglass® was suspended in ultra-pure water. Produced scaffolds could then be wet with this Bioglass®-water suspension by using this simple methodology. After drying for a certain time under air flow, each sample was immersed in 40ml of simulated body fluid (SBF) (x1) (see Figure 1).

The ion concentrations of SBF were approximately equal to those of human blood plasma. The tubes were put in an incubator at 37°C for 7 days. The



solution and the tubes were renewed next day. After the first day of immersion, renewal was every 2 days for the solution. In the end of the immersion period, samples were washed with distilled water and dried at room temperature.

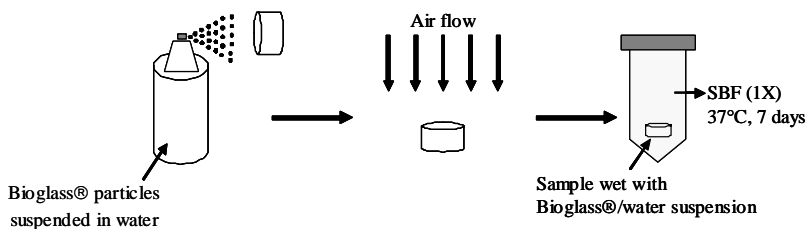


Figure 1. Schematic representation of a novel biomimetic Ca-P coating process using a simple spray.

### 2.3. Characterization of Ca-P Coated Scaffolds

In order to analyze the morphology of the Ca-P layer formed on the scaffolds, the samples were mounted onto brass stubs, sputter coated with gold and analyzed under a Scanning Electron Microscope (SEM) at an accelerating voltage 15kV. Electron Dispersive Spectroscopy (EDS) was also used to determine the presence of Ca and P in bioactive layers. To evaluate the changes on the chemical structure of sample surface, Fourier Transform Infrared Spectroscopy (FTIR-ATR) was used. Thin Film X-ray diffraction (TF-XRD) was used for identifying the crystalline phases present, and characterizing the crystalline/amorphous nature of the formed Ca-P bioactive layers.

### 2.4. Cell Culture Studies with Osteoblasts

A human osteoblasts SaOs-2 cell line was selected to study cell morphology, attachment and proliferation onto Ca-P coated chitosan fiber meshes scaffolds. Cells cultured in DME Media (Sigma), enriched with 10% FBS (Biochrome) and 1% antibiotic/antimicrobial solution (Sigma) were seeded directly over samples in a concentration of  $2 \times 10^6$  cells/scaffold. Incubation was performed at 37 °C (5%

CO<sub>2</sub>, 100% humidity) for 3 weeks. Uncoated samples were used as a control. After each incubation period, samples were washed with Phosphate Buffer Saline (PBS, Sigma) solution and fixed in gluteraldehyde 2.5% (v/v). For Scanning Electronic Microscopy (SEM) observation, samples were previously dehydrated in increasing alcohol concentrations (50%, 70%, 90% and 100%), air-dried and sputter coated with gold.

### *Cell viability*

A MTS assay was carried out to determine the cell viability after 3 weeks of culture by using Cell Titer 96<sup>®</sup> Aqueous One Solution Cell proliferation Assay kit (Promega, USA). This test is based on the bioreduction of the substrate, (3-(4,5-dimethylthiazol-2-yl)-5-(3-carboxymethoxyphenyl)-2(4-sulfophenyl)-2H tetrazolium) (MTS), into a brown formazan product by NADPH or NADP produced by dehydrogenase enzymes in metabolically active cells. According to the standard procedure, the triplicates of samples were placed in a new plate and fresh medium was added to each well. MTS reagent in 5/1 ratio was added to each well and then incubated for three hours at 37 °C in a humidified atmosphere containing 5% of CO<sub>2</sub>. A 100µl of incubated medium was transferred to 96-well plate culture plate and the optical density was read at 490nm in a micro-plate reader (Synergy HT, Bio-tek).

### *Alkaline Phosphatase (ALP) Activity*

In order to determine the amount of alkaline phosphatase (ALP) produced by the cells seeded on the scaffolds, scaffolds/ cells constructs were washed, freeze-thawed and sonicated after 3 weeks of culture. p-Nitrophenyl phosphate (pNPP) was added to the supernatant in the ratio of 1/3 and incubated at 37°C for 1 h. The enzyme reaction was then stopped by a solution containing 2 M NaOH and 0.2 mM EDTA in distilled water. The absorbance of p-nitrophenol (pNP) formed was determined at 405 nm with a reference filter at 620 nm. A standard curve was made using pNP values ranging from 0 to 600 µmol/ml. The results were expressed as µmol of pNP produced/ml/h.

### 3. Results&Discussion

#### 3.1. Biomimetic Coating

The scaffolds used in this study were porous chitosan fiber meshes of a cylindrical shape with a diameter of 1cm (Figure 2).

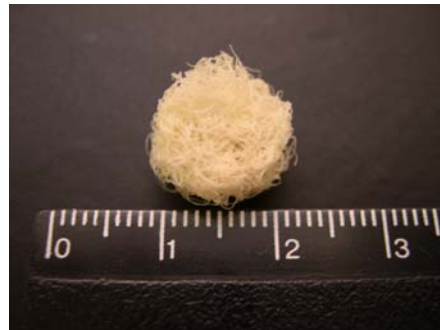


Figure 2. Chitosan fiber mesh scaffolds produced by wet spinning

The structure is made of randomly oriented fibers with an average diameter of 100 $\mu$ m and these fibers form a highly interconnected nest-like structure as it can be seen from SEM micrographs (see Figure 3.A and B). As we have reported before [21], these scaffolds have a very high water uptake ability, which can of course provide better adhesion of Bioglass® particles on the surface of the fiber during the biomimetic coating process. However the coating of biodegradable scaffolds with biomimetic Ca-P layers is rather difficult and not many examples of this can be found on the literature [22, 23].

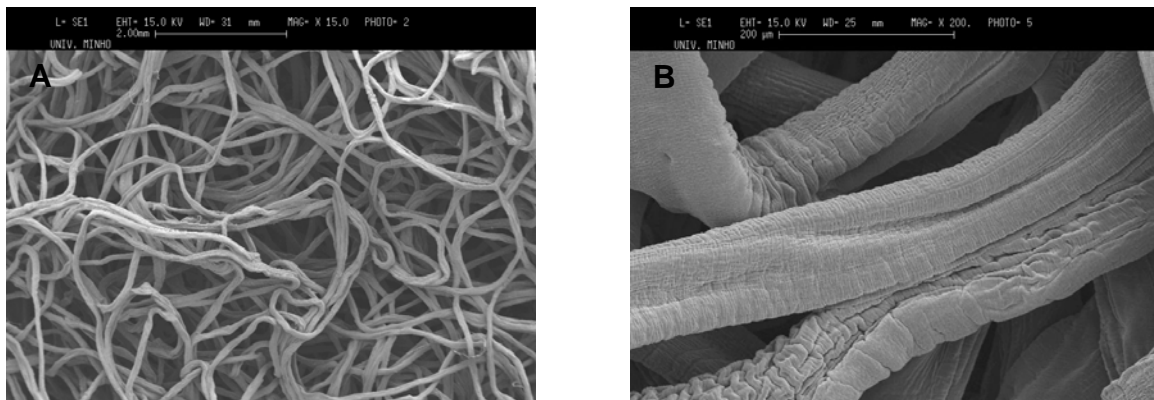


Figure 3. SEM micrographs of chitosan fiber mesh scaffolds; A) x15, B) x200

SEM micrographs of Ca-P coated chitosan fiber mesh scaffolds were given in Figure 4.

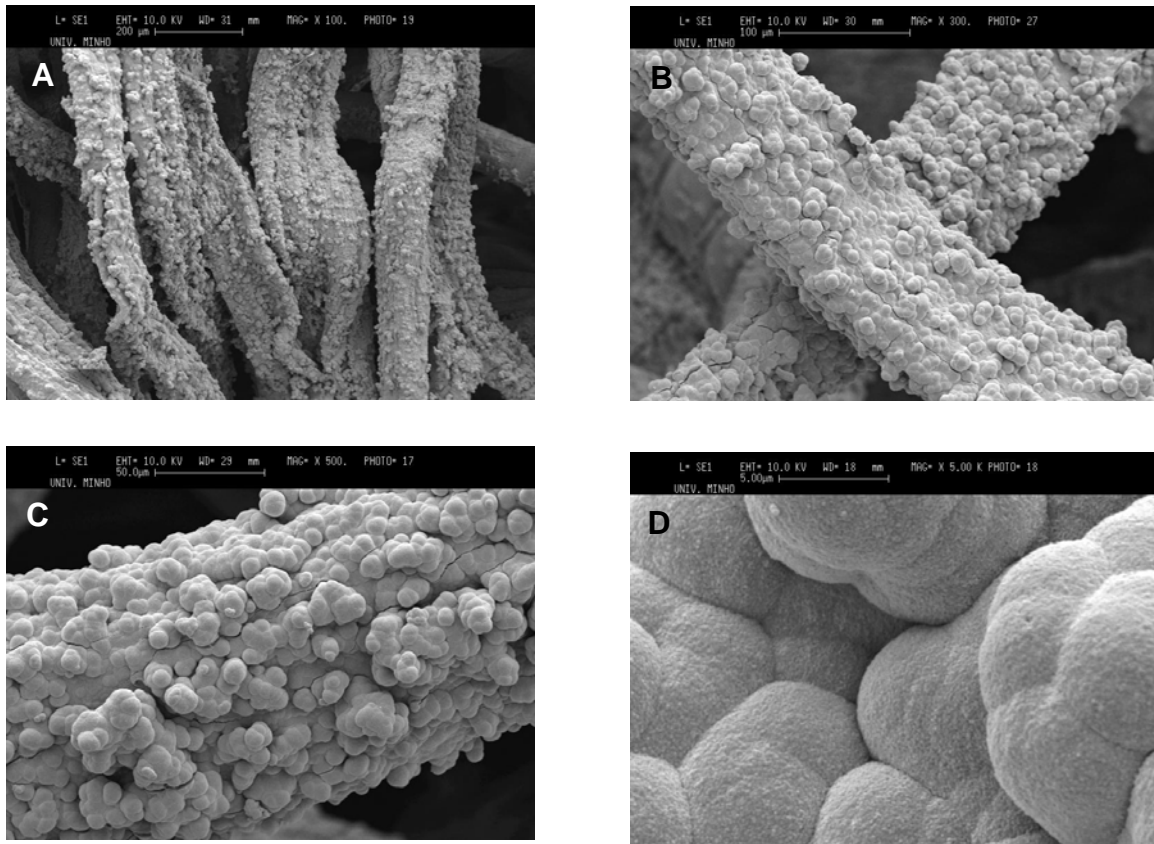


Figure 4. SEM micrographs of the developed coated scaffolds, exhibiting a fine and homogenous Ca-P layer onto chitosan fiber meshes surfaces; A) x100, B) x300, C) 500, D) x5000

After Bioglass® spraying to the samples, a fine and homogenous Ca-P layer was observed on their surface after 7 days soaking in SBF solution. Kokubo et al. [24, 25] proposed the mechanism of bone-like apatite formation on polymeric surfaces when CaO-SiO<sub>2</sub> glass particles are used as a nucleation-inducing agent. According to this mechanism, silicate ions released from the glass particles are attached on the polymer surface and Si-OH groups in the silicate ions induce the apatite nucleation on the surface. At the same time, the release of calcium ions from glass particles increases the ionic activity product of SBF with respect to apatite and accelerates the apatite nucleation. Finally, the apatite nuclei formed on the surface grow spontaneously by consuming Ca and P

ions from the fluid. Using this approach, many flat polymeric surfaces have been coated with bone-like apatite by rolling the samples in Bioglass®/water suspension [26]. However, the rolling process is not suitable for more complex surfaces due to the non-homogenous distribution of Bioglass® particles. Therefore, we developed a simple spraying method which allowed a homogenous distribution of glass particles on the scaffold surface as well as inside the structure. As a result of this method, a homogenous bone-like apatite layer was observed on the individual fibers. Moreover, it was also possible to see the typical cauliflower morphology of bone-like apatite layer in SEM micrographs with a higher magnification (Figure 4.D).

The EDS spectra of the coated samples confirmed the formation of apatite layer by showing the Ca and P elements (Figure 5). The typical Ca-P ratio was around  $1.6 \pm 0.10$  which is similar to natural bone apatite.

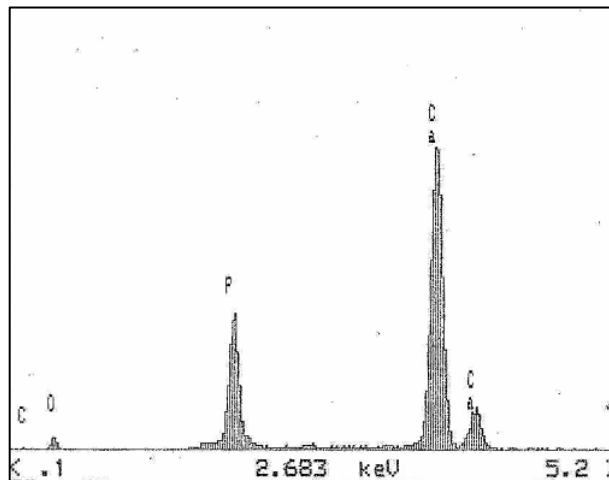


Figure 5. EDS spectra of Ca-P coated chitosan fiber mesh scaffolds.

Figure 6 shows FTIR spectra of control (uncoated chitosan fiber meshes) and biomimetic Ca-P coated chitosan fiber meshes. Uncoated samples presented the characteristic absorption bands of chitosan which are a wide band associated with  $\text{-OH}$  group at around  $3400\text{cm}^{-1}$  and a band associated with glycosidic linkage at around  $1050\text{cm}^{-1}$ . After Ca-P coating of the surface, the characteristic band attributed to  $\text{-OH}$  tend to disappear while a sharp band

appeared at  $1030\text{cm}^{-1}$  which is a characteristic P-O stretching band. The decrease in the intensity of  $-\text{OH}$  stretching group might be due to the increase in the carbonate substitution as has been reported by the others [27, 28]. It has been suggested that when the carbonate substitution increase, carbonate ions replace with hydroxyl ions [28]. These results demonstrated that the surfaces of the chitosan fibers were completely coated by a carbonated apatite layer.

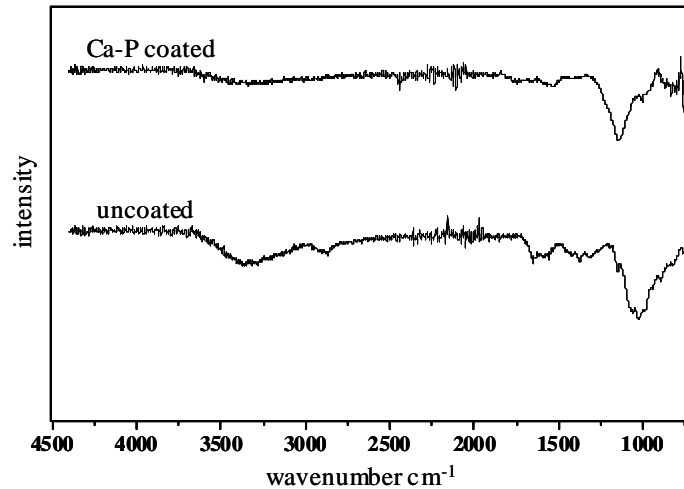


Figure 6. FTIR spectra of Ca-P coated sample and uncoated sample.

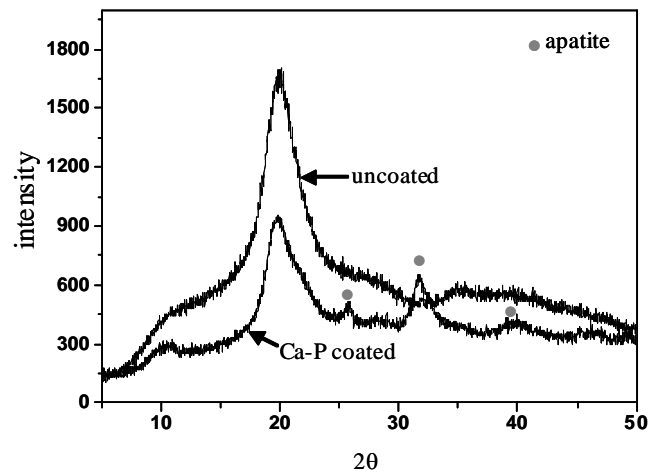


Figure 7. Thin-film XRD patterns of the chitosan fiber meshes immersed in SBF for 7 days.

Thin-film XRD of the samples immersed in SBF for 7 days is presented in Figure 7. The main diffraction peak at  $2\theta=32^\circ$  is a contribution of (211), (300) and (202) planes of apatite. Another main diffraction peak at  $2\theta=26^\circ$  indicated the (002) lattice plane of apatite crystals. Other diffraction peak of apatite appeared around at  $2\theta=40^\circ$  as it was marked in Figure 7. The broad peak at around  $2\theta=20^\circ$  was due to the chitosan. The intensity of this peak decreased after coating which confirms once again the apatite layer on the surface of fibers.

### 3.2. Cell Culture Studies with Osteoblasts

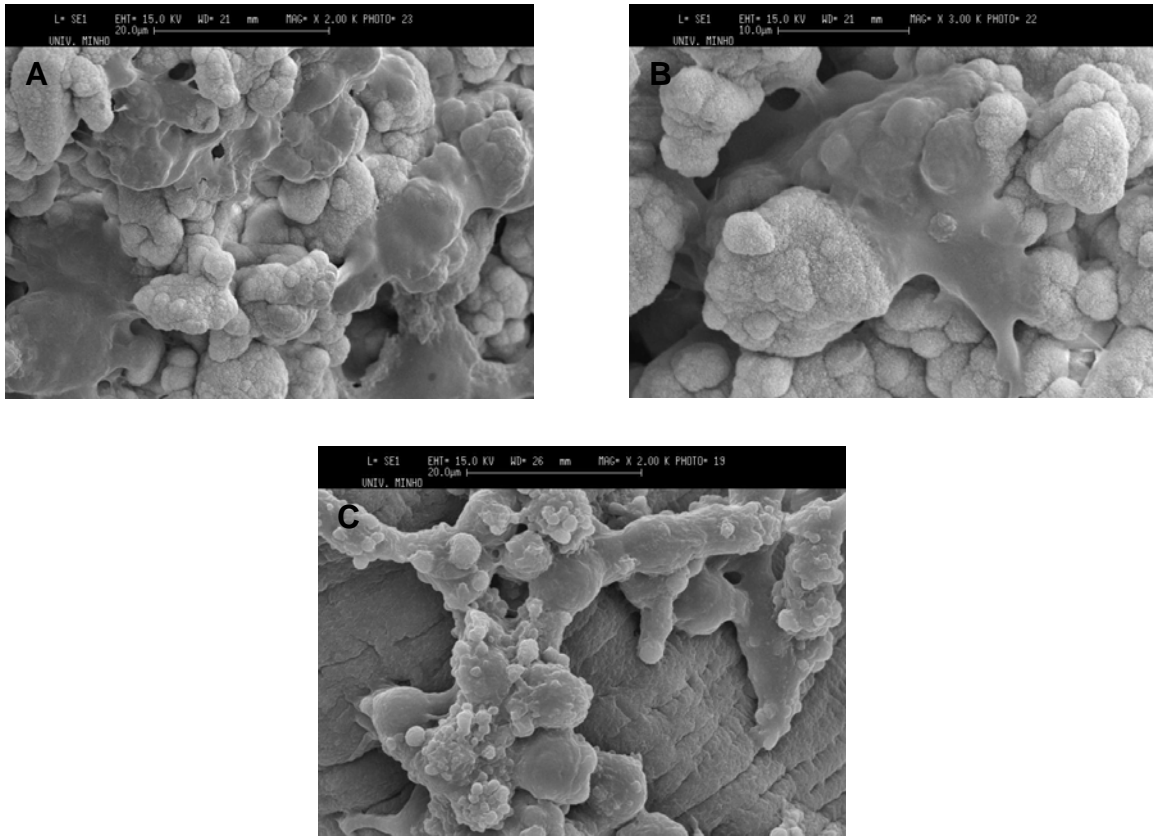


Figure 8. Human osteoblast like cells seeded on A) Ca-P coated (x2000), B) Ca-P coated (x3000) and C) uncoated (x2000) chitosan fiber mesh scaffolds after 2 weeks of culture.

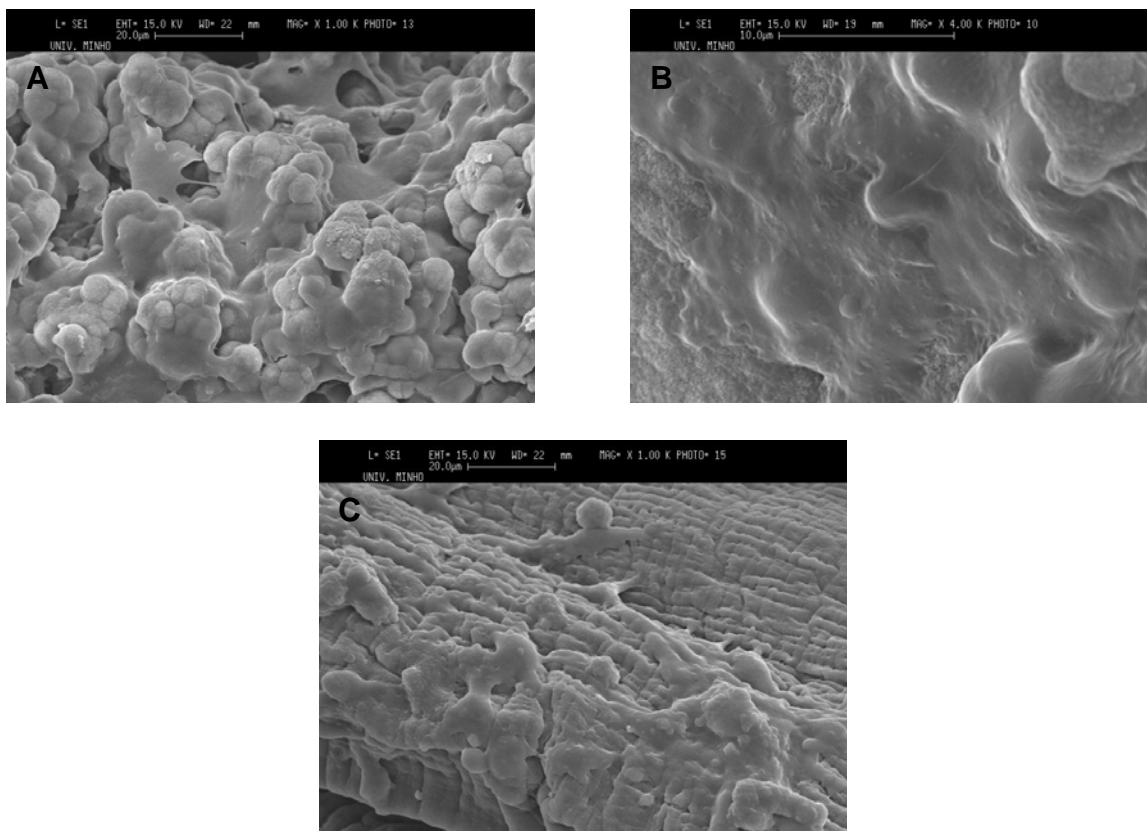


Figure 9. Human osteoblast like cells (SaOs-2) seeded on A) Ca-P coated (x1000), B) Ca-P coated (x4000) and C) uncoated (x1000) chitosan fiber mesh scaffolds after 3 weeks of culture.

Figure 8 and 9 exhibit the SEM micrographs of osteoblasts seeded on the surface of Ca-P coated and uncoated samples after 2 and 3 weeks of culture, respectively. The cells were observed to be able to attach and to proliferate in both surfaces. However, they seemed to be more spread and presented a different morphology when the surface was pre-coated with a Ca-P layer. This is a result of the changes in the surface chemistry of the scaffolds. Several investigators have reported that the surface chemistry and the topography can directly affect the osteoblast response and determine cell attachment and alignment [29-31]. Depending on the surface composition and the topography, protein, ligands and integrins can adsorb to the surface in different structures and adhesion kinetics [32]. Due to the different interaction between the adhesion ligands adsorbed to different surfaces and the adhesion receptors of the cells, cells can generate different adhesion signals. These adhesion signals influence



further cell attachment and morphology. In the present study, it was not possible to evaluate the effect of surface topography because of the irregular surface structure of the chitosan fibers. However, we can say that the surface chemistry has a clear influence on cell attachment and morphology. The difference on the cell spreading behaviour could also be observed clearly with a longer culturing time. The osteoblasts started to form a complete layer on the surface of fibers after 3 weeks of culture (Figure 9. B).

The Ca-P coating also influenced the long-term cell viability on the scaffolds. Figure 10 shows the MTS results after 3 weeks of culture. MTS is an indirect assay to determine the metabolic activity and number of the cells. As it can be seen, osteoblasts seeded on the Ca-P coated scaffolds showed higher O.D. value than control samples which means metabolic activity and number of cells were higher in the Ca-P coated samples. This can be related to the enhanced cell attachment on the Ca-P coated samples. In fact, it has been reported that initial cell attachment affects further proliferation of the cells [33].

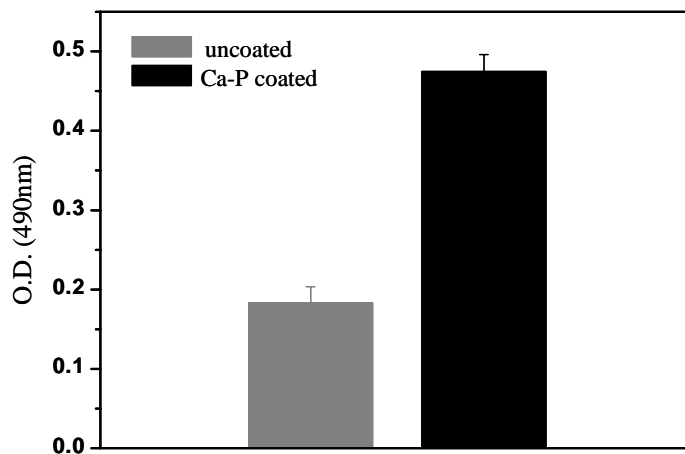


Figure 10. Cell viability and proliferation of human osteoblast like cells determined by MTS after 3 weeks of culture. Error bars represent means  $\pm$  SD for n=3.

ALP is a well-known enzyme used as a marker of the osteogenic phenotype, which catalyzes the hydrolysis of phosphate esters at an alkaline pH [34]. It has been also demonstrated that it plays an important role in bone matrix mineralization process. Figure 11 presents the ALP activity of the cells cultured

on the coated and control scaffolds. ALP activity of the cells seeded on the Ca-P scaffolds were found significantly higher than that on control. One possible reason for that can be the release of the  $\text{Ca}^{2+}$  ions from the coating to the culture medium. Matsuoka et al. [35] showed that ALP activity and osteogenic differentiation of osteoblastic cells increased if there is an increase of Ca concentration in culture medium by release from the apatite. However, further studies are still needed to understand the details of mechanism of the cellular response to Ca-P coating that is described herein.

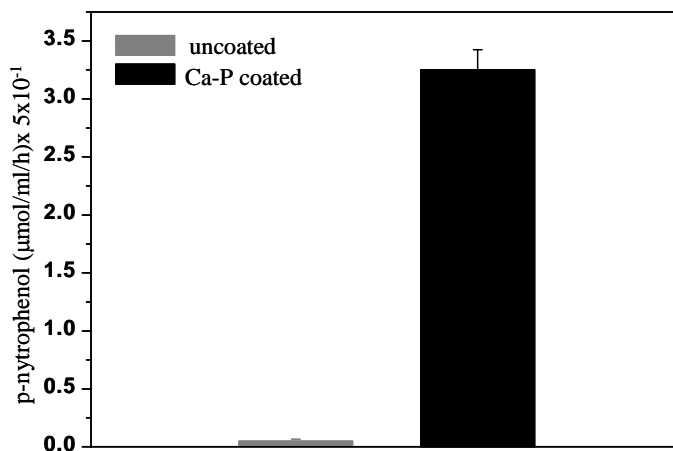


Figure 11. The ALP activity of human osteoblast like cells seeded on Ca-P coated scaffolds and control (uncoated scaffolds). Error bars represent means  $\pm$  SD for n=3

#### 4. Conclusions

A novel and simple biomimetic approach was described for the preparation of bone-like apatite coated chitosan scaffolds. Fiber mesh type scaffolds could be prepared from chitosan by a wet spinning method. A homogenous Ca-P coating was produced on the surface and the bulk of chitosan scaffolds by means of using the proposed methodology. After 7 days of immersion in the SBF solution, a fine and homogenous bone-like apatite layer was observed on the surface of chitosan fibers. Furthermore, osteoblasts adhered on Ca-P coated samples showed a more spread and distinct morphology. Higher cell numbers were observed on the coated scaffolds as compared to the uncoated samples. On the basis of these results, Ca-P coated scaffolds obtained by the proposed

biomimetic process can be useful to be used as a bone tissue engineering scaffolds.

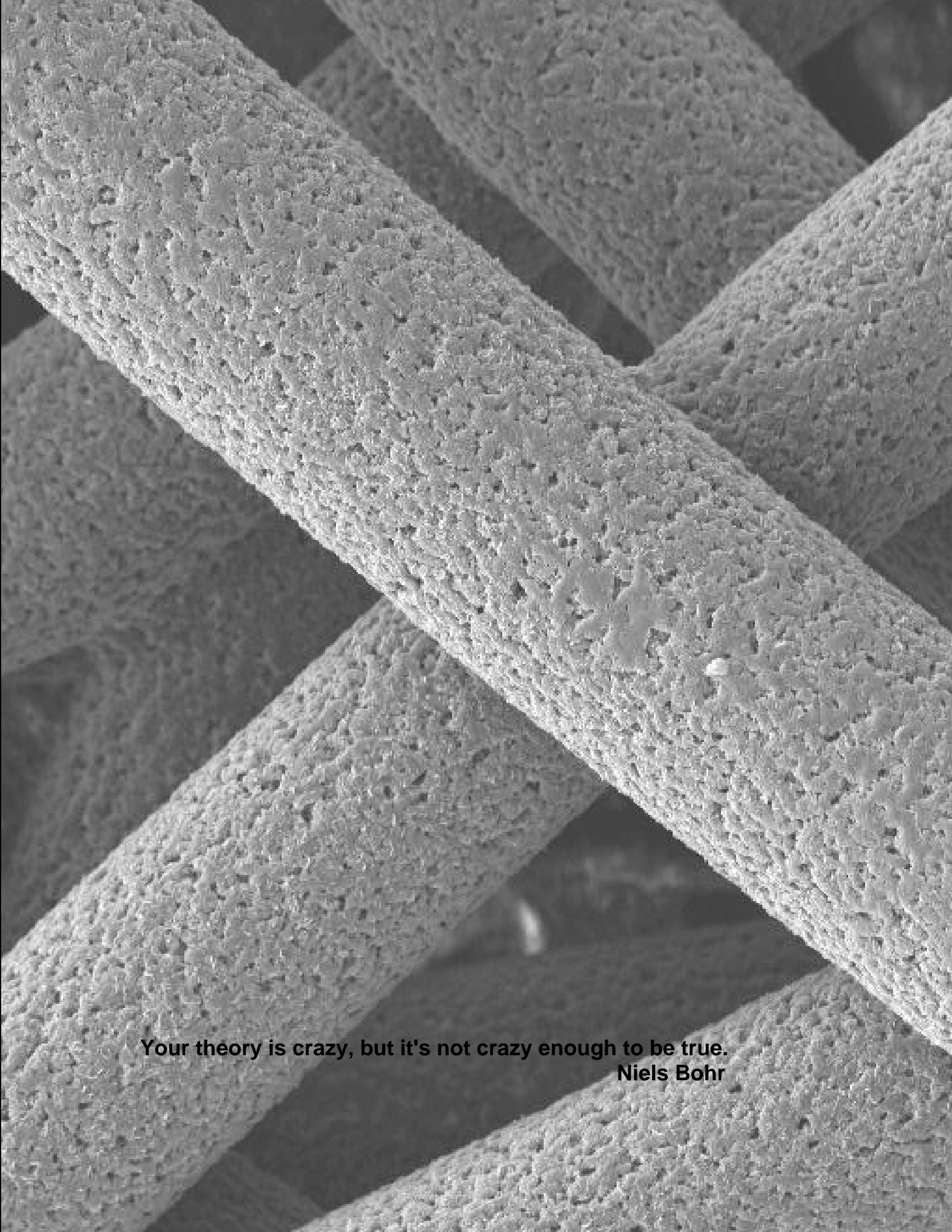
## References

1. Weiner, S. and H.D. Wagner, The material bone: Structure mechanical function relations. *Annual Review of Materials Science*, 1998. **28**: p. 271-298.
2. Mikos A.G., a.T.J.S., Formation of highly porous biodegradable scaffolds for tissue engineering. *J. Biotech.*, 2000. **3**: p. 114-119.
3. Arinze, T.L., et al., A comparative study of biphasic calcium phosphate ceramics for human mesenchymal stem-cell-induced bone formation. *Biomaterials*, 2005. **26**(17): p. 3631-3638.
4. Kruyt, M.C., et al., Bone tissue engineering in a critical size defect compared to ectopic implantations in the goat. *Journal of Orthopaedic Research*, 2004. **22**(3): p. 544-551.
5. Ramires, P.A., et al., The influence of titania/hydroxyapatite composite coatings on in vitro osteoblasts behaviour. *Biomaterials*, 2001. **22**(12): p. 1467-1474.
6. Hutmacher, D.W., Scaffolds in tissue engineering bone and cartilage. *Biomaterials*, 2000. **21**(24): p. 2529-2543.
7. Gomes, M.E., et al., Alternative tissue engineering scaffolds based on starch: processing methodologies, morphology, degradation and mechanical properties. *Materials Science & Engineering C-Biomimetic and Supramolecular Systems*, 2002. **20**(1-2): p. 19-26.
8. Salgado, A.J., O.P. Coutinho, and R.L. Reis, Novel starch-based scaffolds for bone tissue engineering: Cytotoxicity, cell culture, and protein expression. *Tissue Engineering*, 2004. **10**(3-4): p. 465-474.
9. Sun, L.M., et al., Material fundamentals and clinical performance of plasma-sprayed hydroxyapatite coatings: A review. *Journal of Biomedical Materials Research*, 2001. **58**(5): p. 570-592.
10. Cui, F.Z., Z.S. Luo, and Q.L. Feng, Highly adhesive hydroxyapatite coatings on titanium alloy formed by ion beam assisted deposition. *Journal of Materials Science-Materials in Medicine*, 1997. **8**(7): p. 403-405.

11. Bigi, A., et al., Human osteoblast response to pulsed laser deposited calcium phosphate coatings. *Biomaterials*, 2005. **26**(15): p. 2381-2389.
12. Sato, M., E.B. Slamovich, and T.J. Webster, Enhanced osteoblast adhesion on hydrothermally treated hydroxyapatite/titania/poly(lactide-co-glycolide) sol-gel titanium coatings. *Biomaterials*, 2005. **26**(12): p. 1349-1357.
13. Kim, C.S. and P. Ducheyne, Compositional Variations in the Surface and Interface of Calcium-Phosphate Ceramic Coatings on Ti and Ti-6Al-4V Due to Sintering and Immersion. *Biomaterials*, 1991. **12**(5): p. 461-469.
14. Abe, Y., T. Kokubo, and T. Yamamuro, Apatite Coating on Ceramics, Metals and Polymers Utilizing a Biological Process. *Journal of Materials Science-Materials in Medicine*, 1990. **1**(4): p. 233-238.
15. Kim, H.M., et al., Composition and structure of the apatite formed on PET substrates in SBF modified with various ionic activity products. *Journal of Biomedical Materials Research*, 1999. **46**(2): p. 228-235.
16. Tanahashi, M., et al., Apatite Coated on Organic Polymers by Biomimetic Process - Improvement in Its Adhesion to Substrate by Naoh Treatment. *Journal of Applied Biomaterials*, 1994. **5**(4): p. 339-347.
17. Oliveira, A.L., C.M. Alves, and R.L. Reis, Cell adhesion and proliferation on biomimetic calcium-phosphate coatings produced by a sodium silicate gel methodology. *Journal of Materials Science-Materials in Medicine*, 2002. **13**(12): p. 1181-1188.
18. Oliveira, A.L., P.B. Malafaya, and R.L. Reis, Sodium silicate gel as a precursor for the in vitro nucleation and growth of a bone-like apatite coating in compact and porous polymeric structures. *Biomaterials*, 2003. **24**(15): p. 2575-2584.
19. Azevedo, H.S., et al., Incorporation of proteins and enzymes at different stages of the preparation of calcium phosphate coatings on a degradable substrate by a biomimetic methodology. *Materials Science & Engineering C-Biomimetic and Supramolecular Systems*, 2005. **25**(2): p. 169-179.

20. Tanahashi, M., et al., Apatite Coating on Organic Polymers by a Biomimetic Process. *Journal of the American Ceramic Society*, 1994. **77**(11): p. 2805-2808.
21. Tuzlakoglu, K., et al., Production and characterization of chitosan fibers and 3-D fiber mesh scaffolds for tissue engineering applications. *Macromolecular Bioscience*, 2004. **4**(8): p. 811-819.
22. Oyane, A., et al., Simple surface modification of poly(epsilon-caprolactone) for apatite deposition from simulated body fluid. *Biomaterials*, 2005. **26**(15): p. 2407-2413.
23. Zhang, R.Y. and P.X. Ma, Biomimetic polymer/apatite composite scaffolds for mineralized tissue engineering. *Macromolecular Bioscience*, 2004. **4**(2): p. 100-111.
24. Ohtsuki, C., T. Kokubo, and T. Yamamuro, Mechanism of Apatite Formation on Cao-Sio2-P2O5 Glasses in a Simulated Body-Fluid. *Journal of Non-Crystalline Solids*, 1992. **143**(1): p. 84-92.
25. Li, P.J., et al., Apatite Formation Induced by Silica-Gel in a Simulated Body-Fluid. *Journal of the American Ceramic Society*, 1992. **75**(8): p. 2094-2097.
26. Reis, R.L., et al., Treatments to induce the nucleation and growth of apatite-like layers on polymeric surfaces and foams. *Journal of Materials Science-Materials in Medicine*, 1997. **8**(12): p. 897-905.
27. Rehman, I. and W. Bonfield, Characterization of hydroxyapatite and carbonated apatite by photo acoustic FTIR spectroscopy. *Journal of Materials Science-Materials in Medicine*, 1997. **8**(1): p. 1-4.
28. Elliott, J.C., D.W. Holcomb, and R.A. Young, Infrared Determination of the Degree of Substitution of Hydroxyl by Carbonate Ions in Human Dental Enamel. *Calcified Tissue International*, 1985. **37**(4): p. 372-375.
29. Lincks, J., et al., Response of MG63 osteoblast-like cells to titanium and titanium alloy is dependent on surface roughness and composition. *Biomaterials*, 1998. **19**(23): p. 2219-2232.

30. Webster, T.J., R.W. Siegel, and R. Bizios, Osteoblast adhesion on nanophase ceramics. *Biomaterials*, 1999. **20**(13): p. 1221-1227.
31. Ong, J.L., et al., Osteoblast responses to as-deposited and heat treated sputtered CaP surfaces. *Journal of Materials Science-Materials in Medicine*, 2001. **12**(6): p. 491-495.
32. Villarreal D.R., S.A.a.O.J.L., Protein adsorption and osteoblast responses to different calcium phosphate surfaces. *J Oral Implant.*, 1998. **24**(2): p. 67-73.
33. Anselme, K., Osteoblast adhesion on biomaterials. *Biomaterials*, 2000. **21**(7): p. 667-681.
34. Harris, H., The Human Alkaline-Phosphatases - What We Know and What We Dont Know. *Clinica Chimica Acta*, 1990. **186**(2): p. 133-150.
35. Matsuoka, H., et al., In vitro analysis of the stimulation of bone formation by highly bioactive apatite- and wollastonite-containing glass-ceramic: Released calcium ions promote osteogenic differentiation in osteoblastic ROS17/2.8 cells. *Journal of Biomedical Materials Research*, 1999. **47**(2): p. 176-188.



**Your theory is crazy, but it's not crazy enough to be true.  
Niels Bohr**





## **CHAPTER VI**

### **A NEW ROUTE TO PRODUCE STARCH-BASED FIBER MESH SCAFFOLDS BY WET SPINNING AND SUBSEQUENT SURFACE MODIFICATION AS A WAY TO IMPROVE CELL ATTACHMENT AND PROLIFERATION**

## **Abstract**

This study proposes a new route for producing fiber mesh scaffolds from a starch-polycaprolactone blend. It was demonstrated that the scaffolds with 77% porosity could be obtained by a simple wet spinning technique based on solution/precipitation of a polymeric blend. In order to enhance the cell attachment and proliferation, Ar plasma treatment was applied to the scaffolds. It was observed that the surface morphology and chemical composition were significantly changed due to the etching and functionalization of the fiber surfaces. XPS analyses showed an increase of the oxygen content of the fiber surfaces after plasma treatment (untreated scaffolds O/C:0.26 and plasma treated scaffolds O/C:0.32). Both untreated and treated scaffolds were examined using a SaOs-2 human osteoblast-like cell line during 2 weeks of culture. The cell seeded on wet-spun SPCL fiber mesh scaffolds showed high viability and alkaline phosphatase enzyme activity, being those values were even higher for the cells seeded on the plasma treated scaffolds.

## 1. Introduction

Tissue engineering offers a promising new approach to create biological alternatives for regeneration of different tissues. It involves the use of tissue-specific cells seeded in a scaffold which can guide the cell growth and tissue formation in three dimensions. To bring about the desired biological response, a scaffold should possess a number of characteristics such as three dimensional highly porous and interconnective structure, large surface area, adequate pore size, suitable surface chemistry and mechanical properties, etc. [1]

Biodegradable polymeric fiber structures can provide a large surface area and a relatively large porosity which can be optimized for specific applications. Besides these, many tissues, such as nerve, muscle, tendon, ligament, blood vessel, bone, and teeth, have tubular or fibrous bundle architectures and anisotropic properties. Therefore, fiber-based structures find a number of applications in tissue engineering, including soft tissue repair [2], vascular prostheses [3], bone [4, 5] and cartilage scaffolds [6], among others.

There are three main techniques to produce fibers to be used in biomedical applications: melt spinning, dry spinning and wet spinning. Melt spinning is based on the extrusion of polymeric melt while the spinning process starts from polymeric solution in the case of dry and wet spinning. Most of the synthetic polyester fibers used in tissue engineering are produced by a conventional melt spinning technique [7, 8]. However, excessively high processing temperatures may result in monomer formation during extrusion process. The excess monomer can catalyze the hydrolysis of the material. The wet spinning technique is an alternative way to produce biodegradable polyester fibers for the use in tissue engineering [9-12]. The fiber properties can be tailored depending on the spinning rate, the concentration of the polymer solution and coagulation bath. A highly viscous solution and high spinning rate allow fiber precipitation at the bottom of the coagulation bath. This approach could be used to form scaffolds during the processing.

In design of a tissue engineering scaffold, surface physicochemistry is one of the most important issues to be considered. The physicochemical properties of the surface directly influence the scaffold performance by effecting the cellular response and ultimately effecting the new tissue formation [13]. In

order to improve the cell affinity, the surface hydrophilicity, surface energy, surface roughness and surface charge can be modified by different methods, including mechanical treatments, wet chemical treatments and plasma treatments. Chemical treatments have been widely used to modify the biomaterial surfaces [14, 15]. However, the main problem of these treatments is the influence of the treatment on the bulk properties of the material. The surface of the materials can be modified by plasma treatment without altering the bulk properties of the material [16, 17]. By this technique, it is possible to introduce or graft desired functional groups and polymer chains onto the surface. The surface roughness which plays an important role for cell attachment can be also changed by plasma treatment. Therefore, plasma is a valuable method for improve cell affinity to the tissue engineering scaffolds.

In the present study, we describe a new route for the production of starch-based fiber mesh scaffolds which allows forming of scaffolds during spinning. This new route also avoids polymer degradation which is the main problem of melt-based systems. The surface properties of the produced scaffolds are tailored by plasma treatment in order to enhance cell attachment and proliferation

## **2. Materials&Methods**

### **2.1. Materials**

A blend of starch/polycaprolactone (SPCL) (30/70 wt %) was used to produce fiber mesh scaffolds. More information on these materials can be found elsewhere. All the reagents used were analytical grade unless specified otherwise.

### **2.2. Wet Spinning Process**

Starch-based fiber mesh scaffolds were originally produced by wet spinning. In order to obtain a polymer solution with proper viscosity, SPCL was dissolved in chloroform at a concentration of 40% (w/v). Please note that, it was possible to obtain a homogenous suspension of starch particles into the solution even though the only the synthetic part of the blend was soluble in the chloroform. Methanol was used as a coagulant. The polymer solution was loaded into a

syringe and placed in a syringe pump (World Precision Instruments, UK). A certain amount of polymer solution was subsequently extruded into a coagulation bath. The fiber mesh structure was formed during the processing by the random movement of the coagulation bath. The formed scaffolds were then dried at room temperature overnight in order to remove any remaining solvents.

After spinning, the internal architecture of the produced fiber meshes was characterized by micro-computed tomography ( $\mu$ CT) [18]. The surface morphology of the fibers was analyzed under a scanning electron microscope (SEM, Leica Cambridge S360 microscope). Specifically, three specimens were scanned in air using a  $\mu$ CT imaging system ( $\mu$ CT40, Scanco Medical AG, Bassersdorf, Switzerland) with a nominal resolution of 12  $\mu$ m. The reconstructed images were filtered using a constrained 3D Gaussian filter to partially suppress noise in the volumes ( $\mu = 1.2$  voxel, support = 1 voxel), and binarized using a global threshold. Standard 3D morphometry as developed for trabecular bone was used to assess structural parameters for the scaffolds. These parameters included porosity and scaffold surface-to-volume ratio and were derived from a triangulated mesh allowing for computation of surface and volume [19]. In addition, pore size and fiber thickness were determined using the distance transformation method [20]. In this method, each pore (fiber) is filled with a non-redundant set of maximal spheres. Mean pore (fiber) size was then calculated as the volume-averaged diameter of all spheres making up the pore (fiber).

### **2. 3. Plasma Surface Treatment**

In order to improve cell attachment and proliferation, a plasma treatment was performed using a plasma reactor PlasmaPrep<sub>5</sub> (Gala Instrument GmbH, Germany) with a chamber size of 15 cm diameter and 31 cm length (5L) and with a fully automated process control. In order to maximize the surface area to be exposed to the plasma, the samples were wired (necklace like) with a distance of 1 cm between them. The wire was fixed to a metal support which was placed into the chamber. The chamber was flushed with argon five times prior to treatment. A radio frequency (RF) source was used and a power of 30 W was applied for 15 minutes. Argon was used as a working gas and the

pressure in the reactor was controlled (0.18 mbar) by adjusting its flow rate. The samples were kept 24 hours after being removed from the reactor and then characterized.

#### *X-ray Photoelectron Spectroscopy (XPS)*

X-ray photoelectron spectroscopy (XPS) was used to quantitatively determine the surface composition of the scaffolds. The XPS analysis were performed using an 250 iXL ESCA instrument (VG Scientific) equipped with two X-Ray sources: a source with Al  $K\alpha_{1,2}$  monochromatized radiation at 1486.92 eV and another one (Dual) equipped with two anodes: Mg and Al.

The nonconductive nature of the samples required the use of an electron flood gun to minimize surface charging. Charge compensation at the surface was performed by using both a low energy flood gun (electrons in the range 0 to 14 eV) and an electrically grounded stain steel screen placed directly on the sample surface.

The first attempt to measure the samples was the use of the monochromatic X-ray source. However, this was impossible due to the high roughness of the samples which caused problems to build up the charge. Generally, charge neutralization for 3D surfaces is more difficult because of the “holes” on the surface. The best choice for these cases is Mg source which helps to neutralize the surface charge. Therefore, the measurements were carried out using non-monochromatic Mg- $K\alpha$  radiation ( $h\nu=1253.6$  eV). Photoelectrons were collected from a take off angle of  $90^\circ$  relative to the sample surface. The measurements were performed in the constant analyzer energy mode (CAE) with a 100 eV pass energy for survey spectra and 20eV pass energy for high resolution spectra. C1s high resolution scans were taken before and after experiments in order to check out the efficiency of charge compensation.

Charge referencing was done by setting the lower binding energy C1s hydrocarbon ( $CH_x$ ) peak at 285.0 eV.

The atomic composition of the samples was determined from the survey spectra using the standard Scofield photoemission cross sections. The chemical functional group identification was obtained from the high-resolution

peak analysis of C1s envelopes. The spectra fitting were performed using the “Chi-squared” algorithm to determine the goodness of a peak fit.

#### **2. 4. Cell Culture Studies**

A human osteoblast-like cell line (SaOs-2) was used to test the cell attachment and proliferation on the scaffolds. A 1ml of cell suspension containing  $3 \times 10^5$  cells in a culture medium (DMEM low glucose supplemented with 10% Fetal Bovine Serum and 1% antibiotics/antimicrobials) were dropped onto scaffolds (n=3). The cells on scaffolds were then allowed to grow for 2 weeks at 37°C in humidified atmosphere containing 5% CO<sub>2</sub> with medium changes every 2-3 days.

##### *Morphological Analysis*

For the morphological examination, cell/scaffold constructs were rinsed with Phosphate Buffer Saline (PBS, Sigma, USA) and then fixed in 2.5% glutaraldehyde. The samples were dehydrated through graded series of ethanol and dried before mounting onto brass stubs, sputter coated with gold. Finally, the samples were analyzed under a scanning electron microscope (SEM) at an acceleration voltage of 15kV.

##### *Cell Proliferation-DNA Assay*

Cell proliferation was evaluated by quantifying DNA content using the PicoGreen dsDNA kit (Molecular Probes, USA). PicoGreen dsDNA Quantitation Reagent is an ultra-sensitive fluorescent nucleic acid stain for quantitative analysis of double-stranded DNA (dsDNA) in solution.

For the assay, the scaffold/cell constructs (n=3) were rinsed with PBS and incubated with sterile ultra pure water at 37°C for 1h before putting at -80°C. The samples were then thawed and put in an ultrasonic bath for 15 min. An aliquot of each sample was transferred to the 96-well plate. A certain ratio of Tris-EDTA buffer and PicoGreen reagent prepared in the same buffer was added to the each well. The fluorescence was read at 485nm and 528nm excitation and emission, respectively. The DNA amount of each samples was then calculated using a standard curve.



### *Alkaline Phosphatase (ALP) Activity*

Alkaline phosphatase (ALP) activity from the scaffolds/cells constructs (n=3) was quantified by the specific conversion of p-nitrophenyl phosphate (pNPP) into p-nitrophenol (pNP). To perform the assay, the seeded scaffolds were rinsed with PBS and transferred individually into eppendorf containing sterile ultra pure water. They were then frozen at  $-80^{\circ}\text{C}$  and defrosted at room temperature before starting the assay. A buffer solution containing 0.2% w/v p-nitrophenyl phosphate was added to the samples in a ratio of 1:3. The enzyme reaction was carried out at  $37^{\circ}\text{C}$  for 1 h and then stopped by a solution containing 2 M NaOH and 0.2 mM EDTA in distilled water. The absorbance of p-nitrophenol formed was determined at 405 nm with a reference filter at 620 nm. A standard curve was made using pNP values ranging from 0 to 600  $\mu\text{mol/ml}$ . The results were expressed as  $\mu\text{mol}$  of pNP produced/ml/h.

### *Statistical Analysis*

All the quantitative results were obtained from triplicate samples. Data were expressed as a mean  $\pm$ SD. For statistical analysis, a two-tailed Student's *t*-test was used. Differences were considered to be significant at  $p < 0.05$ .

## **3. Results and Discussion**

### **3.1. Morphology of the scaffolds**

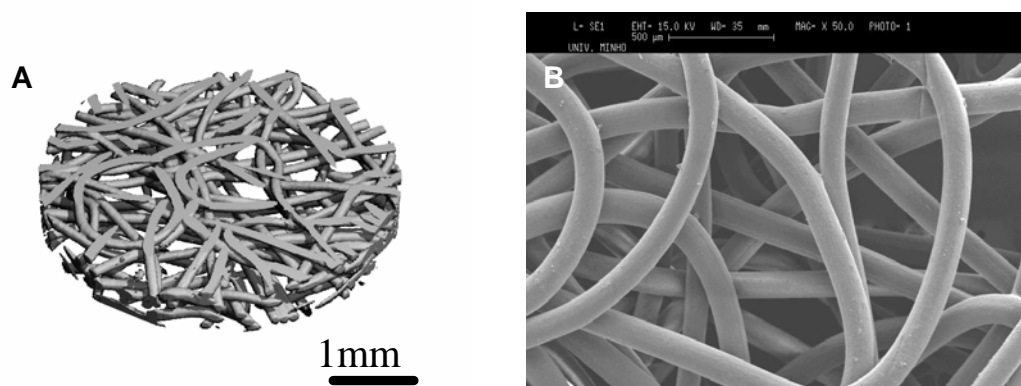


Figure 1. Morphology of the wet-spun SPCL fiber mesh scaffolds analysed by; A)  $\mu\text{CT}$ , showing thin section of sample, B) SEM

Figure 1.A and B present respectively the  $\mu$ CT and SEM images of SPCL fiber mesh scaffolds produced by wet spinning. It can be clearly seen that, the SPCL fibers were randomly formed into a 3D structure. The porosity of the scaffolds, determined by  $\mu$ CT, was 77%.  $\mu$ CT morphometry showed that fiber diameter was  $100\mu\text{m}$ ; mean pore size was  $250\mu\text{m}$ , which is in the range of ideal pore size for bone regeneration [21]. The scaffolds have a high surface to volume ratio: the specific scaffold surface was  $29\text{ mm}^2/\text{mm}^3$ , similar to that of native bone [20]. Moreover,  $\mu$ CT showed that wet-spinning was a very reproducible procedure; the coefficient of variation (CV) for fiber thickness was 4.2%; for the other parameters, CV was 1.2% or below.

Previous studies have reported that 2D polymer surfaces could be easily modified by different plasma techniques [22-24]. However, it becomes more complicated in the case of 3D porous polymeric structure due to the pore structures and low interconnectivity which do not allow the penetration of plasma exposition in the interior part of the structure because of the shadow effect. In the present study, the wet-spun scaffolds produced presented a highly porous and interconnected structure that can overcome this problem of plasma surface modification. In the case of wet-spun scaffolds, the treatment is very similar to treatment of a single fiber. As a result, the surface exposed to the plasma is much higher, which allows for a more uniform and effective surface treatment.

### 3.2. Plasma Treatment

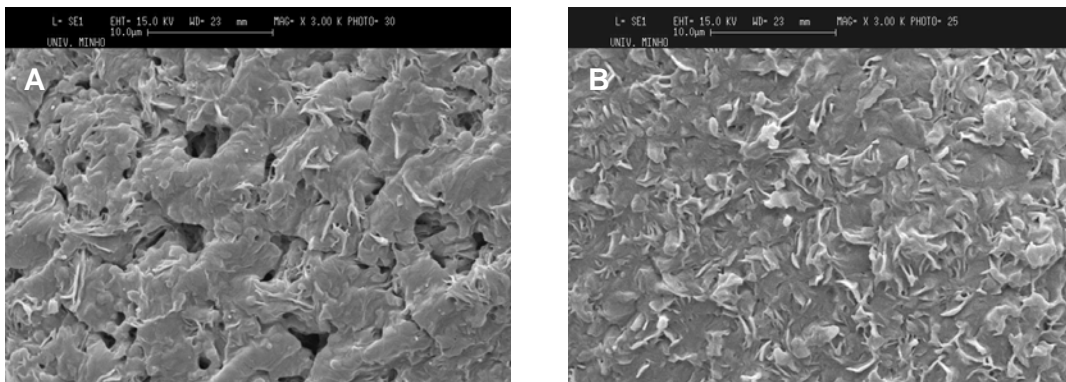


Figure 2. The surface of the SPCL fiber mesh scaffolds; A) before (x3000) and B) after Ar plasma treatment (x3000).

Due to phase inversion during precipitation, the surface of the fibers exhibited a non-smooth morphology (Figure 2.A). After plasma treatment, a significant difference on the fiber surfaces was observed (Figure 2.B). It is well known that the surface roughness typically tends to increase after a plasma treatment due to the so-called etching process [25]. When the plasma is composed of an inorganic gas such as argon, helium, hydrogen, nitrogen, and oxygen, it leads to the etching reactions on the topmost layer of the polymer surface [26]. This etching is a result of stripping off the topmost layer of the polymer because of the weight loss of the polymer during the plasma exposure. However, the SPCL fiber surfaces showed a denser and smaller nano-size roughness after plasma treatment. Since SPCL has a very low glass transition temperature (-60°C), it can be explained by melting and etching that consecutively occurred on the surface during the plasma process.

X-ray photoelectron spectroscopy (XPS) analysis was performed in order to obtain more detailed information for the chemical structures and groups presented on the surface before and after the performed modification. The results obtained are summarized in Table 1.

Table 1. XPS data for wet spun SPCL scaffolds before and after modification

	C%	O%	O:C/C:O ratio
Theoretical PCL	69.2	30.8	0.45/2.25
Theoretical SPCL	62.7	37.3	0.59/1.68
Fiber mesh, untreated	76.9	20.4	0.26/3.77
Fiber mesh modified	69.7	22.1	0.32/3.15

As it can be seen from the table the measured oxygen content on the surface is lower than the theoretical one calculated for PCL. The difference between the bulk and surface composition of the material is not a surprise. It has been reported [27, 28] that in polymeric systems, the composition near to the surface can be markedly different from the bulk. In fact, due to the high complexity of blend chemistry, different components may predominate at the

surface, depending on the blend composition, crystallinity of the components, complexity and degree of miscibility of the system, processing conditions and also the nature of surrounding environment [27-29]. However, after plasma modification the oxygen content on the surface increase and an O/C ratio of 0.32 was measured (compared to 0.26 for the untreated material). Oxidation is not the only process which is taking place on the surface during the plasma treatment. As can be seen from the table the percentage of carbon was also changed after the treatment; it reduced from 76.9 to 69.7 confirming the presence of some etching.

More detailed analyze of C1s core level spectra of SPCL fiber mesh samples (Figure 3) showed that they contain three main peaks – at 285 eV, which was assigned to the main carbon backbone, at 286.4 eV for –C–O– and at about 288.8eV for carboxyl bonded carbons. This is not unexpected since the main component of the blend poly( $\epsilon$ -caprolactone) has all of those bonds present in its structure.

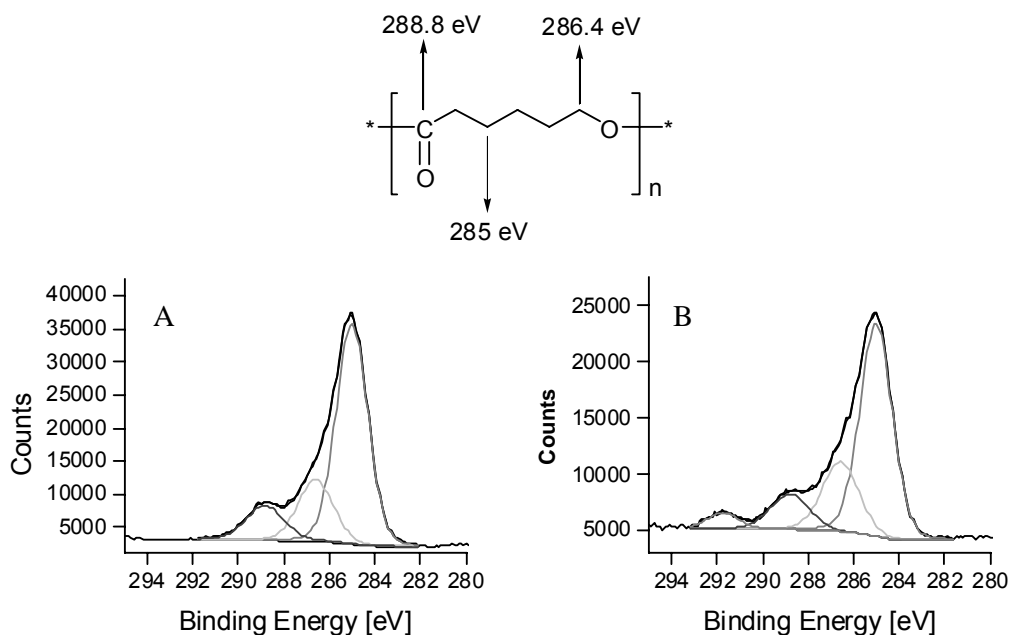


Figure 3. C1s core level spectra for wet-spun SPCL fiber meshes A) before and B) after Ar plasma treatment

The intensity of the peaks at 286.4 eV and 288.8 eV increased after treatment as it can be seen from Figure 3. The created active species on the surface by Ar plasma are very reactive and can recombine with the oxygen from

the air. As a result surface functionalization with different oxygen containing groups occurs on the surface and this is the reason for the observed differences in the C1s core level spectra. It should be noted that the occurred surface oxidation is not as powerful as the one in which oxygen plasma is employed; in the latter case much more hydrophilic surfaces are produced which do not promote protein adsorption and consequently do not favour cell adhesion.

### 3.3. Cell Culture

#### *Morphological Analysis*

The morphology and the shape of the osteoblast seeded onto both untreated and plasma treated fiber meshes showed a clear difference after different time of culturing (Figure 4, 5, and 6). It was observed that the cells were able to grow and making a film on the treated surface while they were in spindle-like shape with cytoplasmic extension on the untreated surface after 3 days of culture (Figure 4).

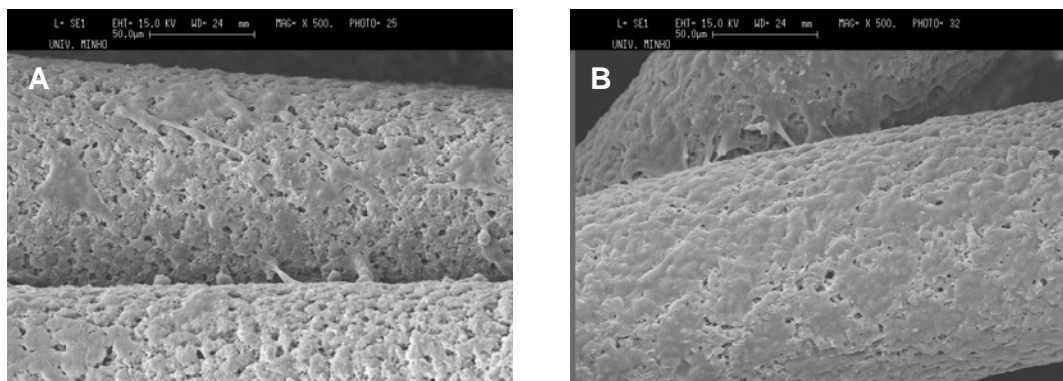


Figure 4. SEM micrographs of osteoblast-like cells seeded on SPCL fiber mesh scaffolds after 3 days of culture; A) untreated, B) Ar plasma treated scaffold

This was more evident after 7 days of culture (Figure 5.A and B). Both scaffolds were completely covered by cells, which indicate the ability of the scaffolds for osteoblast cell attachment and proliferation.

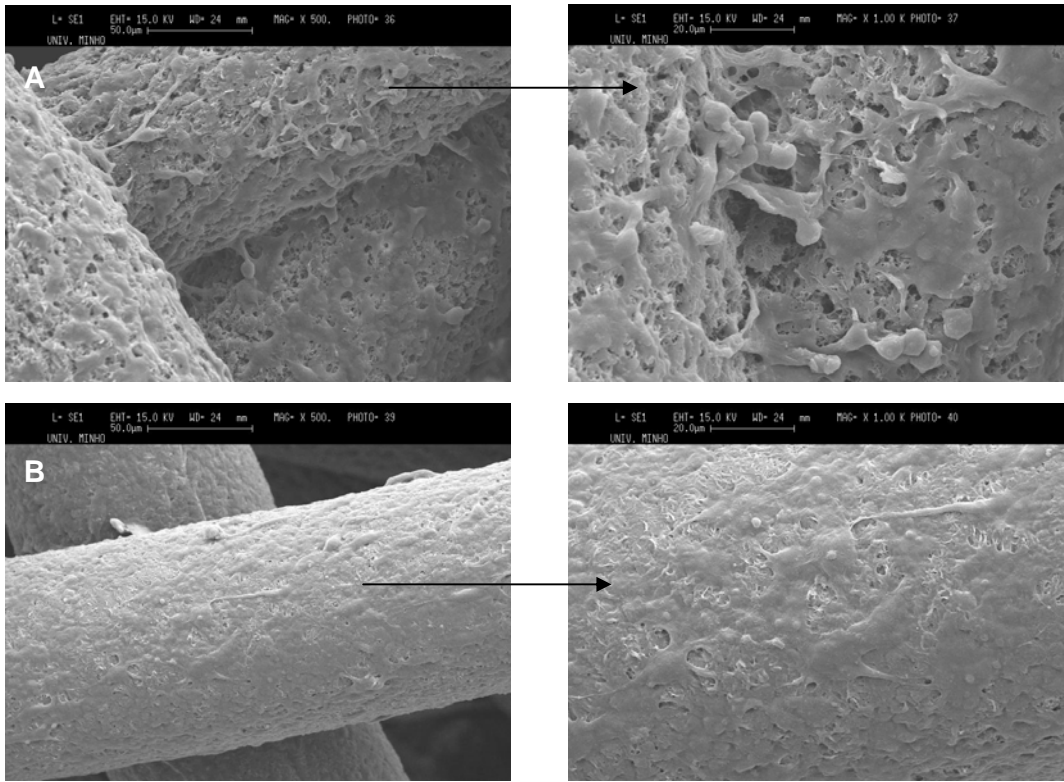


Figure 5.B. SEM micrographs of osteoblast-like cells seeded on A) untreated and B) Ar plasma treated SPCL fiber mesh scaffolds after 7 days of culture. (Picture at right shows the cells on the surface with higher magnification, (x1000))

However, the osteoblasts seeded on the treated fiber meshes were able to bridge between the fibers after 14 days of culture (Figure 6.A).

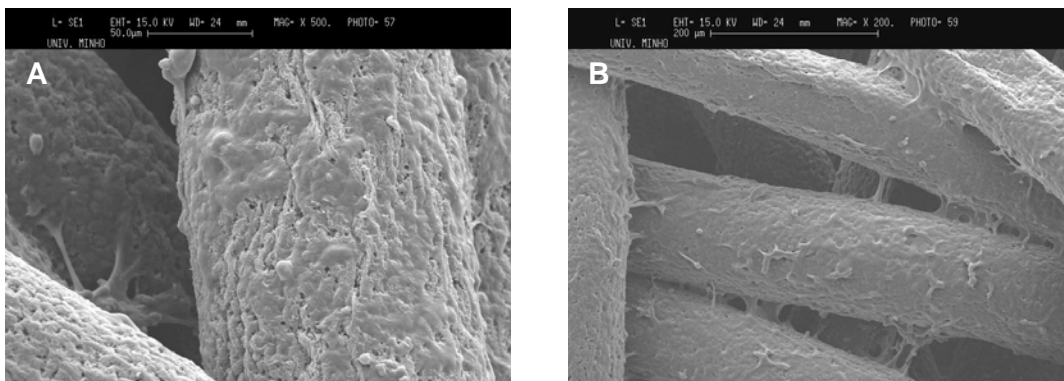


Figure 6. SEM micrographs of osteoblast-like cells seeded on SPCL fiber mesh scaffolds after 3 days of culture; A) untreated, B) Ar plasma treated scaffold

### Cell Viability

Besides the cell morphology, changing the surface chemistry and topography also influenced the metabolic activity of the cells. As it was discussed above, the oxygen content of the fiber surfaces significantly increased after plasma treatment due to degradation and functionalization of the fiber surfaces. It is known that osteoblasts are attachment-dependent cell [30]. They can only produce and mineralize their extracellular matrix if they attach in a proper surface that allows specific cell-surface interaction. They also can recognize the changes in the surface topography if it is above 0.5  $\mu\text{m}$  [31]. Therefore, DNA amount was significantly different between untreated and treated scaffolds after 3 and 7 days of culture ( $p=0.045$  and  $p=0.015$  for 3 and 7 days, respectively) while it was not significant after 14 days (Figure 7).

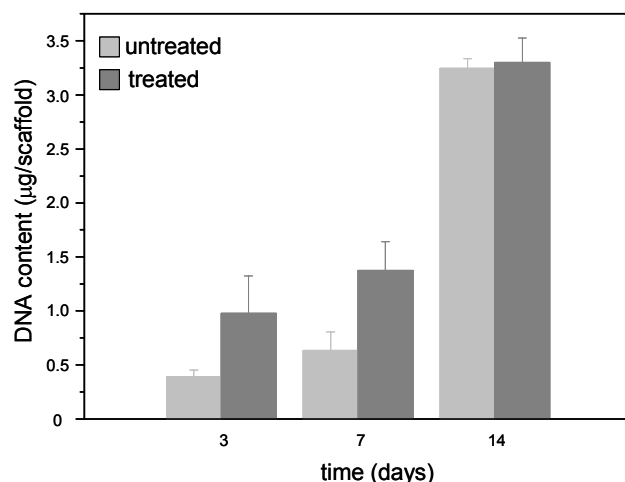


Figure 6. Cell viability and proliferation of human osteoblast like cells determined by DNA. Error bars represent means  $\pm$  SD for  $n=3$ .

This can be explained by the effect of plasma treatment in the initial stage of culture. By plasma treatment, it is possible to increase the serum protein adsorption on the surfaces which would be resulted in an increase of initial cell attachment. Once they reached confluency, the rate of cellular death and proliferation becomes equal and hence the proliferation stops. This fact can explain the decrease in the difference between untreated and treated samples after 14 days of culture.

### *ALP activity*

Alkaline phosphatase is an enzyme which is used as an early marker for osteoblast differentiation. Although its exact role is not very clear, it is known that it plays an important role in bone matrix mineralization process [30]. Regarding the present experiments, ALP activity of the cells cultured onto the SPCL fiber meshes increased with the culture period (Figure 8). The enzyme activity of the cells was found to be even higher if the scaffolds were treated by plasma. On the other hand, the differences in the enzymatic activity between the cells seeded on untreated and treated scaffolds decreased after 14 days of culture. It has been reported that the deposition of extracellular matrix occurs before the mineralization starts [32]. This latest stage of cell differentiation precedes mineralization and thereby ALP enzyme activity which is associated with calcification tends to decrease [33, 34]. This phenomenon can explain the ALP results from the present study indicating that the cells cultured on untreated and treated scaffolds might be in different stage of differentiation.

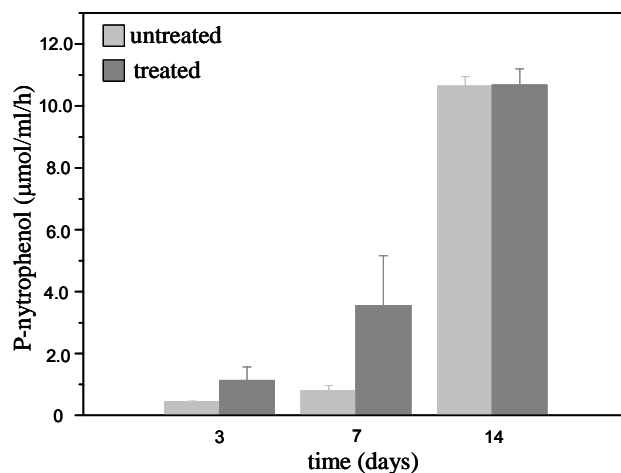


Figure 8. The ALP activity of human osteoblast like cells seeded on untreated and Ar plasma treated wet-spun SPCL fiber meshes. Error bars represent means  $\pm$  SD for n=3.

### **4. Conclusions**

A new route was described to produce starch-based fiber mesh scaffolds. The results of this study indicated that a simple wet-spinning technique could be used to obtain highly porous fiber mesh scaffolds from a biodegradable starch-



polycaprolactone blend. The scaffolds could be formed, in a very reproducible manner, during the process by means of optimizing the processing conditions. Furthermore, the developed scaffolds were able to support osteoblast-like cell attachment and proliferation. As a second step, the scaffolds surfaces were modified by using Ar plasma. After plasma treatment, the surface morphology and surface chemical composition of the fibers were significantly changed. Osteoblast-like cells were able to recognize these physical and chemical changes on the surface and they showed higher cell viability and ALP enzyme activity on the treated scaffolds.

As a final conclusion, these results suggested that starch-based fiber mesh scaffolds can be easily processed by a wet spinning technique into adequate scaffolds. Subjecting these scaffolds to Ar plasma can enhance their suitability for tissue engineering applications.

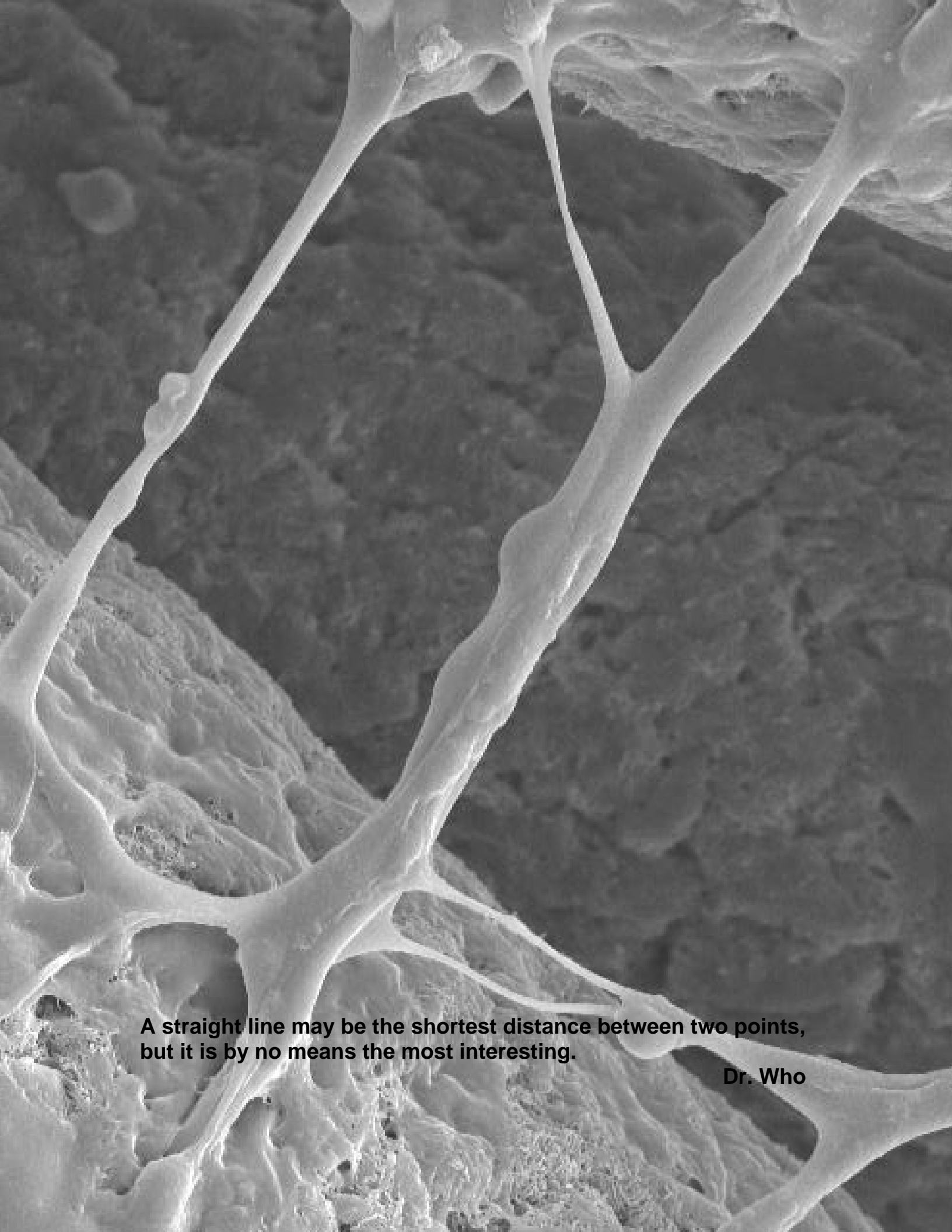
## References

1. Hutmacher, D.W., Scaffold design and fabrication technologies for engineering tissues - state of the art and future perspectives. *Journal of Biomaterials Science-Polymer Edition*, 2001. 12(1): p. 107-124.
2. Chen, G.P., et al., Culturing of skin fibroblasts in a thin PLGA-collagen hybrid mesh. *Biomaterials*, 2005. 26(15): p. 2559-2566.
3. Gafni, Y., et al., Design of a filamentous polymeric scaffold for in vivo guided angiogenesis. *Tissue Engineering*, 2006. 12(11): p. 3021-3034.
4. Gomes, M.E., et al., Influence of the porosity of starch-based fiber mesh scaffolds on the proliferation and osteogenic differentiation of bone marrow stromal cells cultured in a flow perfusion bioreactor. *Tissue Engineering*, 2006. 12(4): p. 801-809.
5. Tuzlakoglu, K., et al., Nano- and micro-fiber combined scaffolds: A new architecture for bone tissue engineering. *Journal of Materials Science-Materials in Medicine*, 2005. 16(12): p. 1099-1104.
6. Woodfield, T.B.F., et al., Design of porous scaffolds for cartilage tissue engineering using a three-dimensional fiber-deposition technique. *Biomaterials*, 2004. 25(18): p. 4149-4161.
7. Schmack, G., et al., Biodegradable fibers of poly(3-hydroxybutyrate) produced by high-speed melt spinning and spin drawing. *Journal of Polymer Science Part B-Polymer Physics*, 2000. 38(21): p. 2841-2850.
8. Yuan, X.Y., Mak, A. F. T. Kwok, K. W. Yung, B. K. O., Yao, K. D., Characterization of poly(L-lactic acid) fibers produced by melt spinning. *Journal of Applied Polymer Science*, 2001. 81(1): p. 251-260.
9. Williamson, M.R. and A.G.A. Coombes, Gravity spinning of polycaprolactone fibres for applications in tissue engineering. *Biomaterials*, 2004. 25(3): p. 459-465.
10. Nelson, K.D., et al., Technique paper for wet-spinning Poly(L-lactic acid) and poly(DL-lactide-co-glycolide) monofilament fibers. *Tissue Engineering*, 2003. 9(6): p. 1323-1330.
11. Williamson, M.R., H.I. Chang, and A.G.A. Coombes, Gravity spun polycaprolactone fibres: controlling release of a hydrophilic

- macromolecule (ovalbumin) and a lipophilic drug (progesterone). *Biomaterials*, 2004. 25(20): p. 5053-5060.
12. Williamson, M.R., R. Black, and C. Kielty, PCL-PU composite vascular scaffold production for vascular tissue engineering: Attachment, proliferation and bioactivity of human vascular endothelial cells. *Biomaterials*, 2006. 27(19): p. 3608-3616.
  13. Mwale, F., et al., The effect of glow discharge plasma surface modification of polymers on the osteogenic differentiation of committed human mesenchymal stem cells. *Biomaterials*, 2006. 27(10): p. 2258-2264.
  14. Pashkuleva I., Reis R.L., Surface activation and modification- a way for improving the biocompatibility of degradable biomaterials, in *Biodegradable Systems in Tissue Engineering and Regenerative Medicine*. 2004, CRC Press: Boca Raton. p. 429-454.
  15. Garbassi F., M.M., Occhiello E, *Polymer Surfaces: from Physics to Technology*. 1994: John Wiley&sons. 241-274.
  16. Huang, F.L., et al., Dynamic contact angles and morphology of PP fibres treated with plasma. *Polymer Testing*, 2006. 25(1): p. 22-27.
  17. Tsal, P.P., Surface modification of fabrics using a one-atmosphere glow discharge plasma to improve fabric wettability. *Tex. Res. J.*, 1997: p. 359.
  18. Ruegsegger, P., B. Koller, and R. Muller, A microtomographic system for the nondestructive evaluation of bone architecture. *Calcified Tissue International*, 1996. 58(1): p. 24-29.
  19. Muller, R., T. Hildebrand, and P. Ruegsegger, Noninvasive Bone-Biopsy - a New Method to Analyze and Display the 3-Dimensional Structure of Trabecular Bone. *Physics in Medicine and Biology*, 1994. 39(1): p. 145-164.
  20. Hildebrand, T., et al., Direct three-dimensional morphometric analysis of human cancellous bone: Microstructural data from spine, femur, iliac crest, and calcaneus. *Journal of Bone and Mineral Research*, 1999. 14(7): p. 1167-1174.

21. Maquet, V. and R. Jerome, Design of macroporous biodegradable polymer scaffolds for cell transplantation. *Porous Materials for Tissue Engineering*, 1997. 250: p. 15-42.
22. Pashkuleva I., M.A.P., Vaz F. and Reis R. L., Surface modification of starch based biomaterials by oxygen plasma or UV-radiation. submitted, 2006.
23. Khang, G., et al., Cell and platelet adhesions on plasma glow discharge-treated poly(lactide-co-glycolide). *Bio-Medical Materials and Engineering*, 1997. 7(6): p. 357-368.
24. Gugala, Z. and S. Gogolewski, Attachment, growth, and activity of rat osteoblasts on polylactide membranes treated with various lowtemperature radiofrequency plasmas. *Journal of Biomedical Materials Research Part A*, 2006. 76A(2): p. 288-299.
25. Tahara, M., N.K. Cuong, and Y. Nakashima, Improvement in adhesion of polyethylene by glow-discharge plasma. *Surface & Coatings Technology*, 2003. 174: p. 826-830.
26. Inagaki, N., Plasma surface modification and plasma polymerization. 1996, Pennsylvania: Technomic Publishing company. 22-28.
27. Cho, K., J. Lee, and P.X. Xing, Enzymatic degradation of blends of poly (epsilon-caprolactone) and poly(styrene-co-acrylonitrile) by Pseudomonas lipase. *Journal of Applied Polymer Science*, 2002. 83(4): p. 868-879.
28. Vikman, M., et al., Morphology and enzymatic degradation of thermoplastic starch-polycaprolactone blends. *Journal of Applied Polymer Science*, 1999. 74(11): p. 2594-2604.
29. Duguay, D.G., et al., Development of a Mathematical-Model Describing the Enzymatic Degradation of Biomedical Polyurethanes.1. Background, Rationale and Model Formulation. *Polymer Degradation and Stability*, 1995. 47(2): p. 229-249.
30. Boyan, B.D., et al., Mechanisms involved in osteoblast response to implant surface morphology. *Annual Review of Materials Research*, 2001. 31: p. 357-371.
31. Anselme, K., Osteoblast adhesion on biomaterials. *Biomaterials*, 2000. 21(7): p. 667-681.

32. Chim, H., et al., Efficacy of glow discharge gas plasma treatment as a surface modification process for three-dimensional poly (D,L-lactide) scaffolds. *Journal of Biomedical Materials Research Part A*, 2003. 65A(3): p. 327-335.
33. Salgado, A.J., et al., Preliminary study on the adhesion and proliferation of human osteoblasts on starch-based scaffolds. *Materials Science & Engineering C-Biomimetic and Supramolecular Systems*, 2002. 20(1-2): p. 27-33.
34. Holy, C.E., M.S. Shoichet, and J.E. Davies, Engineering three-dimensional bone tissue in vitro using biodegradable scaffolds: Investigating initial cell-seeding density and culture period. *Journal of Biomedical Materials Research*, 2000. 51(3): p. 376-382.



**A straight line may be the shortest distance between two points,  
but it is by no means the most interesting.**

**Dr. Who**



## **CHAPTER VII**

### **NANO- AND MICRO-FIBER COMBINED SCAFFOLDS:**

### **A NEW ARCHITECTURE FOR BONE TISSUE ENGINEERING**



## **Abstract**

One possible interesting way of designing a scaffold for bone tissue engineering is to base it on trying to mimic the biophysical structure of natural extracellular matrix (ECM). This work was developed in order to produce scaffolds for supporting bone cells. Nano and micro fiber combined scaffolds were originally produced from starch based biomaterials by means of a fiber bonding and a electrospinning, two step methodology. The cell culture studies with SaOs-2 human osteoblast-like cell line and rat bone marrow stromal cells demonstrated that presence of nanofibers influenced cell shape and cytoskeletal organization of the cells on the nano/micro combined scaffolds. Moreover, cell viability and Alkaline Phosphatase (ALP) activity for both cell types was found to be higher in nano/micro combined scaffolds than in control scaffolds based on fiber meshes without nanofibers.

Consequently, the developed structures are believed have a great potential on the 3D organization and guidance of cells that is provided for engineering of 3-dimensional bone tissues.

## 1. Introduction

Bone tissue engineering has become a rapidly expanding research area since it offers a new and promising approach for bone repair and regeneration. Several requirements have been considered for engineering bone, including choosing a cell type that matures/differentiates into bone cells with the proper form and phenotype, regulating the growth factors and designing a so-called ideal scaffold [1]. The requirements for the design and production of an ideal scaffold are also very complex and not yet fully understood. An ideal scaffold must be biocompatible both in bulk and degraded form, exhibit a porous, interconnected, and permeable structure to permit the ingress of cells and nutrients, and should exhibit the appropriate surface structure and chemistry for cell adhesion and proliferation. The processing techniques used to obtain polymeric scaffolds include solvent casting and particulate leaching, gas foaming, freeze drying, rapid prototyping, thermally induce phase separating, fiber bonding, melt molding and electrospinning, as reviewed elsewhere [2]. Several techniques aim to produce a scaffold which can mimic in some way the architecture of the natural extracellular matrix (ECM).

Natural extracellular matrix (ECM) is composed of various protein fibrils and fibers interwoven within a hydrated network of glycosaminoglycan chains [3]. This network structure serves as a scaffold which can support tensile and compressive stresses by the fibrils and hydrated networks. Besides providing an appropriate microenvironment for cells, ECM is responsible for transmitting signals to cell membrane receptors that reach nucleus via intracellular signaling cascades. Therefore, the fibrillar and porous structure of ECM have a great influence on cell functionality, mainly on cell adhesion and migration.

In last few years, the electrospinning processes have attracted a great deal of attention as a way to try to mimic the structure of natural ECM by means of producing fibers down to 3nm [4]. This process is based on the generation of an electrical field between a polymeric solution (or a polymer melt) placed in a capillary tube with a pipette or needle of small diameter and a metal collector.

When the electrical field reaches its critical value, repulsive electrostatic force overcomes the surface tension of the polymeric solution and a charged jet is produced. This charged polymeric jet then undergoes a stretching process which is accompanied by the rapid solvent evaporation and results the formation of long and thin fibers [5]. Electrospinning has been used to fabricate nanofibrous structures from a number of both natural synthetic polymers, such as collagen [6], chitosan [7], chitin [8], silk fibroin [9] and polyethyleneoxide [10], poly(DL-lactide-co-glycolide) [11], poly(L-lactide) [12], and polycaprolactone [13], among many others. The produced nanofibrous polymeric networks have been proposed for engineering of many different tissues. For instance, Li et al. [14] reported that electrospun poly( $\epsilon$ -caprolactone) membranes could promote chondrocyte proliferation and provide maintenance of chondrogenic phenotype. In another study, polyurethane and gelatin have been used to design a mesoscopically ordered structure for using as an artificial graft [15]. Recently, it has been shown that nanofibrous PCL mats could be used as a scaffold to support differentiation of human mesenchymal stem cell cultured in specific differentiation media [16]. Silk fibroin based nanofibrous matrices have also been tested with human bone marrow stromal cells and proposed as a scaffold for bone tissue engineering [17].

Though there are many studies that have been proposing nanofibrous polymeric mats for tissue engineering, they have a limitation for 3D applications due to their pore size which is smaller than a cellular diameter and can not allow cell migration within the structure. Furthermore, the small size of the fibers tends not to maximize the points of cell attachment which is a negative effect on the expression of several factors and on cell spreading and differentiation.

In the present study, we have developed a novel structure which combines polymeric micro and nanofibers in the same construct that is aimed to serve as a scaffold and mimic the physical structure of ECM for bone tissue regeneration, but simultaneously still providing the macro support that cells do require.

## **2. Materials&Methods**

### **2.1. Materials**

Starch-based scaffolds with a 70% porosity were prepared from a blend of starch/poycaprolactone (SPCL) (30/70 wt%) by a fiber bonding process as described elsewhere [18]. All the reagents used were analytical grade unless specified otherwise.

### **2.2. Electrospinning Process**

Electrospinning was used to obtain nanofibers onto SPCL fiber mesh scaffolds. The aim was to impregnate, as much as possible, the micro-fiber scaffolds with electrospun nanofibers. The solution used in the electrospinning experiments was prepared by dissolving 1g of SPCL in 7 ml chloroform. After dissolution was completed, 3 ml of dimethylformamide (DMF) which has a high dielectric constant was added to the solution to enhance electrospinning of the solution.

The polymer solution was then electrospun to the both side of the SPCL fiber mesh scaffolds. Briefly, a polymer solution was placed in a simple capillary glass tube vertically. A special designed collector was used to move samples through the electrospun polymeric jets. A 15kV voltage was provided by a high power supply at a distance of 10cm between a collector and a capillary tube for 10s.

#### *Morphological Analysis*

The developed structures were analyzed by optical microscopy (Olympus, MIC-D). To observe more detail in morphology of the nanofibers on the scaffolds, a scanning electron microscope (SEM) (Leica Cambridge S360 microscope) was also used.

### **2.3. Cell Culture**

The developed structures were tested with two different cell type, a human osteoblast-like osteosarcoma SaOs-2 cell line and rat bone marrow stromal cells.

In both experiment sets SPCL fiber mesh scaffolds without electrospun nanofibers were used as controls.

In the cell culture experiments with a human osteoblast-like SaOs-2 cell line, cells were seeded onto the scaffold using a density of  $3 \times 10^5$  cells/scaffolds and allowed to grow for two weeks, with medium (DMEM low glucose supplemented with 10% Foetal Bovine Serum, 1% antibiotics/antimicrobials) changes every 2 days.

Rat bone marrow stromal cells (RBMSC) were obtained from the femoras and tibias of 4 weeks-old male Wistar rats (Charles River, Spain) as described elsewhere [19]. Briefly, femurs and tibias were aseptically excised, cleaned of soft tissue, and washed in  $\alpha$ -MEM (Life Technologies, Grand Island, NY) containing 10 times more amount of normal antibiotics concentration in order to avoid contamination during the harvest. Then, the epiphyses were cut off, and the diaphyses flushed with 5 ml of complete medium [ $\alpha$ -MEM (minimal essential medium); Eagle, Sigma, St. Louis, MO], supplemented with 10 % FBS (foetal bovine serum; Biochrome), 50  $\mu$ g/mL ascorbic acid (Sigma), 50  $\mu$ g/mL gentamycin, 1% antibiotics/antimicrobials, 10 mM  $\beta$ -glycerophosphate (Sigma), and  $10^{-8}$ M dexamethasone (Sigma)]. Cells were cultured at 37 °C in a humidified atmosphere containing 5 % of CO<sub>2</sub>.

The confluent cell monolayers were detached using trypsin/EDTA (0.25% trypsin/0.02% EDTA, Sigma) and resuspended in complete medium. A 50 $\mu$ l of cell suspension containing  $3 \times 10^5$  cells were pipetted onto the each scaffold. Cell/scaffold constructs were incubated at 37C for 2h to allow RBMSC to diffuse into and adhere to the scaffolds before adding 1 ml of culture medium to each well. The cells on the scaffolds were then allowed to grown for 2 weeks at 37°C in a humidified atmosphere containing 5% of CO<sub>2</sub> with medium changes every 2-3 days.

### *Morphological Analysis*

After 7 and 14 days of culture, cell/scaffold constructs were fixed in 2.5% glutaraldehyde, dehydrated through graded series of ethanol and dried. The

samples were mounted onto brass stubs, sputter coated with cold and analyzed under a Scanning Electron Microscope (SEM) at an accelerating voltage 15kV.

#### *Cell proliferation Assay*

After 7 and 14 days of culture, cell viability was assessed by using Cell Titer 96<sup>®</sup> Aqueous One Solution Cell proliferation Assay kit (Promega, USA). This test is based on the bioreduction of the substrate, (3-(4,5-dimethylthiazol-2-yl)-5-(3-carboxymethoxyphenyl)-2(4-sulfophenyl)-2H tetrazolium) (MTS), into a brown formazan product by NADPH or NADP produced by dehydrogenase enzymes in metabolically active cells. For this assay, culture medium was removed, samples were washed with PBS before the addition of serum free medium plus Cell Titer 96<sup>®</sup> Aqueous One Solution (5/1 ratio). The samples were then incubated for three hours at 37 °C in a humidified atmosphere containing 5 % of CO<sub>2</sub>. A 100 µl of incubated medium was transferred to 96-well plate culture plate and the optical density was read at 490 nm in a micro-plate reader (Synergy HT, Bio-tek).

#### *Alkaline Phosphatase (ALP) Activity*

Alkaline phosphatase (ALP) activity from the scaffolds/ cells constructs was quantified by the specific conversion of p-nitrophenyl phosphate (pNPP) into p-nitrophenol (pNP). The enzyme reaction was carried out at 37°C for 1 h and then stopped by a solution containing 2 M NaOH and 0.2 mM EDTA in distilled water. The absorbance of p-nitrophenol formed was determined at 405 nm with a reference filter at 620 nm. A standard curve was made using pNP values ranging from 0 to 600 µmol/ml. The results were expressed as µmol of pNP produced/ml/h. Please note that ALP activity was determined in weekly collected supernatant and lysed cell for SAOS-2 and RBMSC, respectively.

### 3. Results&Discussion

#### 3.1. Nano- and micro fiber combined scaffolds

Figure 1.A presents the images of the newly designed combined nano/micro fiber structures. As it can be seen, nanofibers could be randomly electrospun on the microfibers and they present the structure that looks like a nanobridge between the microfibers which is very similar to the architecture of ECM [20]. The average diameter of produced SPCL nanofiber was measured to be around 400nm (Figure 1.B). Moreover, nanofibers presented a fine morphology without presence of beads which is referred as a common problem of electropsun fibers [4]. These results also confirmed that the processing parameters were successfully optimized in order to produce fine nanofibers from SPCL.

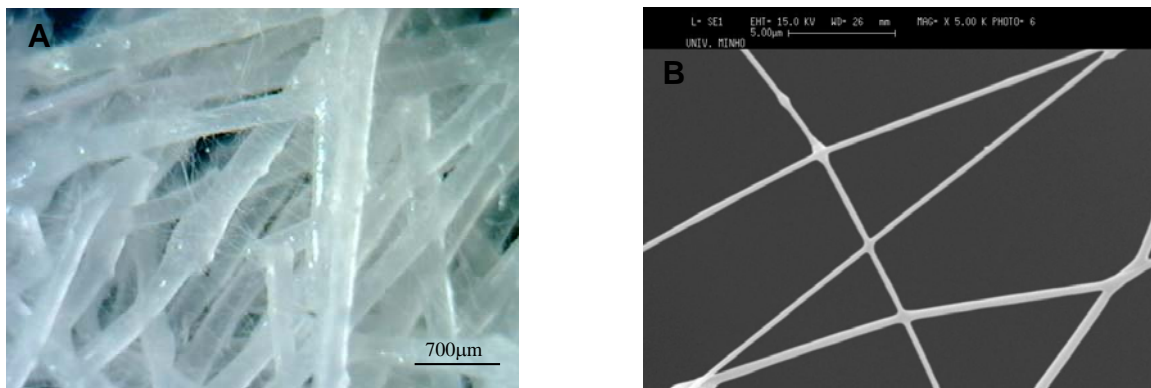


Figure 1. Microscopic images of the scaffolds. Figure B presents a detailed view of nanofibers as observed by SEM.

#### 3.2. Cell Culture

##### *Morphological Analysis*

Regarding cell culture studies with SaOs-2 and RBMSC, cell responses in both cases were clearly different to the nano/micro fiber combined scaffolds when directly compared with the control fiber mesh scaffolds. It was observed that there were significant differences, mainly those related with cell shape and morphology, which could indicate that the patterned layered by the nanofibers

was leading to a different cytoskeleton rearrangement on the seeded cells. SEM images showed that cells had covered microfibers and started to fill the spaces between the latter using for that purpose the previously laid down nanofibers after 7 days of culture.

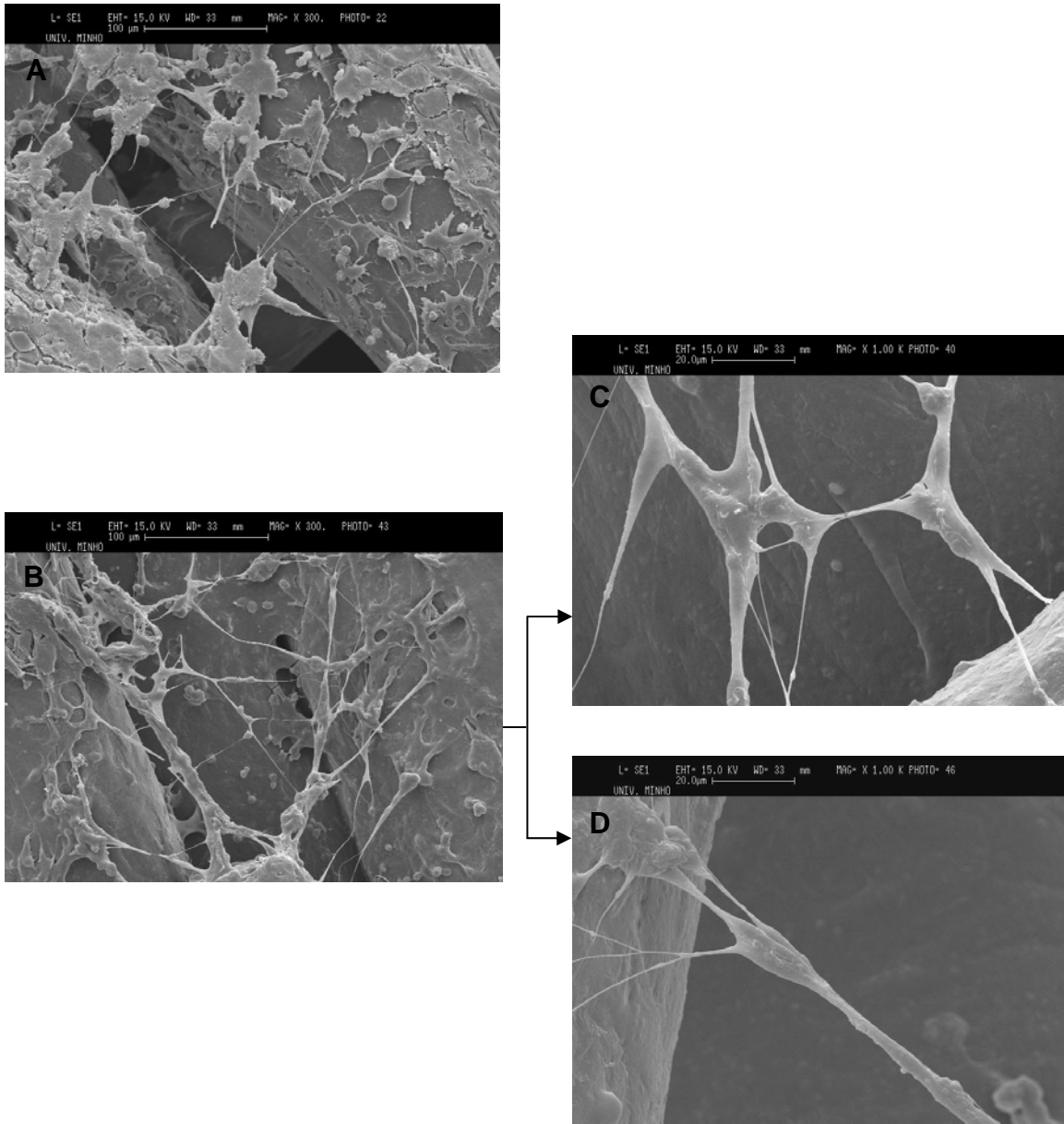


Figure 2. Human osteoblast like cells (SAOS-2) seeded on nano- and micro-fiber combined scaffolds and control (scaffolds without nanofibers); A) after 7 days, B), C) and D) after 14 days of culture.



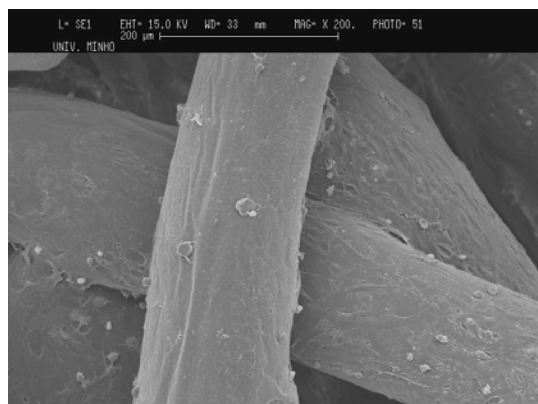


Figure 3. Human osteoblast like cells on control scaffolds after 14 days of culture

Figure 2 shows confluent growth on combined scaffolds and control by the SaOs-2 osteoblast-like cell line. As it can be observed the cell population growing on the combined scaffolds presented a different organization being able to bridge between microfibers. The presence of nanofibers also led to the changes in cell morphology (Figure 2.C and D). Cells along the nanofibers showed very stretched morphology. This fact can be particularly useful as this cytoskeletal rearrangement could affect gene expression, as described by a report of Curtis and Wilkinson [21]. It has been claimed that when the cells stretch themselves, the receptors are also stretched and activated. This results in the expression of different genes than those observed in unstretched cells. This particular hypothesis will be further confirmed in forthcoming (already ongoing) studies. A similar cell response was observed in the study with RBMSC (Figure 4). After 14 days of culture, the scaffolds were covered by cells which used nanofibers to bridge between microfibers (Figure 4.B and C).

It is known that human cells can attach and organize themselves well around the fibers diameter smaller than those of the cells [22]. This approach might explain the behavior of the cells on the developed combined scaffolds. This cell organization could provide better and faster colonization of the scaffolds with cells which is of main importance for tissue engineering approaches.

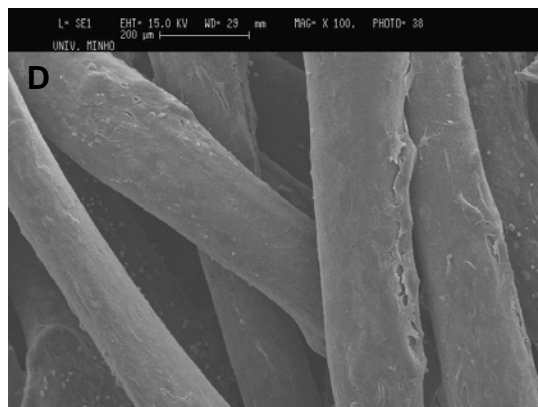
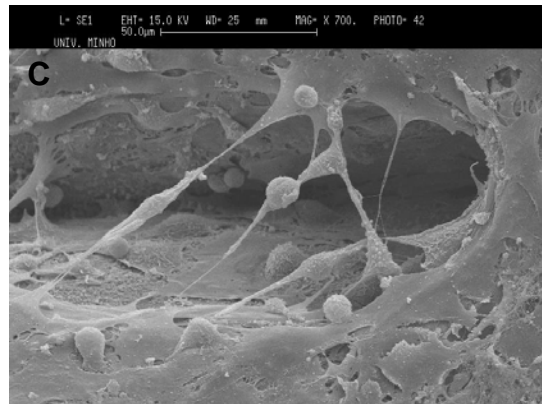
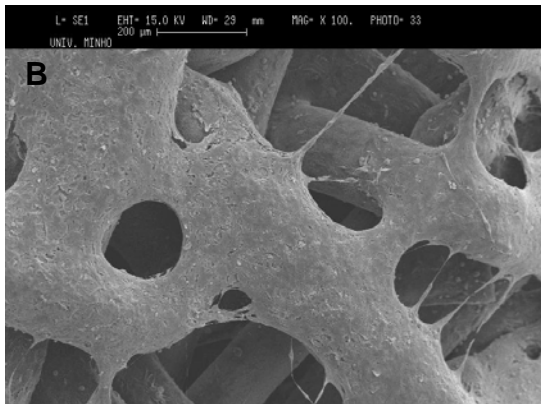
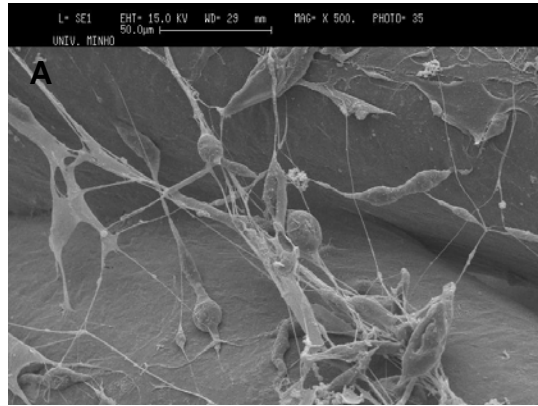


Figure 4. Rat bone marrow stromal cells (RBMSC) seeded on nano- and micro-fiber combined scaffolds and control (scaffolds without nanofibers); A) after 7 days, B) and C) after 14 days of culture. D) Rat bone marrow stromal cells on control scaffolds after 7 days of culture

## Cell viability

The effect of nano/micro fiber combination on cell viability and proliferation of both cell types was tested using a MTS assay. The MTS assay is based on a reduction reaction which reduced MTS reagent to brown formazan product when incubated with viable cells. Thus, the absorbance of formazan indirectly reflected the metabolic activity of cells, which is also associated with cell number.

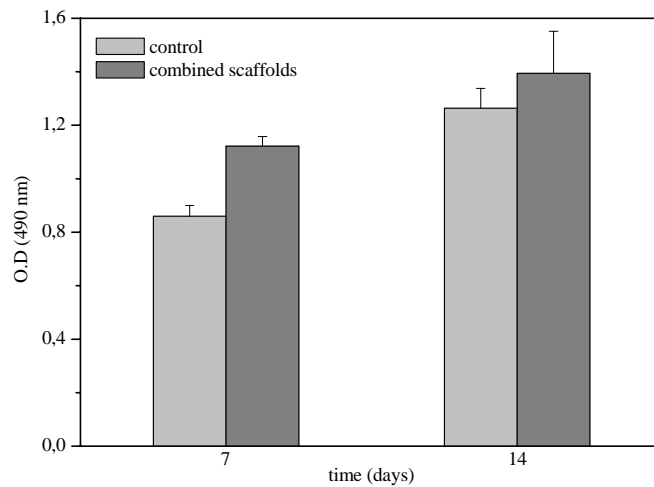


Figure 5. Cell viability and proliferation of human osteoblast like cells determined by MTS. Error bars represent means  $\pm$  SD for n=3.

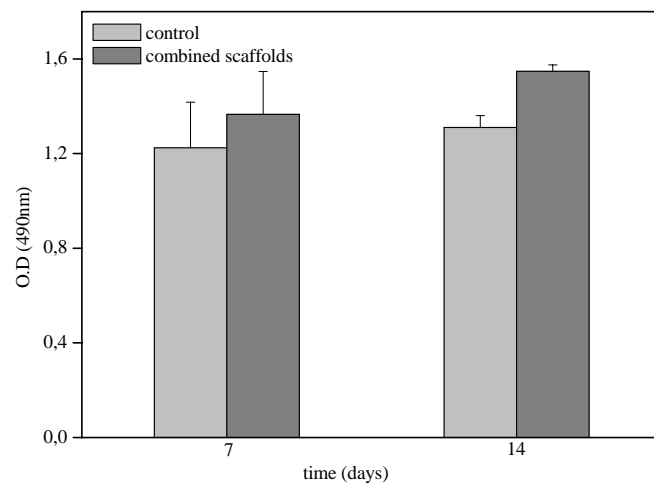


Figure 6. Cell viability and proliferation of rat bone marrow stromal cells determined by MTS. Error bars represent means  $\pm$  SD for n=3.

Figure 5 and 6 present the MTS results of cell culture studies with SAOS-2 and BMSC, respectively. After 7 and 14 days of culturing O.D. values were found to be considerably different for combined scaffolds in both studies. These results indicate that both cell types seeded on combined scaffolds showed increasing metabolic activity and growth rates when directly compared with the control. This fact is closely related with the previously deposited nanofiber mesh. While reducing large void spaces between the pores the mesh is creating additional structures where cells can adhere from the very beginning, avoiding at the same time that the cell suspension drops through the pores until it reaches the bottom of the wells. This particular phenomena shows the validity of the proposed methodology for increasing the cell seeding and culturing conditions during the development of bone tissue engineered constructs.

#### *ALP Activity*

ALP is a well-known enzyme used as a marker of the osteogenic phenotype, which catalyzes the hydrolysis of phosphate esters at an alkaline pH [23]. The skeletal isoform of ALP is a glycoprotein found on the cell membrane of osteoblasts [24]. It has been also demonstrated that it plays an important role in bone matrix mineralization process.

Figure 7 and 8 shows the ALP activity of SaOs-2 and RBMSC cultured on the combined scaffolds and control scaffolds. In both cases, the enzyme activity of scaffolds with nano fibers was higher than that of control in the end of first week. In the case of RBMSC, the differences in enzyme activity became even higher after a second week of culture. This is probably related with the different proliferation rates of the cells seeded on the different scaffolds and at the same time with a probable more induced osteogenic phenotype. The latter hypothesis might be related with the cytoskeleton rearrangement caused by the nanofibers. However further studies are needed to evaluate the influence of these structures on the differentiation of osteogenic cells.

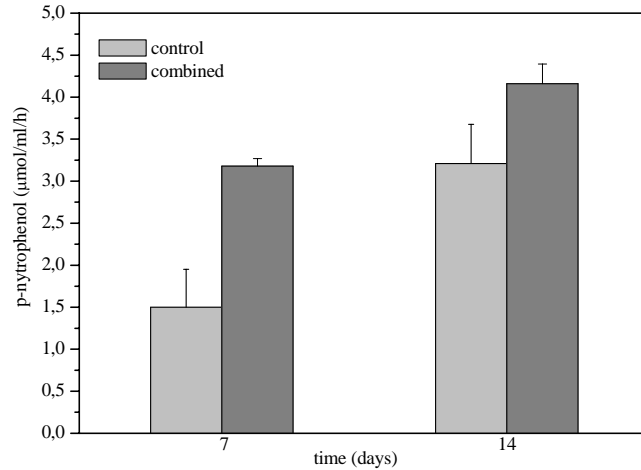


Figure 7. The ALP activity of human osteoblast like cells seeded on SPCL nano- and micro-fiber combined scaffolds and control (scaffolds without nanofibers). Error bars represent means  $\pm$  SD for n=3.

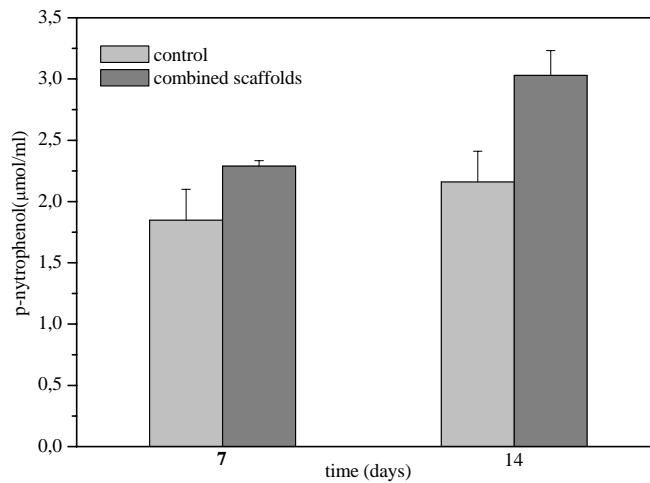


Figure 8. The ALP activity of rat bone marrow stromal cells seeded on SPCL nano- and micro-fiber combined scaffolds and control (scaffolds without nanofibers). Error bars represent means  $\pm$  SD for n=3.

#### 4. Conclusions

An electrospinning technique was used to produce nanofibers on SPCL fiber meshes in order to combine nano- and microfibers in the same 3D scaffold architecture. It was clearly demonstrated that cell response changed completely with the addition of nanofibers on the fiber meshes. Osteoblasts were organized

to bridge between microfibers and this resulted in scaffolds completely filled with cells after two weeks of culture. Moreover, the presence of nanofibers had an influence in cell morphology which was observed to be much more stretched and spread. The scaffolds without nanofibers did not show this kind of organization and the morphology of cells remained normal, and forming a continuous cell monolayer over microfibers. Furthermore, cells seeded on combined scaffolds showed higher viability and ALP activity than that on control.

The results from this study indicate that nano- and micro-fiber scaffolds can provide an ideal structure for cell deposition and organization. Their unique architecture which supports and guides the cells makes them a suitable candidate for bone tissue engineering applications

## References

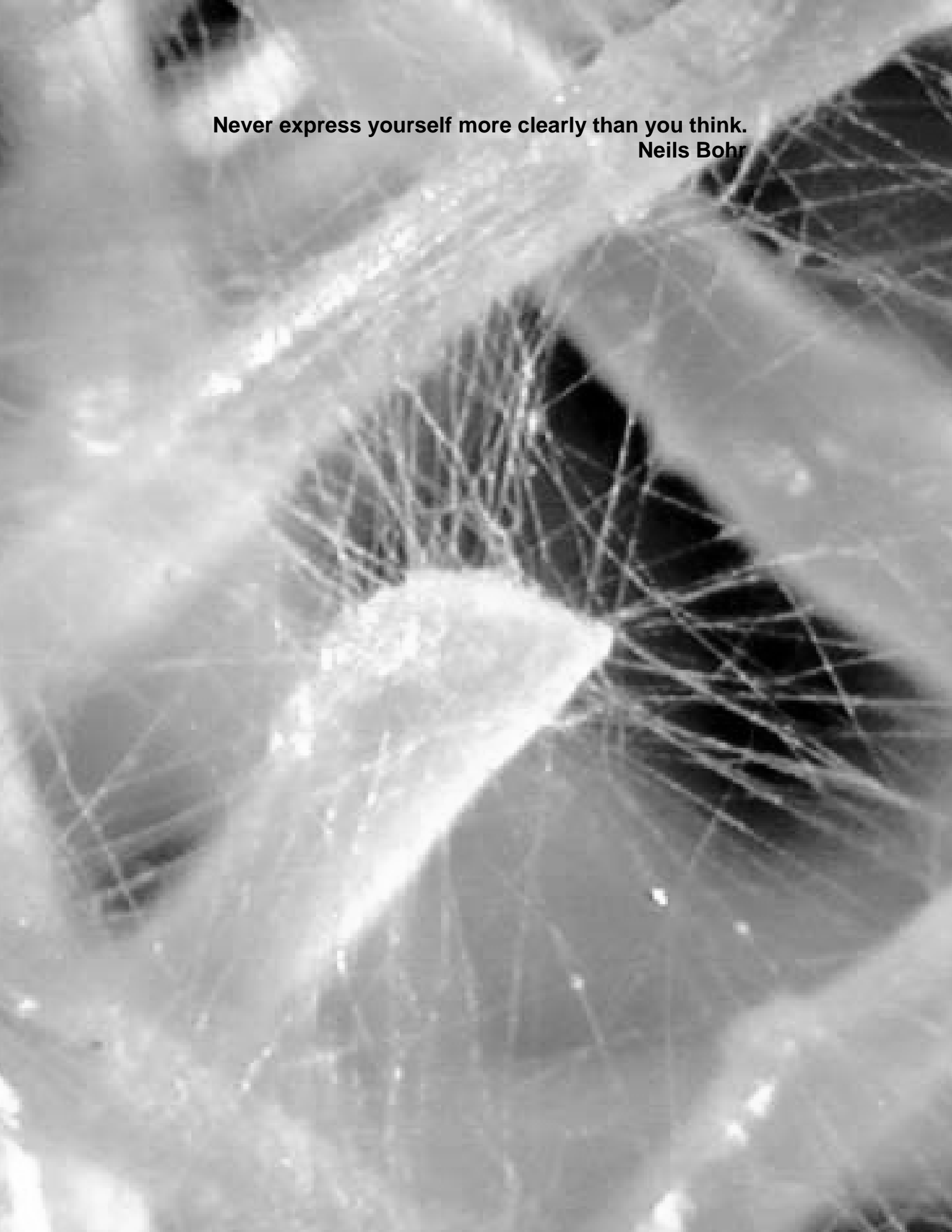
1. Gomes, M.E. and R.L. Reis, Tissue engineering: Key elements and some trends. *Macromolecular Bioscience*, 2004. 4(8): p. 737-742.
2. Liu, X.H. and P.X. Ma, Polymeric scaffolds for bone tissue engineering. *Annals of Biomedical Engineering*, 2004. 32(3): p. 477-486.
3. Lutolf, M.P. and J.A. Hubbell, Synthetic biomaterials as instructive extracellular microenvironments for morphogenesis in tissue engineering. *Nature Biotechnology*, 2005. 23(1): p. 47-55.
4. Huang, Z.M., et al., A review on polymer nanofibers by electrospinning and their applications in nanocomposites. *Composites Science and Technology*, 2003. 63(15): p. 2223-2253.
5. Li, D., Y.L. Wang, and Y.N. Xia, Electrospinning nanofibers as uniaxially aligned arrays and layer-by-layer stacked films. *Advanced Materials*, 2004. 16(4): p. 361-366.
6. Matthews, J.A., et al., Electrospinning of collagen nanofibers. *Biomacromolecules*, 2002. 3(2): p. 232-238.
7. Ohkawa, K., et al., Electrospinning of chitosan. *Macromolecular Rapid Communications*, 2004. 25(18): p. 1600-1605.
8. Min, B.M., et al., Chitin and chitosan nanofibers: electrospinning of chitin and deacetylation of chitin nanofibers. *Polymer*, 2004. 45(21): p. 7137-7142.
9. Jin, H.J., et al., Electrospinning *Bombyx mori* silk with poly(ethylene oxide). *Biomacromolecules*, 2002. 3(6): p. 1233-1239.
10. Son, W.K., et al., The effects of solution properties and polyelectrolyte on electrospinning of ultrafine poly(ethylene oxide) fibers. *Polymer*, 2004. 45(9): p. 2959-2966.
11. Li, W.J., et al., Electrospun nanofibrous structure: A novel scaffold for tissue engineering. *Journal of Biomedical Materials Research*, 2002. 60(4): p. 613-621.

12. Yang, F., et al., Electrospinning of nano/micro scale poly(L-lactic acid) aligned fibers and their potential in neural tissue engineering. *Biomaterials*, 2005. 26(15): p. 2603-2610.
13. Yoshimoto, H., et al., A biodegradable nanofiber scaffold by electrospinning and its potential for bone tissue engineering. *Biomaterials*, 2003. 24(12): p. 2077-2082.
14. Li, W.J., et al., Biological response of chondrocytes cultured in three-dimensional nanofibrous poly(epsilon-caprolactone) scaffolds. *Journal of Biomedical Materials Research Part A*, 2003. 67A(4): p. 1105-1114.
15. Kidoaki, S., I.K. Kwon, and T. Matsuda, Mesoscopic spatial designs of nano- and microfiber meshes for tissue-engineering matrix and scaffold based on newly devised multilayering and mixing electrospinning techniques. *Biomaterials*, 2005. 26(1): p. 37-46.
16. Li, W.J., et al., Multilineage differentiation of human mesenchymal stem cells in a three-dimensional nanofibrous scaffold. *Biomaterials*, 2005. 26(25): p. 5158-5166.
17. Jin, H.J., et al., Human bone marrow stromal cell responses on electrospun silk fibroin mats. *Biomaterials*, 2004. 25(6): p. 1039-1047.
18. Gomes, M.E., et al., Alternative tissue engineering scaffolds based on starch: processing methodologies, morphology, degradation and mechanical properties. *Materials Science & Engineering C-Biomimetic and Supramolecular Systems*, 2002. 20(1-2): p. 19-26.
19. Gomes, M.E., et al., Effect of flow perfusion on the osteogenic differentiation of bone marrow stromal cells cultured on starch-based three-dimensional scaffolds. *Journal of Biomedical Materials Research Part A*, 2003. 67A(1): p. 87-95.
20. Rosso, F., et al., From cell-ECM interactions to tissue engineering. *Journal of Cellular Physiology*, 2004. 199(2): p. 174-180.
21. Curtis, A. and C. Wilkinson, Topographical control of cells. *Biomaterials*, 1997. 18(24): p. 1573-1583.



22. Laurencin, C.T., et al., Tissue engineering: Orthopedic applications. Annual Review of Biomedical Engineering, 1999. 1: p. 19-46.
23. Harris, H., The Human Alkaline-Phosphatases - What We Know and What We Dont Know. Clinica Chimica Acta, 1990. 186(2): p. 133-150.
24. Stigbrand, T., Present Status and Future Trends of Human Alkaline Phosphatases. Human Alkaline Phosphatases, ed. A.R. Liss. 1984, New York. 3.

**Never express yourself more clearly than you think.  
Neils Bohr**





## **CHAPTER VIII**

### **GENERAL CONCLUSIONS**

## **GENERAL CONCLUSIONS**

The main goal of this thesis was to be able to design adequate fiber structures from natural origin polymers for being used in tissue engineering applications, particularly in bone tissue repair approaches. The studies discussed herein can be divided in two main parts:

- Development of chitosan-based fiber structures;
- Development of starch-based fiber structures.

### **Development of chitosan-based fiber structures;**

In the studies of this part, chitosan, which is a biocompatible, biodegradable and non-toxic natural polymer, was chosen for fiber production. Fibers with different diameters were produced by means of wet spinning for use in different purposes. Chitosan fibers with diameter around 200 $\mu$ m presented an oriented surface morphology due to rolling up procedure during processing, which could be called as a kind of stretching. This property of the fibers would then provide a mechanical strength for the combined architecture where the chitosan fibers were used to reinforce the structure. These combined architectures were developed from coralline origin hydroxyapatite particles, chitosan membranes and chitosan fibers being aimed serve as a scaffold for tissue engineering or to be used in guided tissue regeneration by mimicking the arrangements in natural bone.

Chitosan fibers with a smaller diameter were also produced, with the same processing procedure, and shaped into 3D randomly oriented fiber meshes. These fiber meshes showed to support well cell adhesion of osteoblast-like cells. Considering the use of these scaffolds in bone regeneration, it was important to have osteoconductivity in order that osteoblast and osteoprogenitor cells can easily attach and migrate in the scaffold. Based on this fact, the surface of chitosan fiber mesh scaffolds were pre-coated with a bone-like apatite layer. A new coating approach, using a spray, applied in these experiments due the

complex structure of chitosan fiber meshes, was herein proposed. As a result of coating, the osteoblast cell behaviour completely changed when they were cultured on the coated scaffolds.

### **Development of starch-based fiber structures**

In this part, two different types of scaffolds were developed from a starch/polycaprolactone blend: (i) wet-spun SPCL fiber meshes and (ii) nano- and micro-fiber combined scaffolds.

The wet spinning technique was also used in this part as an alternative route for production of SPCL fiber mesh scaffolds. By this technique, the physical properties (such as diameter, thickness, porosity, etc.) of the scaffolds can be adjusted depending on the specifications. Another important advantage of using this technique is that the scaffolds can be formed during processing without any need for a further processing step. In this part of the studies, it was possible to obtain the fiber mesh scaffolds with adequate porosity and the mean pore size which were in the proposed range for an ideal scaffold for bone tissue engineering. Considering the relation between cell attachment and surface properties of a scaffold, the ability of the scaffold surface for cell attachment could be enhanced by applying an Ar plasma treatment. The results from the cell culture studies demonstrated that the treatment worked quite effectively on enhancing cell attachment and proliferation.

It is known that, the ideal scaffold should be one which closely mimics the natural extracellular matrix (ECM). Having this in consideration, we originally developed nano- and micro-fiber combined scaffolds from the same blend in the final study of the thesis. The basic point of this concept was to use nanofibers for mimicking the physical structure of natural ECM. The micro support for cells was provided by SPCL microfiber meshes produced by melt spinning. The presence of nanofibers in the structure showed great influence on cell morphology, viability and differentiation. In fact, cells cultured on combined scaffolds presented different cell organization than that on SPCL fiber meshes without nanofibers.

The cells tended to stretch themselves along the nanofibers and to bridge between microfibers. This stretched morphology led to a difference in differentiation rate which could be related with the different gene expression profiles.

Furthermore, the presence of nanofibers seemed to be an advantage for increasing the cell seeding efficiency, resulting in an increase in cell viability.

### **Final Remarks/Future Research**

The results obtained in the studies discussed in this thesis showed that, tissue engineering scaffolds with different shapes and properties can be designed by using fibers from natural origin polymers. One of the most promising designs seemed to be the one which combines the nano and microfibers in the same structure. By means of following the same concept, new scaffolds can be designed in the presence of different natural polymers such as collagen, silk fibroin (consists of glycosaminoglycans), which are presented in the natural extracellular matrix. The author of the present thesis wants to play an active role on taking forward these kind of approaches.